THERAPEUTIC IMPLICATIONS OF UBIQUITIN PROTEASOME SYSTEM IN NEURODEGENERATIVE DISEASES

A Thesis Submitted
In Partial Fulfilments of the Requirements for the degree of

DOCTOR OF PHILOSOPHY

By

NEETU RANI

(2K21/PHD/BT/05)

Under the supervision of

PROF. PRAVIR KUMAR

Professor and Dean IA
Department of Biotechnology
Delhi Technological University

Department of Biotechnology

DELHI TECHNOLOGICAL UNIVERSITY

(Formerly Delhi College of Engineering)

Shahbad Daulatpur, Main Bawana Road, Delhi-110042. India

November, 2024

DELHI TECHNOLOGICAL UNIVERSITY
(Formerly Delhi College of Engineering)
Shahbad Daulatpur, Main Bawana Road, Delhi- 110042. India

CANDIDATE'S DECLARATION

I, Neetu Rani, 2K21/PHDBT/05 student of Ph.D. Biotechnology, hereby declare that the project synopsis titled **"THERAPEUTIC IMPLICATIONS OF UBIQUITIN PROTEASOME SYSTEM IN NEURODEGENERATIVE DISEASES,"** which is submitted by me to the Department of Biotechnology, Delhi Technological University, Delhi in partial fulfillment of the requirement for the award of the degree of doctorate in philosophy, is original and not copied from any source without paper citation. is an authentic record of my own work carried out during the period from 02.08.2021 to 06.08.2024 under the supervision of Prof. Pravir Kumar, Department of Biotechnology, Delhi Technological University The work has not previously formed the basis for the award of any Degree, Diploma Associateship, Fellowship, or other similar title or recognition.

Candidate's Signature

Neetu Rani
2K21/PHDBT/05
Ph.D. scholar
Department of Biotechnology

This is to certify that the student has incorporated all the corrections suggested by the examiners in the thesis and the statement made by the candidate is correct to the best of our knowledge.

Signature of Supervisor (s)

Signature of External Examiner

DELHI TECHNOLOGICAL UNIVERSITY

(Formerly Delhi College of Engineering)

Shahbad Daulatpur, Main Bawana Road, Delhi- 110042. India

CERTIFICATE BY THE SUPERVISOR (s)

Certified that **Ms. Neetu Rani (2K21/PHD/BT/05)** has carried out her research work presented in this thesis entitled **"THERAPEUTIC IMPLICATIONS OF UBIQUITIN PROTEASOME SYSTEM IN NEURODEGENERATIVE DISEASES"** for the award of Doctor of Philosophy from the Department of Biotechnology, Delhi Technological University, Delhi, under the supervision of **Prof. Pravir Kumar,** Department of Biotechnology, Delhi Technological University, Delhi .The thesis embodies results of original work and studies that are carried out by the student herself and the contents of the thesis do not form the basis for the award of any other degree to the candidate or to anybody else from this or any other University/Institution.

Date: 21-10-2024

Pravir Kumar
21/10/2024

Prof. Pravir Kumar
Professor and Dean IA
Department of Biotechnology
Delhi Technological University
Delhi -110042

Yasha Hasija 21.10.24

Prof. Yasha Hasija
Head of Department
Department of Biotechnology
Delhi Technological University
Delhi -110042

AKNOWLEDGEMENT

*First and above all, I bow down to the **GOD, the ALMIGHTY** for his grace, blessings, and countless love from the very inception to the completion of this research work. During the complete course of this work, I have felt the grace of God which enlighten my knowledge and thoughts.* I express my sincere gratitude to many people for providing me constant motivation and guidance of many people for all their contributions that helped me a lot to complete this research. *I would therefore like to acknowledge all of them.*

*I would like to express my gratitude to **Prof. Prateek Sharma**, Vice chancellor, Delhi Technological University, Delhi for providing me the opportunity to carry out this work in this prestigious institute. Further, I express my gratitude to **Prof. Yogesh Singh** and **Prof. Jai Prakash Saini**, former Vice chancellor Delhi Technological University, Delhi for providing me opportunity and infrastructure to complete this work. Here, I would also like to thanks **Prof. Yasha Hasija**, Head of the Department, department of Biotechnology, for providing me the infrastructure and smooth functioning of official work.*

*It is a great pleasure to express my sincere gratitude to my thesis supervisor **Prof. Pravir Kumar,** Department of Biotechnology and Dean, International Affairs, Delhi Technological University for his invaluable advice, constant support, and patience during my PhD study. His immense knowledge and plentiful experience have encouraged me in all the time of my research period. I am very happy to inscribe this page, and I owe a warm thanks to you sir.*

*I would like to thanks to **Dr. Rashmi Ambasta**, Associate professor, SRM University, Haryana, and former CSIR Scientist, Delhi Technological University, Delhi, for her support and motivation in the planning and execution of the experimentations.*

Immeasurable appreciation to my senior colleagues ***Dr. Sudhanshu Sharma, Dr. Rohan Gupta, Dr. Smita Kumari, Dr. Dia Advani, Rahul Tripathi, Dr. Neha Kukreti*** *and* ***Dr. Sonika Kag*** *for their precious support and a cherished time spent together in the lab. I also want to thank my colleague* ***Mehar Sahu*** *and junior colleagues* ***Shefali Kardam*** *and* ***Shruitkirti Vashishth*** *for their support.*

I gratefully acknowledge the fellowship received for my research work from the Council of Scientific and Industrial Research (CSIR), University Grants Commission (UGC), Govt. of India. I wish to acknowledge the Senior Management and technical staff of DTU, for providing support to my work.

Most importantly, credit is due to my parents and family members, who were always there to bring positivity and hope. This PhD study would not have been possible without the corporation and support of my family. I am profoundly grateful to them for their extended love and patience during the difficult times.

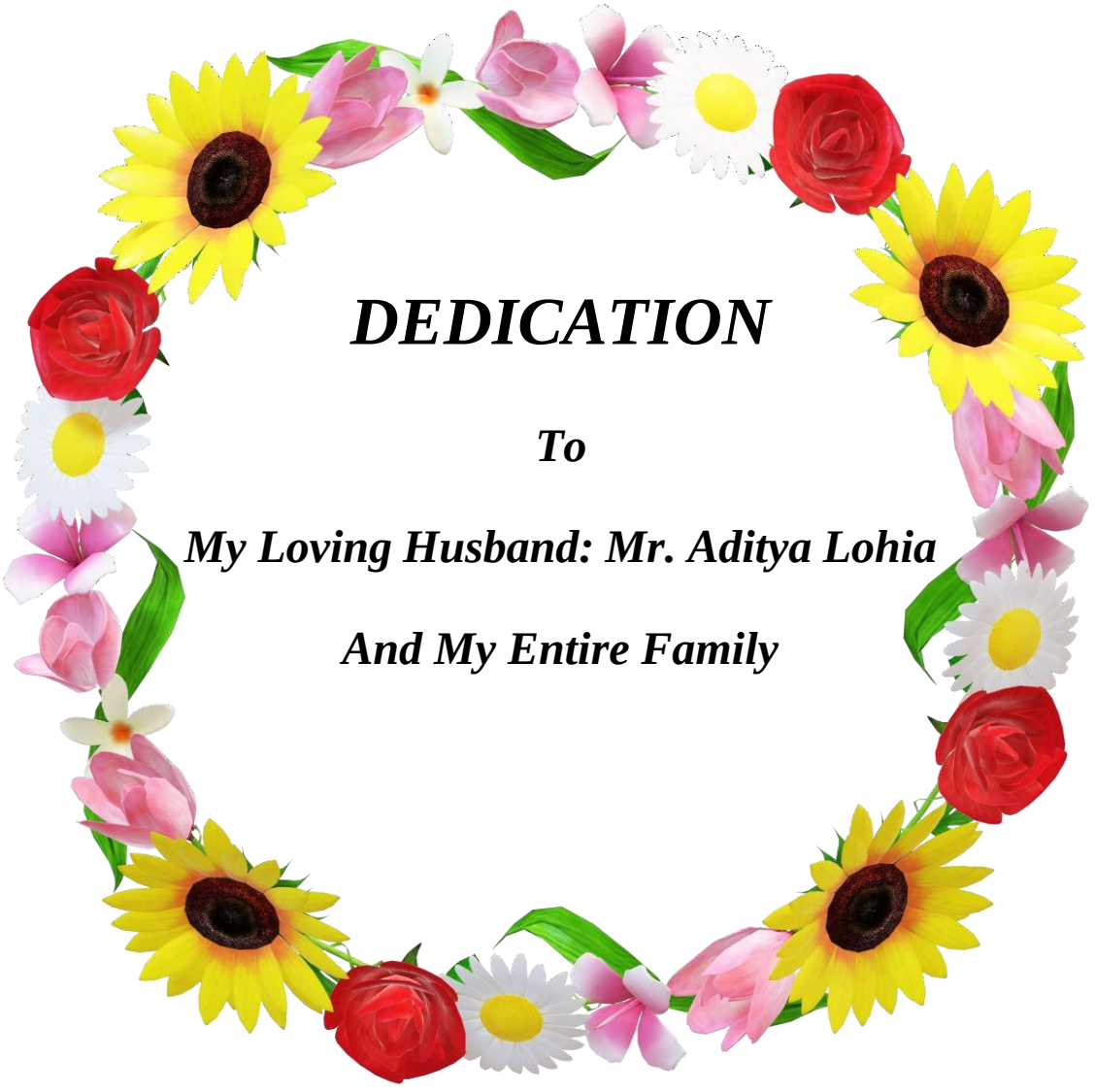

DEDICATION

To

My Loving Husband: Mr. Aditya Lohia

And My Entire Family

LIST OF PUBLICATIONS

1. Rani, N., Kumar, P. Exploring Natural Compounds as Potential CDK4 Inhibitors for Therapeutic Intervention in Neurodegenerative Diseases through Computational Analysis. *Mol Biotechnol* (2024). https://doi.org/10.1007/s12033-024-01258-8 **(SCIE IF-2.4)**

2. Rani, N., Sahu, M., Ambasta, R.K., Kumar, P., 2024. Triaging between post-translational modification of cell cycle regulators and their therapeutics in neurodegenerative diseases. Ageing Res Rev 94, 102174. https://doi.org/10.1016/J.ARR.2023.102174 **(SCIE IF-12.5)**

3. Sahu, M., **Rani, N.** & Kumar, P. Simulation and Computational Study of RING Domain Mutants of BRCA1 and Ube2k in AD/PD Pathophysiology. Mol Biotechnol 66, 1095–1115 (2024). https://doi.org/10.1007/s12033-023-01006-4 **(SCIE IF-2.4)**

4. Rani, N., Kaushik, A., Kardam, S., Kag, S., Raj, V. S., Ambasta, R. K., & Kumar, P. (2024). Reimagining old drugs with new tricks: Mechanisms, strategies and notable success stories in drug repurposing for neurological diseases. Progress in Molecular Biology and Translational Science. https://doi.org/10.1016/BS.PMBTS.2024.03.029 **(IF-3.6)**

5. Rani, N. & Kumar, P. "Understanding the role of alkaloids in therapeutic targeting of UBE3A in Alzheimer's Disease," 2023 3rd International Conference on Innovative Sustainable Computational Technologies (CISCT), Dehradun, India, 2023, pp. 1-4, doi: 10.1109/CISCT57197.2023.10351490.

6. Rani, N. & Kumar, P. “Leuconoxine as a prospective therapeutic candidate targeting CDK6 in combating Alzheimer's disease,” the World Congress of Neurology (WCN 2023) Journal of the Neurological Sciences Volume 455, SUPPLEMENT, 121442, :https://doi.org/10.1016/j.jns.2023.121442 **(IF-3.6)**

7. **Rani, N.** & Kumar, P. “Revolutionizing Antimicrobial Defence: Unleashing CDK5 as a Molecular Maestro Against Drug Resistance,” 3rd International Conference on “Antimicrobial Resistance, Novel Drug Discovery and Vaccine Development: Challenges and Opportunities”, Delhi, India 2024.

THERAPEUTIC IMPLICATIONS OF UBIQUITIN PROTEASOME SYSTEM IN NEURODEGENERATIVE DISEASES

NEETU RANI

(2K21/PHDBT/05)

ABSTRACT

The ubiquitin-proteasome system (UPS) and the regulation of the cell cycle are essential mechanisms that play an indispensable part in maintaining neuronal homeostasis and integrity. Disruption of these pathways has been identified as a significant factor in the development of neurodegenerative diseases (NDDs), which includes Alzheimer's disease (AD), Parkinson's disease (PD), Huntington's disease (HD), and amyotrophic lateral sclerosis (ALS). This study thoroughly examines the therapeutic consequences of focusing on both the UPS and the disruption of the cell cycle in neurodegeneration. We analyze the complex interplay between UPS dysfunction and cell cycle irregularities, emphasizing their combined impact on neuronal dysfunction and degeneration. The study investigates the molecular pathways that cause defective protein degradation, cell cycle re-entry, and abnormal expression of cell cycle proteins in NDDs. The study discusses emerging treatment approaches that focus on UPS function and regulating cell cycle activity. These approaches include pharmaceutical therapies, and the use of cell cycle inhibitors. In addition, we investigate the prospect of using combinatorial techniques to target both pathways to create synergistic neuroprotective effects. The discussion focuses on the challenges related to UPS and cell cycle-targeted medicines, including as medication selectivity, the ability to penetrate the blood- brain barrier, and the possibility for adverse effects. Promising advancements in personalized medicine strategies, therapies directed by biomarkers, and precise targeting of UPS and cell cycle components offer potential for creating of effective medicines to stop or decelerate the course of NDDs. Acquiring a more profound comprehension of the interaction between UPS and the disruption of the cell cycle in neurodegeneration is crucial for promoting therapeutic approaches and for improving patient outcomes.

Firstly, common differentially expressed genes (DEGs) (i.e., Cell Cycle related genes) were screened after comparing DEGs from the GSE5281 dataset and the CCR genes from KEGG database, based on the applied filters of adj p value < 0.05 and Log Fc value. Further Gene set enrichment analysis was performed to assess the biological, cellular, and molecular processes of CCR genes. The CCR genes was further screened for protein-protein interaction (PPI) with the help of STRING and Cytoscape tools, from where 10 CCR genes were extracted. This study identified CCR genes biomarkers (CDK6, EP300, RB1, ATR and CDC25C) based on Gene set enrichment analysis and pathway analysis. CDK6 has been selected for further analysis due to its highest Log FC value among selected biomarkers and its active involvement in enrichment interpretation. Natural compounds were used against CDK6. Molecular docking analysis predicted that NPC314329 has maximum binding affinity scores and found to be promising therapeutic agents against AD.

CDK4 is a member of the serine-threonine kinase family, which has been found to be overexpressed in a plethora of studies related to neurodegenerative diseases. CDK4 is one of the most validated therapeutic targets for neurodegenerative diseases. Hence, the discovery of potent inhibitors of CDK4 is a promising candidate in the drug discovery field. Firstly, the reference drug Palbociclib was identified from the available literature as a potential candidate against target CDK4. In the present study, the Collection of Open Natural Products (COCONUT) database was assessed for determining potential CDK4 inhibitors using computational approaches based on the Tanimoto algorithm for similarity with the target drug, i.e., Palbociclib. The potential candidates were analyzed using SWISSADME, and the best candidates were filtered based on Lipinski's Rule of 5, Brenk, blood-brain barrier permeability, and Pains parameter. Further, the molecular docking protocol was assessed for the filtered compounds to anticipate the CDK4-ligand binding score, which was validated by the fastDRH web-based server. Based on the best docking score so obtained, the best four natural compounds were chosen for further molecular dynamic simulation to assess their stability with CDK4.

In this study, two natural products, with COCONUT Database compound ID - CNP0396493 and CNP0070947, have been identified as the most suitable candidates for neuroprotection.

Further, common differentially expressed genes (DEGs) (i.e., E3 ligases) were screened after comparing DEGs from the GSE5281 dataset and the KSBP2 E3 ligases dataset, based on the applied filters of adj p value < 0.05 and Log Fc value. The gene ontology of E3 ligases was identified by performing Gene set enrichment analysis, which was further screened for PPI with STRING and Cytoscape tools. As a result, E3 ligases biomarkers (UBE3A, UBE4B, RCHY1, UBOX5, UBE3C, CBL) were identified. Amongst these biomarkers, UBE3A was selected for further analysis due to its highest Log FC value and active involvement in enrichment interpretation. Molecular docking analysis of UBE3A with natural compounds (alkaloids) predicted that Leuconoxine, Jamine and Panamine have maximum binding affinity scores. However, after MD simulation analysis, leuconoxine was predicted as protective agents against UBE3A in AD.

LIST OF TABLES

LIST OF FIGURES

LIST OF ABBREVIATIONS

AD	Alzheimer's disease
PD	Parkinson's disease
HD	Huntington's disease
ALS	Amyotrophic Lateral Sclerosis
NDDs	Neurodegenerative diseases
UPS	Ubiquitin-proteasome system
Aβ	Amyloid-β
AD	Alzheimer's disease
PD	Parkinson's disease
CDKs	Cyclin-dependent kinases
HDACs	Histone deacetylases
APP	Amyloid precursor protein
BDNF	Brain-derived neurotrophic factor
CKIs	CDK inhibitors
pRb	Retinoblastoma protein
APC	Anaphase promoting complex
SCF	SKP1/Cullin 1/F-box
BH3	Bcl 2 homology 3 BH3
FOXO	Forkhead box O
ATM	Ataxia telangiectasia Mutated
NGF	Nerve growth factor
DUBs	Deubiquitinating enzymes
RING	Really interesting new gene
CRLs	Cullin Ring Ligase
HECT	Homologous to the E6AP carboxy terminus
HERC	HECT and RCC-like domain containing
RBR	Ring Between Ring

SKP1	S-phase kinase-associated protein 1
HPV16	Human papillomavirus type 16
DSBs	Double-stranded DNA breaks
TrkB	Tropomyosin-related kinase B
DCRNs	Differentiating chick retinal neurons
ATR	Ataxia-telangiectasia and Rad-3

LIST OF CONTENTS

CHAPTER 1

INTRODUCTION

Chapter 1
INTRODUCTION

According to research, around 7 million people in the United States are living with Alzheimer's disease (AD) and almost 1 million people are diagnosed with Parkinson's disease (PD) which is expected to reach 1.2 million by 2030 [1], [2] Also, millions of people are suffering from other NDDs such as Huntington's disease (HD), Amyotrophic Lateral Sclerosis (ALS) and others [3], [4]. This brings attention towards an urgent need for upgrading therapeutics management strategies [5]. However, effective therapeutics for neurodegenerative diseases (NDDs) have constituted a significant challenge. Currently, very few therapies are available for treating these NDDs, which are only for symptomatic relief or decelerating the disease progression, demanding the development of NDD-focused therapeutics by scientists and clinicians.

The study of neurodegenerative conditions has focused on two primary systems: the ubiquitin-proteasome system (UPS) and the cyclin-dependent kinases (CDKs). After being discovered to be important cell cycle regulators, CDKs have been linked to a number of neurological functions, such as memory formation, synaptic plasticity and neuronal survival. Numerous NDDs have been linked to dysregulation of CDKs, which is implicated in pathological processes such tau hyperphosphorylation and aberrant cell cycle re-entry. The UPS is the principal system that degrades intracellular proteins and keeps cellular protein balance in check. Misfolded and aggregated proteins build up and are a common feature of many NDDs; this buildup has been connected to UPS dysfunction. Evidence suggests that CDKs can affect UPS activity and vice versa, indicating a complicated relationship between CDKs and the UPS. An overview of various factors involved in NDDs is represented in **Fig 1.1**. Establishing new therapeutic targets for NDDs require an understanding of this dynamic.

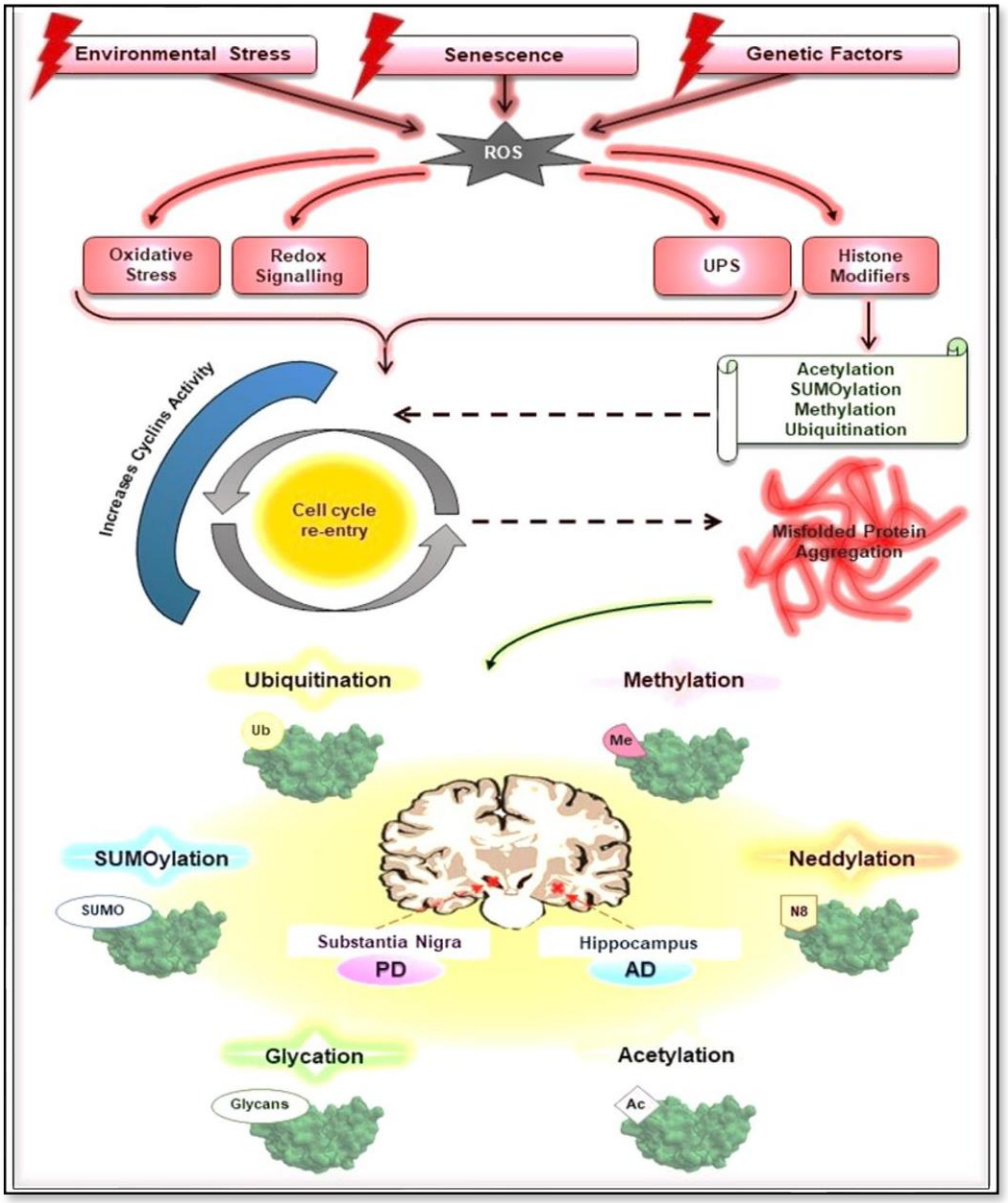

Fig 1.1. Overview of factors involved in NDDs - The role of cell cycle regulators and PTMs in NDDs has been extensively studied in pathogenesis of NDDs. Various factors such as Oxidative stress, UPS, Redox signaling, histone modifiers stimulate various signaling pathways such as JNK, p38/MAPK, GSK3β and others that leads to the upregulations of Cyclins which in turn affects the cell cycle mechanism. Various post-translational modifications also have a crucial role in the progression of NDDs.

1.1 AIM AND OBJECTIVES

1.1.1 Aim

The focus of this thesis is to enquire the potential therapeutic benefits of targeting the ubiquitin-proteasome system (UPS) and cyclin-dependent kinases (CDKs) in NDDs. The goal of the study is to find novel treatment approaches that could modify CDKs and the UPS, to halt the progression of these diseases by investigating their roles in the pathogenesis.

1.1.2 Objectives

1. To identify the potential cell cycle regulators involved in NDDs.
2. To develop the novel therapeutic agents that target CDK4 to control NDDs.
3. To identify the novel UPS molecular signatures implemented in NDDs for prospective novel therapeutics.

1.1.3 Overview of the Thesis

This thesis comprises of six chapters, each emphasizing on a specific area of study of cell cycle regulators, specifically CDKs and the UPS, in the context of NDDs. **Chapter 1** gives and overview of the NDDs and important functions of CDKs and UPS. In this chapter, the dysregulation in various system and its influence on the pathophysiology of disease is discussed. Further, the chapter also comprise of the study's aim and objectives and its possible contribution to the field of therapeutics of NDDs along with the limitations and future direction. **Chapter 2** provides an overview of the research on the involvement of CDKs and UPS in NDDs. It includes a thorough summary of the present knowledge and connections between these system with NDDs. **Chapter 3** elaborates the methods used for identifying putative therapeutic targets in the UPS and CDK pathways. It includes studying the relationship between CDKs, UPS and NDDs through bioinformatics methods and computational analysis. **Chapter 4** presents the results of these studies explaining the function of CDKs and UPS components in the NDDs. It delves into the effects of changes these systems on the disease progression thereby investigating possible

treatment targets. The potential of natural compounds, for targeting UPS components is discussed in **Chapter 5**. The usage of molecular docking, molecular dynamic simulations, and other bioinformatics methods in prediction of the therapeutic efficacy of these drugs is also elaborated in this chapter. Finally, the overall results of the study are summarized, which includes the therapeutic implication of these compounds as potential candidates against NDDs, along with discussing future research possibilities as well as the constraints of the current study.

CHAPTER 2

REVIEW OF LITERATURE

Chapter 2
REVIEW OF LITERATURE

2.1 Overview

Neurodegenerative diseases (NDDs) are manifested by gradual neuronal loss associated with the accumulation of Amyloid-β (Aβ) protein, prion protein, α-synuclein and tau showing altered physio-chemical properties in various parts of the brain [6]. The aberrant re-entry of neurons into the cell cycle has been linked to various NDDs such as Alzheimer's disease (AD) [7], brain and spinal cord injury [8], cerebral ischemia [9] and Parkinson's disease (PD) [10], which are classified based on their protein deposition [11]. Understanding the role of ubiquitination in cell cycle regulation is important to elucidate their impact on various biological processes, including their emerging importance in NDDs. Cell cycle is a sequential mechanism controlling the growth, development, and multiplication of cells. Initiation of cell division is carried out by Cyclins and their enzymatic partners i.e. Cyclin-dependent kinases (CDKs) that are significant proteins for cell cycle advancement. Ubiquitination is enzymatic conjugation of specific chemical groups to amino acid side chains [12].

Ubiquitination is important in modulating the activity of essential cell cycle proteins such as Cyclins, CDKs and their inhibitors. These modifications affect the timing and progression of cell cycle phases and are important for maintaining genomic stability and preventing abnormal cell division. Ubiquitination and autophagy can affect cellular machinery responsible for protein degradation. Dysregulation of UPS can lead to impaired clearance of misfolded proteins, contributing to their accumulation in NDDs. Epigenetic PTMs, including DNA methylation and histone modifications, can influence gene expression patterns in neurons. Altered epigenetic regulation is associated with changes in the expression of genes associated with NDDs. These abnormal PTMs of cell cycle regulators can lead to neuronal re-entry into the cell cycle, which is associated with neuronal death. This dysregulation of the cell cycle is an emerging area of research in the

context of NDDs. Understanding the specific PTMs involved in NDDs is important to unravel their molecular mechanisms and develop potential therapeutic interventions. Targeting the enzymes responsible for these modifications or restoring normal protein homeostasis through PTM-related approaches holds the promise of mitigating the progression of these debilitating diseases.

In NDDs, histone acetylation homeostasis is severely disrupted, switching to hypoacetylation. This histone hypoacetylation is due to direct inhibition of histone deacetylases (HDACs). Interestingly, increasing histone acetylation through the inhibition of HDACs has been associated with potential neuroprotective actions. Methylation in Amyloid precursor protein (APP), Brain-derived neurotrophic factor (BDNF), and α-synuclein genes have been consistently reported in AD and PD. Several pathophysiological conditions like oxidative stress, chromatin remodelling and DNA damage response along with signalling cascades such as JNK/p38MAPK and ERK, actively participate in cell cycle re-entry using PTMs thereby inducing neuronal death [13]. A similar mechanism is also seen in tumor cells; however, its effects are different in both cases. A tumor cell entering the cell cycle survives and continues to divide due to the presence of oncogenes [14]. However, in the cell cycle re-entry of a neuron, it cannot proceed to the subsequent G0 quiescent state or revert to an existing G0 state. When it comes to the influence on other cells, the impact of ubiquitination on cell cycle regulators provides a clear overview that includes many metabolites that might be used as potential targets as well as approaches for suppressing the cell cycle to treat neurodegeneration ailments. Understanding the ubiquitination involved in NDDs is important to unravel their molecular mechanisms and develop potential therapeutic interventions. Targeting the enzymes responsible for these modifications or restoring normal protein homeostasis through UPS related approaches holds the promise of mitigating the progression of these debilitating diseases.

2.2 Implication of Cyclins, CDKs and Ubiquitination in regulation of cell cycle homeostasis

2.2.1 Cyclins, CDKs, and CKIs key regulators in cell cycle

The cell cycle, a fundamental process governing cellular reproduction, orchestrates a delicate interaction between the phases of growth, DNA replication and division. This intricate interaction, involving interplay among Cyclins, CDK and CDK inhibitors (CKIs), ensures the precise progression through distinct stages. Understanding the regulatory mechanisms of the cell cycle is crucial for maintaining cellular integrity and preventing aberrant proliferation.

The cell cycle, a ubiquitously controlled process, is a crucial feature of life that determines the reproductive potential of the cells [15]. The cell cycle can simply be conceptualized as having two phases- Interphase and Mitosis (M) phase [16]. During the interphase, the cell accumulates the enzymes and proteins required for DNA replication, while in M phase the cell carries out an equal distribution of genetic and cytoplasmic components. Some non-dividing cells remain in G0 phase (quiescent stage). Rendering previous studies, the regulation of the cell cycle is closely controlled by a complex involving Cyclins, CDKs, and CKIs [17], [18], [19]. CDKs have a catalytic core (serine/threonine-specific) and collaborate with Cyclin-like regulatory subunits that regulates kinase activity and substrate specificity [18]. CDKs govern cell division by creating a heterodimer complex with the regulatory subunit Cyclin in response to stimuli. Cyclins are regulatory subunit, belonging to the family of proteins that binds to CDKs and governing its activity by forming complexes that regulate the progression of the cell cycle [20], [21]. The binding of cyclins activates CDKs, allowing them to phosphorylate target proteins and drive the cell cycle forward [22]. The response to stimuli that influence cyclin-CDK complex formation and activation includes various signals related to the cell's environment and the cell cycle itself [23]. The growth factors such as nerve growth factor, epidermal growth factor, and platelet-derived growth factor, can act as stimuli in the synthesis of specific cyclins, leading to the activation of CDKs and progression through the cell cycle [23]. CDK activity can be influenced by the size

of the cell. Cells often check their size before progressing through the cell cycle, and cyclins play a role in integrating signals related to cell size [24]. Signals indicating DNA damage can lead to changes in cyclin-CDK activity. In response to DNA damage, checkpoint mechanisms can inhibit CDK activity, temporarily halting the cell cycle to allow for DNA repair [25]. The availability of nutrients and the cell's metabolic state can also influence cyclin expression and CDK activity, ensuring that cells only divide under favorable conditions.

Human cells have around 29 Cyclins and 20 CDKs [26] out of which CDKs 1-7 are directly involved in cell division and cell cycle transitions, whereas, CDKs 7–11 are involved in gene transcription. The expression of Cyclins oscillates cyclically throughout the cell cycle, [27] while the CDKs level remains uniform throughout the cell cycle, but their function varies with the concentration of Cyclins. D-type Cyclins (D1-3) are produced by the cell in response to mitogens and are associated with CDK4/6. Once this complex is engaged, phosphorylation of retinoblastoma protein (pRb) is triggered, followed by Cyclin E-CDK2 complex initiation, leading to hyperphosphorylation of pRb and controlling progression through the G1 to S Phase, thereby initiating DNA replication by activation of E2F transcription factor. The role of pRb in limiting S phase entry and cell development has been established [15]. The tumor suppressor pRb negatively controls the cell cycle and tumor growth, however, pRb proteins are functionally inactivated when they are phosphorylated. Cyclin D, E, and their kinase partners are important for G1 to S phase transition. In the late G2 phase, Cyclin A/CDK1 complex initiates mitosis. Finally, B-type Cyclins activate CDK1, causing chromosomal condensation and mitotic entry once the nuclear lamina is broken [15]. Cyclin B must be disintegrated to complete mitosis and subsequently initiate the replication; otherwise, the cell will go into quiescence (G0). WEE kinases are also playing crucial role in cell cycle regulation by inhibiting CDK1 by phosphorylating at residues threonine 14 and tyrosine 15 and preventing its binding with cyclin B [28]. When cell is ready for mitosis, cdc25 phosphatase inhibits the activity of WEE kinases by removing phosphate group Once the cell is ready to proceed into mitosis, the phosphatase and all transition from G2 to M phase [29]. Finally, for the successful formation of

daughter cells, checkpoints must tightly coordinate the sequential activity of CDK/Cyclin complexes so that it can move to the next phase [30]. Each CDK's activity is also influenced by the expression of specific CKIs, placed into two classes: INK4 and CIP/KIP. The INK4 proteins i.e., p15, p16, p18, and p19 bind to monomeric CDK4 and 6 proteins and inhibit them [31]. CIP/KIP proteins (including p21, p27, and p57) result in inactive trimeric complexes [Cyclin A-CDK2, Cyclin B-CDK1, Cyclin D-CDK4/6, and Cyclin E-CDK2] and blocks CDK activity, with significant impact on cell cycle progression [18], [32]. DNA damage and transforming growth factors activate these inhibitors involving p53 cascade, INK4 proteins regulate the cell cycle progression by inhibition of pRb phosphorylation and p14 stimulates the stabilization of mdm2 which is an E3 ligase involved in the ubiquitination of p53. SKP1/Cullin 1/F-box (SCF) and (Anaphase promoting complex) APC complex are two important E3 ligase groups associated with the regulation of the cell cycle involving the process of ubiquitination. Role of various Cyclins, CDKs, CKIs and the UPS in NDDs has been demonstrated in **Fig 2.1**. Impairment of these E3 ligases has resulted in various NDDs.

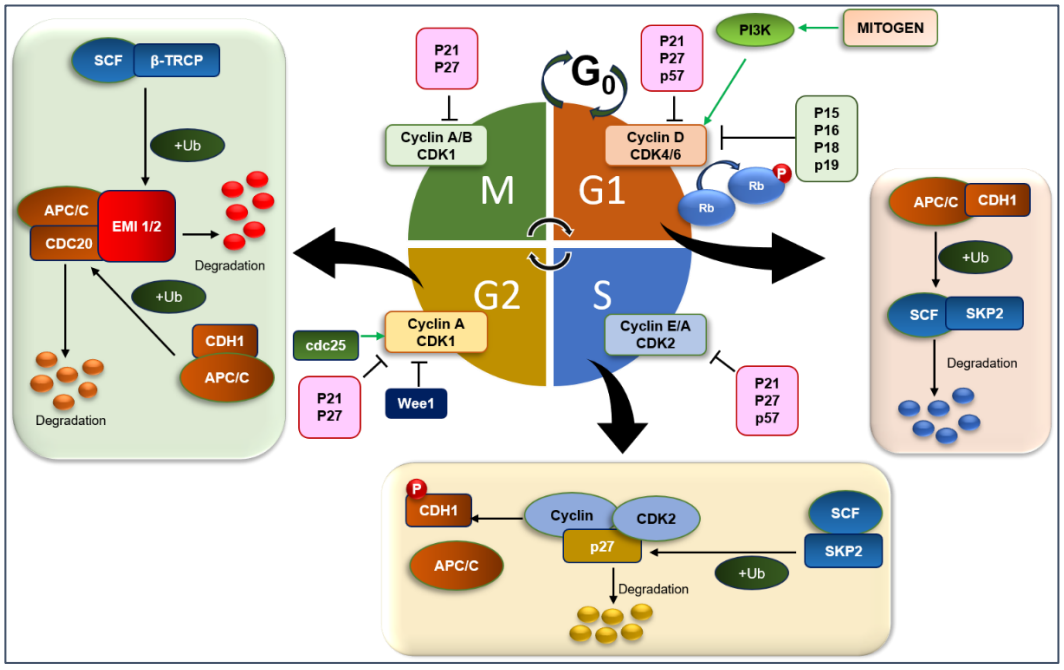

Fig 2.1. Role of Cyclins, CDKs, CKIs and UPS in NDDs. Neuronal cells move through G1, S, G2, and mitotic stages of cell cycle. Under pathological conditions, a post-mitotic neuron in G0 phase may re-enter the cell cycle. The cell then goes through the interphase but is stopped at the end of G2 phase. Tetraploid cells may endure apoptosis rather than enter the M phase. Wee1 is a protein kinase that is involved in the inactivation of CDK1/ Cyclin B and CDK1/Cyclin A, resulting in cell cycle arrest at G2 phase that is degraded by SCF1β-TrCP which also inhibits cdc25A and Emi. Phosphorylation by Wee1 inhibits CDKs, whereas dephosphorylation of CDKs by Cdc25 phosphatases activates them. Cdh1 downregulation by SCF-Cyclin F promotes premature S-phase entry. CDK inhibitors (i.e., p21, p27, and p53) block cell cycle progression whereas downregulation of these CDK inhibitors by SCF-Skp2 promotes cell cycle progression. SCF-Skp2 also suppresses the transcription factor E2F and blocks cell cycle progression.

It is well established that the primary function of CDKs is orchestrating cell cycle progression. The association of CDKs with cyclins forms complexes that drive the orderly transition of cells through distinct phases of the cell cycle [33]. This regulation ensures accurate and controlled cell division, a process vital for the maintenance of cellular integrity and development. The association between CDKs and apoptosis becomes particularly noteworthy when considering the dual roles played by CKIs such as p21 and p27 [34]. These CKIs, known for their role in regulating the cell cycle, also participate in apoptosis [35]. Induction of CKIs often in response to cellular stress or DNA damage can result in CDK inhibition, leading to cell cycle arrest. This temporary halt in the cell cycle provides the cell an opportunity to repair damage, highlighting the intricate interplay between CDKs, CKIs, and the maintenance of genomic integrity [36]. Numerous regulatory proteins, including cyclins, CDKs, and cell cycle inhibitors, are known to influence both apoptosis and the cell cycle. For instance, certain checkpoints in the cell cycle, regulated by proteins like p53 and pRb, can determine whether a cell proceeds with division, undergoes cell cycle arrest, or enters apoptosis in response to cellular stress or DNA damage [37], [38]. The intricate interplay between apoptosis and the cell cycle is essential for eliminating damaged cells, preventing aberrant proliferation, and maintaining overall tissue health. Dysregulation of this balance

can contribute to various diseases, highlighting the significance of understanding the crossroads between apoptosis and the cell cycle.

According to recent findings, Cyclin-CDKs regulate apoptosis through the mitochondrial route, controlled by Bcl-2 family members. The Bcl-2 family is classified into three categories: (1) Bcl 2 homology 3 (BH3)-only proteins are pro-apoptotic initiators (Bad, Bid, Bik, Bim, Bmf, Noxa, Puma, Bnip3, etc.); (2) anti-apoptotic proteins (Bcl-2, Bcl-xL, Mcl-1, etc.) and (3) pro-apoptotic effectors (Bax, Bak, Bok). Pro-apoptotic initiators which are (BH3)-only proteins are important for initiating pro-apoptotic effectors mediated mitochondrial impairment. Bim transcription is triggered by the E2F and myc, c-jun, and Forkhead box O (FOXO) family transcription factors, which are sufficient to induce neuronal apoptosis. Cyclin B-CDK1 complex may trigger apoptosis in neurons by phosphorylating Bcl-xL, thereby, inhibiting ATP synthase activity and upregulating Puma and Noxa. In response to oxidative and genotoxic stress, activated CDKs move towards aberrant re-entry in the cell cycle via p53 cascade activation that results in neurodegeneration, which can be prevented by the mutations in Ataxia telangiectasia Mutated (ATM) [39]. Small molecule CKIs such as Olomoucine and Flavopiridol also prevent neuronal death where the major cause eliciting DNA-damaging agents [40]) and NGF (Nerve growth factor) withdrawal [41], [42]. G1/S blockers such as Deferoxamine and Mimosine prevent neuronal apoptosis, but DNA synthesis inhibitors such as N-acetylcysteine and aphidicolin do not. As a result, DNA synthesis is not required for neuronal apoptosis [40]. After traumatic brain injury, further CKIs, such as Roscovitine, provide neuroprotection [43]. CKIs have an anti-apoptotic effect in neurons after NGF deprivation and DNA damage, SOD1 depletion has no protective effect against apoptosis brought on by oxidative stress [40]. The anti-apoptotic activity of CKIs is restricted to differentiated postmitotic neurons because treatment with them paradoxically aggravates apoptosis in proliferation-competent cells [40].

2.2.2 Ubiquitination and their role in cell cycle

The level of Cyclin keeps oscillating during cell division due to proteolysis, which is maintained by the UPS [15] which also maintains the level of CDKs, CKIs and other factors responsible for cell cycle homoeostasis [44]. Ubiquitination, a three-step process involving a group of enzymes (E1, E2, and E3) involving covalent binding of ubiquitin which is a short 76-amino-acid polypeptide, to the lysine of protein of interest [45]. First step is an ATP dependent process in which E1 activating enzyme forms the thioester bond between the glycine at C-terminal of ubiquitin and its own active cysteine residue [46]. Further, activated ubiquitin by the E1 enzyme transferred to the cysteine residue of E2 conjugating enzyme forming a thioester bond [47]. Next step is to recruit activated ubiquitin to the target to perform this mechanism E3 ligase will act as a mediator between ubiquitin charged E2 and target, E3 enzyme transfers the charged ubiquitin directly or indirectly to the substrate at lysine residue via an isopeptide bond [48]. Attachment of a single or series of ubiquitin molecules linked to distinct lysine residues corresponds to mono ubiquitination or polyubiquitination respectively [49]. Importantly, ubiquitin includes seven lysine residues that can be repurposed to catalyze future ubiquitination by the appropriate E2/E3 pair cycles and polyubiquitin chain assembly. The K48 ubiquitin chain is involved in the degradation of substrate protein, while K63 ubiquitin chain is linked by non-proteolytic functions such as signal transduction, kinase activation, and endocytosis [50]. Reversal ubiquitination is done by deubiquitinating enzymes (DUBs); therefore, it becomes necessary to maintain equilibrium between an E3 ligase and a DUB functionality.

E3 ligases are large in numbers approximately 600 above based on their pattern of transfer of charged ubiquitin to the target, they are classified into four categories: RING finger, HECT, RBR and U-box type [51]. All these E3 enzymes have large differences in composition and low sequence homology illustrated in **Fig 2.2**.

RING finger E3 ligases are characterized by the presence of RING (really interesting new gene) domain, during ubiquitination process, there is a direct

binding between RING domain and E2 enzymes, whereas in case of **HECT E3 ligase and RBR** the transfer of charged ubiquitin to the target occurs form the E2 enzymes evading the E3- ubiquitin complex. RING E3 ligases are further classified into two classes monomeric and multi-subunit. Monomeric E3 enzymes have the domain for substrate binding, ubiquitination and for the autoubiquitination examples TRAF6, COP1 and mdm2. Multi-subunit E3 ligases have diverse class having various common features Cullin Ring Ligases (CRLs) are one of them which have an N terminal RING box protein, C terminal substrate binding region and have an adaptor protein some other examples are SCF protein complex and APC/C. HECT E3 ligases are a small family of E3 enzyme (approximately 28 in number in humans) consisting of homologous to the E6AP carboxy terminus (HECT) domain at the C terminal, which have two lobes namely N and C lobe [52]. C-lobe is the site where charged ubiquitin binds to the active cysteine site before binding to the target, whereas the N-lobe binds to E2. Based on N-terminal HECT E3 ligases are classified into three major sub families such as NEDD4 (9 members), HECT and RLD domain containing (HERC 6 members) and other HECT's 13 members [53]. Generally, C terminal of HECT domain of the Nedd4 family is characterized by the presence of WW and C2 domain, C2 domain can bind phospholipids and calcium ions at N-terminal, which is essential for targeting proteins to phospholipid membrane and ubiquitination of target. The HERC (HECT and RCC-like domain containing) subfamily is made up of HERC protein that is small and large in nature and presence of RCC- like domain used to classify them. HERC3 and HERC5 are the small HERC proteins which have fewer number of RLDs but are involved in immune response and antiviral activities. Large HERC namely HERC1 and HERC2 having multiple RLDs are implicated in many cellular processes such as cell proliferation, DNA damage response and chromatin dynamics. E6AP (UBE3A) is multidomain structure, having N-terminal with WW domain, which is crucial for the protein -protein interactions, it helps the UBE3A to identify the substrate. HECT domain is the catalytic region of the UBE3A, this domain has active cysteine residue that forms thioester bond with the ubiquitin, which is then transferred of E2 to the target protein. C- terminal interacts with substrate and other regulatory protein. UBE3A dysfunction have been extensively studied in the Angelman syndrome, recent studies have implicated its role in NDDs. CKIs namely p27 and p21

are the substrate of this E3 ligase, thereby facilitating cell proliferation through CDK4/6 activity.

RBR (Ring Between Ring) E3 ligases are a unique class of E3 ligases that combines the characteristics of both **RING** and **HECT** E3 ligases, exhibiting a hybrid mechanism of action, consisting of three conserved domains such as RING1, IN-between- RING(IBR), RING2 [54]. RING1 is responsible for recruiting ubiquitin charged E2 enzymes, IBR domain is similar to the RING2 domain but lacks a catalytic cysteine residue [55]. RING2 domain have the presence of active cysteine residue that takes part in the formation of thioester bond during the ubiquitin transfer process [56]. Parkin is one of the examples of RBR type E3 enzyme, which plays critical role in mitophagy [57]. RBR E3 ligases play a key role in cellular signaling, protein homeostasis, and disease pathogenesis, especially in NDDs [55].

A hallmark feature of **U- box E3 enzymes** is the presence of U-box domain composed of approximately 70 residues, and resembles with RING type E3 enzymes with the only difference of absence of Zn binding residues [56]. U- box domain is pivotal for mediating interaction with ubiquitin charged E2 enzymes, where E3 enzymes Ubiquitin transfers directly from E2 enzymes to the target [56]
.

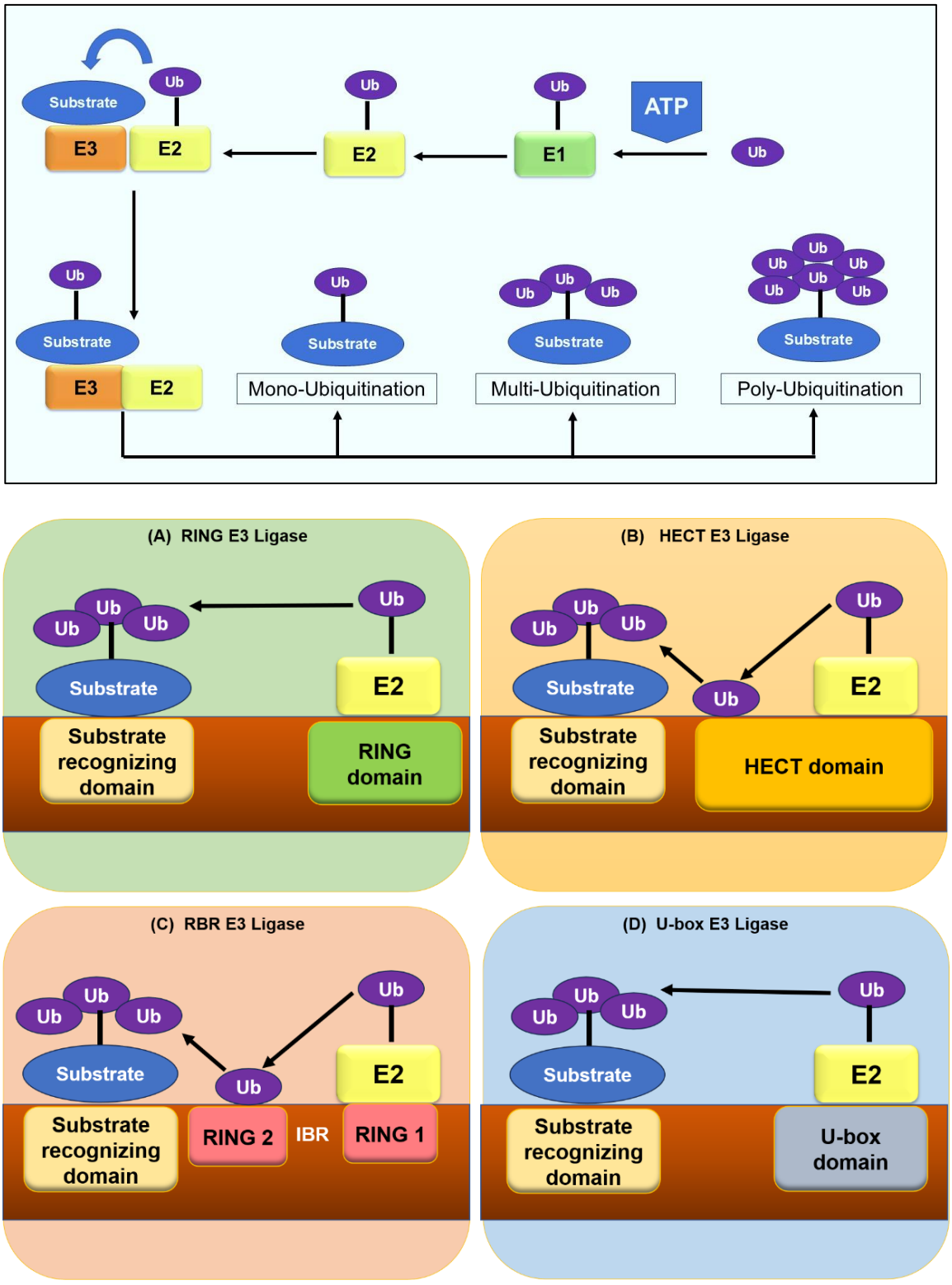

Fig 2.2. Ubiquitination mechanism and types of E3 Ligases.

2.2.3 E3 ligases as a controller of cellular progression

The key E3 ligases involved in the cell cycle homeostasis are APC/C, and SCF complex [58]. APC/C a large multi-subunit ubiquitin (Ub)-protein ligase, are responsible for controlling Cyclins in mammalian cells [59]. APC/C is significant for the eukaryotic cell division cycle controlled by targeting out and destroying critical cell-cycle regulators namely mitotic cyclin and securin [60]. APC/C is crucial for mitotic exit and prevention of untimely entry into S phase [61], [62], [63], [64]. Activators such as cdc20 in metaphase and cdh1 in telophase, regulate APC/C. The cell cycle proteins are deteriorated by APC^{Cdc20} and APC^{Cdh1}. The prometaphase–metaphase transition is the first site of APC^{Cdc20} activation where it downregulates Nek2 and Cyclin A. APC^{Cdc20} causes further breakdown of Cyclin B, Xkid, and securing it at metaphase whereas, the kinesins Kip1, and Cin8 at anaphase. From the late anaphase and till G1 phase, these proteins are regulated by APC^{Cdh1}. The deterioration of Tome-1, Prc1, Plk1, Aurora A, and Cdc20 at mitotic exit is induced by APC^{Cdh1} followed by the proteolysis of Cdc6, Orc1, and Geminin in the early G1 phase. The SCF complex, a group of E3 ligase, transfers active ubiquitin to target protein substrates in a precise manner. S-phase kinase-associated protein 1 (SKP1) is a necessary component of the SCF complex [65]. The ligase's final component is a RING-domain-containing protein from the Roc1/Rbx1 family [66]. The F-box protein (FBP) component of SCF is the one that binds to substrates specifically. As a result, it is the SCF's primary specificity determinant and FBP function has been linked to a range of cellular and developmental events. Ubiquitin-mediated proteolytic degradation is post-translational, ubiquitin ligases like SCF are well adapted to regulate multi-component molecular machines like DNA synthesis and mitotic apparatus as well as transition sites like cell-cycle checkpoints [66]. SKP2 degrades negative regulators of the cell cycle such as p27, p21, and p57, facilitating cell cycle advancement throughout the S and G2 phases. SKP2 is often overexpressed in NDDs FBXW7 promotes the breakdown of positive cell cycle regulators such as MYC, JUN, cyclin E, and Notch. β-TRCP is a flexible F-box protein that

recognizes multiple cell cycle regulators, including EMI1/2, WEE1A, and CDC25A/B, as well as its canonical substrates, β-catenin and IκB.

2.2.4 UBE3A as a therapeutics target

E6AP, also known as UBE3A, was initially identified as a ubiquitin-protein ligase that degrades the tumour suppressor p53 [67]. This finding was especially relevant in the context of human papillomavirus type 16 (HPV16) infections, which are linked to malignant tumours and cervical cancer [68]. HPV16 encodes the oncoprotein E6, which causes the degradation of p53 in cells with infection [69]. A 100 kDa protein known as E6AP mediates the degradation process, which is essential for the ubiquitination and subsequent degradation of p53 in cancer cell [70]. E6AP acts through the HECT domain, a region common with multiple E3 ligases and necessary for ubiquitin ligase action. The binding site in E6 is found at the N-terminal of E6AP (amino acids 391-408), with final 84 amino acids of E6AP causing p53 degradation [70]. The catalytic site of E6AP is located at Cys833, and mutations in this cysteine residue makes the ligase inactive [67]. Notably, E6AP may self-ubiquitinate in HPV16-positive cells, resulting in its own deterioration [68]. In addition to its function in viral oncogenesis, E6AP regulates cell proliferation by targeting the cell cycle inhibitor p27 for destruction [71]. The cell cycle is regulated by p27 by inhibiting CDK, which halts the transition from the G1 to the S phase. E6AP increases p27 ubiquitination, which marks it for destruction by the proteasome [72]. This degradation of p27 reduces its inhibitory impact on cyclin-CDK complexes, enabling the cell cycle to continue and boosting cell proliferation [73]. The crystal structure of E6AP revealed that the HECT domain is made up of two loosely packed lobes joined by a three-residue hinge [74]. The COOH-terminal lobe includes the catalytic cysteine required for ubiquitination, and mutations in this area have been associated to Angelman syndrome (AS) and other NDDs [75]. Inhibition of UBE3A may affect its ubiquitination activity decrease the degradation of critical substrates, including p27.

As illustrated in **Fig 2.3.**, E3 Ligases such as Mdm2, CHIP, Nedd4, TRAF6, FbxW7, and Fbxo2 play crucial roles in the regulation of post-mitotic neurons. Mdm2 ubiquitinates p53 at K120, thereby reducing p53 levels and consequently inhibiting p53-mediated cell apoptosis [76]**.** Mdm2 also promotes parkin-dependent mitophagy which is reduced by its knockdown. Thus, Mdm2 may enhance Parkin's neuroprotective activity [77]. FBXW7 induces degradation of PS1 and other positive regulators of cell cycle i.e., cyclin E, myc, jun, and notch. Fbxo5 independently inhibits the APC/C activity in SCF by interacting with Cdc20 and Cdh1 which recruits APC/C substrates. Thus, Fbxo5 upregulates the cyclin B level. Similarly, Nedd4 and TRAF6 regulates PI3K/Akt pathway that leads to upregulation of cyclin E. Regulation of CKI (i.e., p21, p27, Cyclin E, Cdc25a and Wee1) by SCF (fbxo2 & fbxw7) and its other inter regulatory partner APC/C ubiquitin ligase can be simplified in a view of SCF ligases that control the cell cycle by degrading CDK subunits, and their regulators as shown in **Table 2.1.** Therefore, E3 ligase may be a crucial therapeutic target in NDDs.

Table 2.1. E3 Ligases involved in Cell Cycle regulation

E3 ligases	Binding partner	Motif	substrates	Significance of E3 ligases	References
UBE3A	Ubc4/5	LxxLL	p21, p27, p57	Ubiquitination of p53, p21, and p27	[78]
APC/C	CDC20	D box	CYCLIN A	Mitotic progression	[79], [80]
		-	CYCLIN B	activation of CDK1/CDK2 and transition at level of G1/S, G2/M	[80]
		(RxxLxxxxN)	Securin	Promotes chromosome Segregation	[81]
		D box and (KENxxxN)	FOXM1	inhibit cell cycle progression	[82]
		A box motif	AURORA	inhibits mitotic Progression indirectly linked to APC/C	[83]

		D box	SKP2	regulates G1/S transition by inhibiting the degradation of p21, p27	[84], [85]
		KEN box	CDC20	Activator of APC/C	[86]
		KEN box	PLK1	Mitotic progression	[87]
SCF	SKP2	NA	p21, p27, p57	Cell proliferation	[88]
	βTrCP	DpSGXX(X)pS	p130		
			NFκB	Cell cycle inhibition	[89]
			Emi1	Activation of APC/C complex in M Phase	[90]
			WEE	Activation of CDK1(G1 Phase)	[91]
			lκB	activation of NFκB	[89]
			β-catenin	Inhibition of cell cycle	[92]
			CDC25A	inhibit cell cycle progression	[93]
			FOXOM1	inhibit cell cycle progression	[94]
	FBXW7	S/TPPx S/T	Cyclin E	positive regulation of cell cycle	[95]
			MYC		
			JUN		
			Notch		

The intertwining roles of CDKs, Cyclins, and CKIs in the cell cycle and apoptosis highlight the intricate sustaining cellular homeostasis. This is orchestrated with precision, ensures proper cell division, guards against aberrant proliferation, and responds appropriately to cellular stress. Dysregulation of this delicate balance can contribute to various diseases, emphasizing the importance of deciphering the intricate connections between the cell cycle and apoptosis.

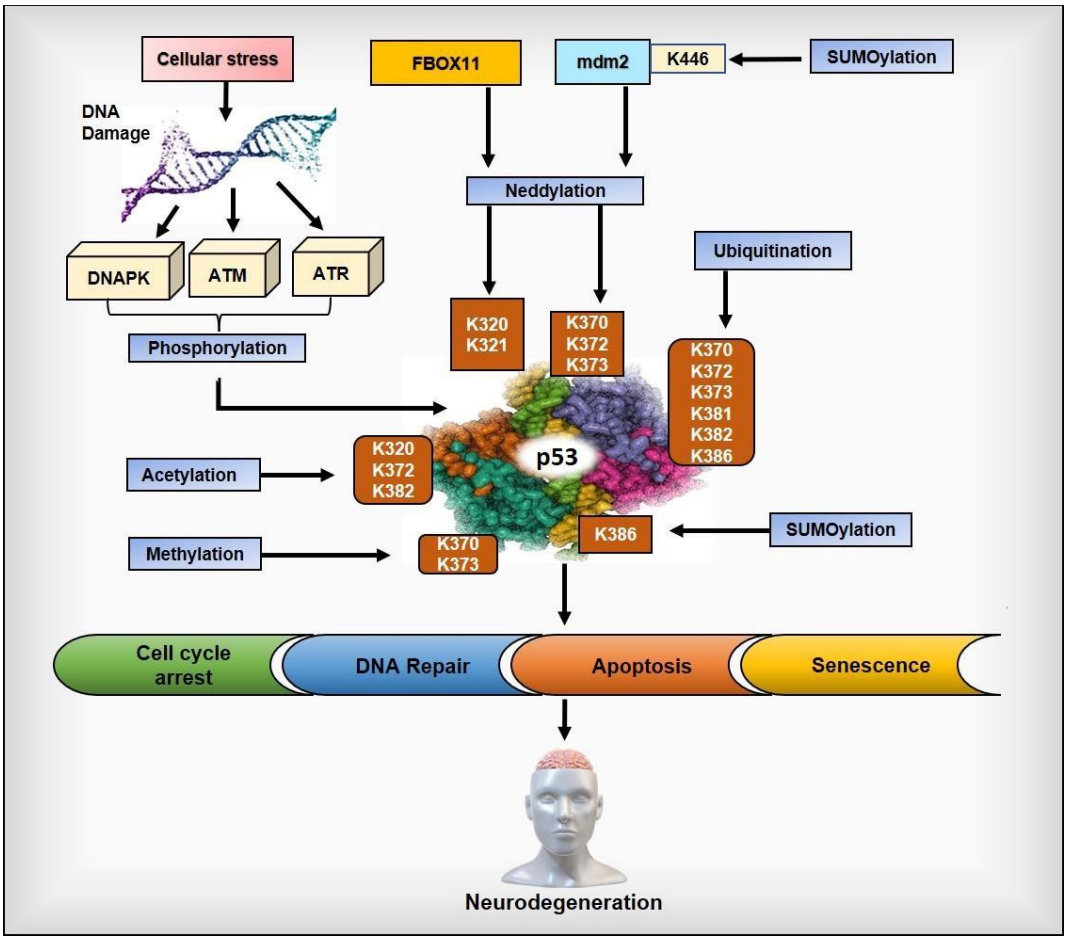

Fig 2.3. Lysine sites involved in post-translational modification of p53 in NDDs - p53 level rises due to cellular stress which increases its activity and is responsible for various mechanisms such as DNA repair, apoptosis, cell cycle arrest, and senescence, which triggers neurodegeneration. Several PTM-modified lysine sites regulate p53 transcriptional activity in different ways like acetylation at K320, K370, K372, and K382 upregulates its activity, and methylation of p53 at diMeK370 and K372 also works in a similar way whereas methylation at K370, K373, and K382 suppresses p53 action. Methylated p53 can act both as a positive as well as negative regulator of acetylated p53. Mdm2 ubiquitinates p53 at K370, K372, K373, K381, K382, K386 and Neddylation ubiquitinates p53 at K370, K372, and K371 by FBOX11 and SUMOylation at K446 site of mdm2 stimulates neddylation of p53 at K320, K321 leading to ubiquitination. SUMOylation at the K386 position of p53 suppresses its function.

2.3 Revival of cell cycle in neurons

Neurons are usually post-mitotic and seized in G0 stage throughout their life span. However, growing evidence implies that the neurons actively participate in aberrant cell-cycle re-entry due to various growth factors, which results to neuronal death

[96]. A possible explanation for this situation may be that the neurons constantly face death unless they prevent cell cycle reactivation. One such cell cycle marker is the pRb protein, which regulates the cell cycle in adult neurons (Herrup & Yang, 2007). Further, the ATM induces the DNA damage response and keeps the neurons in a quiescent stage [98]. Similarly, CDK5 prevents the interaction of transcription factors with its activation subunit. CDK5 is transported to the cytoplasm in response to the encountered neuronal stress. Therefore, ATM and CDK5 degradation also contribute to the pathogenesis of NDDs [99], [100].

However, further evidence shows the subsistence of distinct cell cycle biomarkers in mature neurons which is linked to their role in neurogenesis and synaptic plasticity. Cell cycle stimulation is also considered necessary for the repair of double-stranded breaks associated with high ROS in chronic inflammation. Neurons remain in G1 phase as manifested by an increased expression of cell cycle biomarkers namely BrdU and Cyclin E, ultimately leading to cell death, for example, pRb in association with E2F3 plays a key role in neuronal migration [101]. CDC20-mediated marker drives dendritic trimming and withdrawal. Furthermore, CDK5 phosphorylation leads to disruption of Cofilin-actin complex, p27 a microtubule-binding protein thereby promoting neuronal migration [102]. Similarly, in post-mitotic neurons, p57 mediates cell cycle withdrawal, thus facilitating differentiation and maturation. It has been observed that Cdh1-APC regulates axonal growth and patterning through an additional substrate other than SnoN which is a transcriptional factor. As a result, the cell cycle is redesigned to meet the needs of post-mitotic cells. However, due to several external factors such as oxidative stress, hypoxia, and DNA damage, neuron apoptosis is seen due to its cell cycle re-entry. The content of DNA at-risk in neurons, as well as the resulting cell death, has been associated to the progression of NDDs. Further, the tetraploid neurons had considerable levels of Cyclin B1 which showed cell cycle re-entry. Tetraploid neurons refer to neurons that have duplicated their DNA, however, are not able to go through a cell division. Instead of progressing via cell cycle, these neurons remain stuck in S and M phases, and culminate in an abortive cell cycle. [103].

The intriguing phenomena of cell cycle biomarkers present in post-mitotic neurons, their ability to re-enter the cell cycle under specific conditions, and the resulting consequences provoke us to reconsider our conventional understanding of neurobiology. In neurons, cell cycle-related processes serve functional purposes, yet they may also give rise to neurodegeneration in specific situations. The intricate and dynamic nature of neuroscience and its relevance to neurodegenerative diseases are highlighted by the complex interplay between the cell cycle and neurons.

2.4. Factors provoking cell cycle re-entry in neurons

Few types of neurons such as cortical and sympathetic neurons, upregulate the expression of biomarkers of the cell cycle and attempt to revive the cell division when exposed to DNA damage, oxidative stress, neurotrophic factor deprivation, activity withdrawal, and excitotoxicity [104]. Further, axonal guidance and brain wiring signalling pathways are prone to be hampered by the proteolytic imbalance of cell cycle regulators [105].

2.4.1. Neurotrophic factor deprivation

Neurotrophins such as neuron growth factors, neurotrophic factors derived from the brain, and neurotrophin-3 play important roles in differentiation, regeneration, and plasticity mechanisms [106], [107]. These BDNFs protect the neurons from oxidative stress and excitotoxicity by binding with its receptor which results in phosphorylation of Tropomyosin-related kinase B (TrkB), triggering three essential intracellular signalling cascades in brain cells i.e., Phospholipase C, PI3K/AKT, and MAPK [107]. However, there is evidence of a direct impediment of Aβ protein in the proteolytic conversion of pro-BDNF to BDNF, thus lowering its levels [108]. As per a study on differentiating chick retinal neurons (DCRNs), TrkB and CDK1 co-express in vivo and BDNF requires the suppression of CDK1 through phosphorylation at Tyr15 by TrkB to maintain the tetraploid state of neurons [109]. The stimulation of the p75 neurotrophin receptor by NGF results in an aberrant cell cycle. However, as per the same study, binding of NGF to the p75 neurotrophin

receptor does not result in the translocation of p75 to the nucleus. Instead, this association causes nuclear activation of p38MAPK and Tyr15 phosphorylation of E2F4, which can mimic the signal that triggers DCRN cell cycle re-entry and apoptosis [110]. According to recent research, neurotrophin deficiency is connected to NDDs pathophysiology mediated by abnormal cell cycle re-entry.

2.4.2. Double-stranded DNA breaks (DSBs)

DSBs in G0 phase cells are irreparable and maintain an active p53 pathway [111]. Increased DSBs stimulate cell cycle reactivation, which is a key characteristic of NDDs. These neurons that have been driven into the cell cycle have a tendency for apoptosis [112] DSB is checked by MRE11/RAD50/NBS1 complex which also repairs any potential DNA damage by activating the ATM, PI3K-like kinase family containing ataxia -telangiectasia and Rad-3 related (ATR) and DNA-dependent protein kinase (DNA-PKcs) [111].

In DSB adjacent chromatin, histone H2AX is phosphorylated by ATM on Ser139 (γH2AX), which involves MDCI (i.e., DNA damage checkpoint protein 1 mediator) as an identifier for this phosphorylation. The MRN complexes (through an interaction with NBS1) are then engaged by γH2AX-bound MDC1, thereby initiating a positive ATM feedback loop leading to augmentation of the γH2AX chromatin domain [111]. DSB response and diffusible signalling trigger DNA-damage checkpoints (DDR) which can inhibit cell cycle continuation allowing DNA repair. TP53 orthologs activated DNA damage induce apoptosis through inhibition of p21 inhibitor. Cyclin D1 regulates DNA damage repair and inactivation of Cyclin D1 leads to the inactivation of DNA-PKcs which is responsible for the impairment of DNA damage response by NHEJ (non-homologous end joining). The DNA damage leads to phosphorylation of p53 which stimulates the CBP/p300 interaction with p53 and increases its stability through the mechanism of acetylation. SET8 methyltransferase inhibits the p53 during normal processes but in case of DNA damage, SET8 is downregulated and the activity of p53 is restored [113]. SUMOylation at K386 position of p53 increases the chances

of apoptosis by activating the p53-Bax pathway [114]. Mdm2 is well known for the ubiquitination of p53. Further, as per a study, it is also reported that neddylation of p53 at K320 and K321 may affect its nuclear localization, thus suggesting that K320 Neddylation leads to the suppression of p53 [115]. Maintaining genomic integrity and preventing the spread of damaged DNA relies on a delicate equilibrium between DNA repair, cell cycle arrest, and apoptosis induction. Understanding the pathogenesis of diseases, such as NDDs, becomes even more relevant when considering these processes.

2.4.3. Implication of oxidative stress in cell cycle progression

ROS (Reactive oxygen species) is maintained in normal cells by tight homeostasis controlled by various biological antioxidants like glutathione, α-tocopherol, carotenoids, and ascorbic acid reacting with oxidants. NADPH oxidase and Mitochondria are major sources of O^{2-}, OH^{-} and H_2O_2 (ROS) formation. O^{2-} can be converted into H_2O_2 by Superoxide dismutase (SOD1 or SOD2), which can further be converted into water by glutathione peroxidase (GPX), peroxiredoxin (PRX) and catalase (CAT) in mitochondria and cytosol [116]. Antioxidants that are expressed by the cells keep ROS (produced during normal cellular function and homeostasis) stable [116]. Reduced ROS is essential for the maintenance of normal cellular proliferation. [105], [116], [117].

Moderate to high ROS acts as an indicator for enhanced cellular proliferation, tumor initiation, survival, metastasis, and angiogenesis. However, extremely elevated ROS is hazardous leading to unrepairable DNA damage, apoptosis, and cell cycle arrest [116]. Mitochondrial dysfunction [105] in turn affects Ca^{2+} homeostasis, induces apoptotic pathway activation, and affects ATP production. This negative impact on ATP synthesis also triggers the AMPK pathway, which prevents cells from transitioning from G1 to S phase [105], [118]. An experimental study revealed that there is a close link in morpho dynamic change of mitochondria and cell cycle arrest. In human mitochondrial fission 1 protein (hFis1)-knockdown cells shows elongated mitochondria and upregulated cell cycle regulators of G2/M phase, including Cyclin A, Cyclin B1, CDK1, polo-like kinase1 (Plk1), aurora

kinase A and Mad2. This study also gives evidence of the upregulation of cell cycle regulators' double knockdown of hFis1 and Opa1[119] In a genetic model of Harlequin (Hq) mutant mice study, a connecting link between cell cycle re-entry and oxidative stress has been revealed, resulting in neurodegeneration in the aging CNS. Mutated cerebellar granule cells are prone to apoptosis which can be controlled by apoptosis-inducing factor (AIF) expression [120], [121]. In another study involving rat cortical neuron exposed to H_2O_2-mediated oxidative stress, it is observed that DNA double-strand break and cell cycle re-entry is substantiated by elevating the level of proliferation markers such as pRb and Cyclin D. H_2O_2 treatment redirects the cells to apoptosis at S phase which can be inhibited by siRNAs of CDK4/6 and CDK2 [105], [122]. Yet another study revealed that camptothecin (CPT) topoisomerase I inhibitor elicits cell cycle-related death in cortical neurons. CPT treatment induces cell cycle regulator (Cyclin D1, CDK4, E2F1) and initiates proliferation leading to acute neuronal apoptosis [123]. Increased ROS is responsible for mitochondrial disruption which has been observed in NDDs.

Understanding these complex interactions provides crucial insights into potential therapeutic targets for diseases characterized by disrupted cell cycle regulation, oxidative stress, and impaired DNA repair in neurons. The delicate equilibrium maintained by neurons in response to stressors underscores the intricate molecular pathways crucial for their survival and function.

2.5 Altered signaling due to cell cycle re-entry

The deviation in signalling cascade is one among the numerous shreds of evidence indicating the involvement of various risk factors connected with abnormal cell cycle re-entry. There are several signalling pathways like β-catenin, Notch, and GSK3β/AKT implicated in cell cycle re-entry. Further, β-catenin and Cyclin D1 are enhanced in cortical neurons of M146V mutant mice (homozygous) having familial AD (FAD) leading to cell cycle-associated apoptosis [124]. Jiang et al., in a study published in 2019, found that prolonged fluoride treatment causes neuronal death and impairs neurogenesis by reducing β-catenin pathway activity. It was

summarized in the same study that the expression of c-myc and Cyclin D1 was reduced by Fluoride [125]. In another study by Singh et al, it has been revealed that the knockdown of axin inhibition protein-2 upregulates the β-catenin pathway in SNpc PD rats and reduces ROS, mitochondrial dysfunction, and apoptosis [126]. CDK5 interacts with various targets such as Cyclin I, peroxiredoxin-2 (Prx2), ATM, Ape1 and p53 by the process of phosphorylation regulate apoptosis and DNA repair mechanism [127]. CDK5 interacts with various signalling pathways such as c-JNK, $P^{38/}$MAPK, and GSK3β/AKT and phosphorylates MEF2D which is a good substrate for caspases-dependent degradation and neuron apoptosis [127]. CDK5-dependent phosphorylation of Ape1 downregulates the DNA damage repair mechanism. Phospho-Ape1 is present in mid-brain dopamine neuron nuclei in patients with PD or AD [127], [128]. Further, in a study by Das et al, it has been shown that curcumin downregulates the p38/MAPK and GSK3β/AKT signalling cascade and Tau phosphorylation [129].

2.6 Cell cycle re-entry and NDDs

The question, of whether cell cycle markers re-expression is a normal part of the cell cycle mechanism or a result of an abnormal event has been the subject of numerous studies. The aberrant cell division in the neurons has been associated with the re-expression of a cell cycle marker and cell division in dormant neurons is fatal and has been associated with NDDs as shown in **Fig 2.4**.

2.6.1. Alzheimer's Disease and aberrant cell cycle

AD is pervaded by neurodegeneration, dementia, neurofibrillary tangles, and the emergence of Aβ plaques composed of hyperphosphorylated tau [130]. Several reputable studies point to the etiology of AD having a close association with cell division. In addition, cell cycle abnormalities are attributed to a surge in pathological Aβ build-up and tau hyperphosphorylation. Cdc7, a kinase-active cell division cycle protein, is vital for the G1/S transition in the cell cycle by activating the pre-replication complex. At least two serine-threonine kinases, CDK and Cdc7

are involved in this process [130]. In several studies, in AD and aged-matched control brain, phosphorylation of Ser40/41 Mcm2 has been compared and the results further strengthen the notion of neuron's abortive entry in the cell cycle in AD [96]. In the case of DNA damage, Chk1 and Chk2 are activated by ATR and ATM playing a major role in various processes such as metabolic stress, oogenesis, neuronal survival, and tissue growth [131]. In AD patient's brains and other animal models, upregulation of DNA damage response has been observed [131], [132]. In many investigations using the transgenic drosophila model, it has been found that neurodegeneration was not generated when the mutation occurs in Ser262Ala, indicating that the Ser262 site is important for pathological tau-Aβ42 interaction. At this position, tau is phosphorylated by ChK2, and the tau toxicity is upregulated in transgenic drosophila. This study provides significant results which indicates that the Ser262 Ala phosphorylation site is important for Aβ42-induced tau toxicity *in vivo*. DNA repair mechanism can reduce Aβ42 accumulation but it may also upregulate the phosphorylation of tau and AD pathogenesis [132].

APP-BP1, an important regulator of Nedd8 conjugation pathway, was identified through its interaction with the intracellular carboxyl terminus of APP [133] Increased APP-BP1 levels drive S phase-mediated DNA replication in neurons accompanied by expression of Cyclin B1 and cdc2 [134]. According to another study, the failure of APP-mediated pathways may be one reason for cell cycle protein reactivation in AD brain. In the case of PS2 (N141I) mutation potentiates the G1 phase of the cell cycle [135]. Results from a study on mice with the PS1 knock-in mutation M146V ($PS1KI^{M146V}$) show aberrant cell cycle reactivation in a β-catenin-dependent manner, triggering an apoptotic response [136]. Quercetin treatment, an interrupter of the β-catenin pathway, reduces Cyclin D1 concentration leading to cell survival [136], [137]. Therefore, a higher concentration of β-catenin seen in the PS1 FAD brain upregulates Cyclin D1 transcription thereby accelerating cell cycle entry [136].

The upregulation of cell cycle markers such as BrdU, PCNA, and Cyclin D1 occurring during neurotoxic stress through signaling cascades are generally associated with neuronal differentiation and survival [138], [139]. Therefore,

Cyclin D1 levels are upregulated resulting in cell cycle re-entry [140]. Various factors like CKIs, are enhanced during neuronal differentiation. The augmented Cyclin E activity correlated to the presence of neuritic plaques in the neocortex. CDK5 has an important function in cell cycle control in AD-affected neurons. While deletion of nuclear CDK5 causes cell cycle re-entry, the crucial role of nuclear CDK5 in maintaining neurons in the postmitotic state has also been demonstrated.

2.6.2. Cell cycle dysregulation in Parkinson's Disease

The cell cycle-related process and molecular pathways upregulations have also been reported in PD. Numerous studies have shown a surge in pRb /E2F pathway in substantia nigra Per compacta (SNc), co-localized with Lewy bodies and primarily composed of aggregated alpha-synuclein, in PD patients' brains [141]. PARK2, a parkin protein, has demonstrated a neuroprotective role against neuronal cell death by suppression of Cyclin E levels [142]. Since, neurons are mitotically incompetent, cell cycle activation results in cell death and neurotoxicity can result in aberrant surge in Cyclin E, which is controlled by ubiquitination and proteolysis mediated by PARK2. However, inactivation of these processes leads to an escalation in Cyclin E levels [142].

In the nervous system, CDK5 is activated by p35 and p39 in numerous biological functions at cellular levels [140], [143]. In a study, it has been demonstrated that CDK5 knockout increased caspase-3 activity in the brain cortex [143]. In nigral neurons from the post-mortem brain of patients, it has been observed that CDK5 activation reduces Prx2 activity by its phosphorylation, and decreases the capacity to eliminate ROS [144]. CDK5 causes the phosphorylation of PARK2 which gets inactivated, thereby upregulating the level of Cyclin E leading to neuronal cell death [145]. The significance of cell cycle initiation in humans and experimental PD caused by DNA damage is supported by all these studies [141]. Thus, all these experimental studies indicate the effect of abortive cell cycle entry in PD pathogenesis.

2.6.3. Evidence of cell cycle re-entry in Huntington's Disease

HD is interpreted by the mutant huntingtin (mHTT) gene in neurons [146]. It has been discovered that the ubiquitin-proteasome system is hindered by the aggregated huntingtin proteins, resulting in the accumulation of additional misfolded proteins and ER stress [147], [148]. ER stress is also generated in various other NDDs. ATF6α is also vital for the survival of cells that are arrested in the G0 phase of the cell division [149]. Ras-homologue enriched in the brain (Rheb), a small GTPase, mediates this effect suggesting disruption of the ATF6/Rheb pathway in Huntington's disease. These changes result in the abnormal rise of cell cycle re-entry markers leading to apoptosis. Also, NF-ƙB has been associated with neuronal differentiation by the upregulation of Cyclin D [150]. The activity of transcription factors such as c-myc and n-myc in hippocampal neurons leads to uncontrolled cell division [151]. It is also important to set up a link between re-entry of the cell cycle and neuroprotective mechanisms in HD. Recent research has demonstrated that mature neurons interacting with Htt undergo aberrant cell-cycle re-entry while healthy neuron, with enhanced expression of wild-type Htt, are prevented from doing so [149], [152], [153]. A study concluded that cell cycle re-initiation is vital for reversing the harmful effects of DNA damage caused by ROS in mature neurons [154]. However, the DNA repair mechanism becomes inactive ultimately resulting in cell death [155]. Therefore, the understanding of mHtt-related cell cycle events in neurons as well as the mechanism underlying re-entry of cell cycle are important for supplementing the therapeutics involved in HD and enhancing our knowledge in understanding the NDDs.

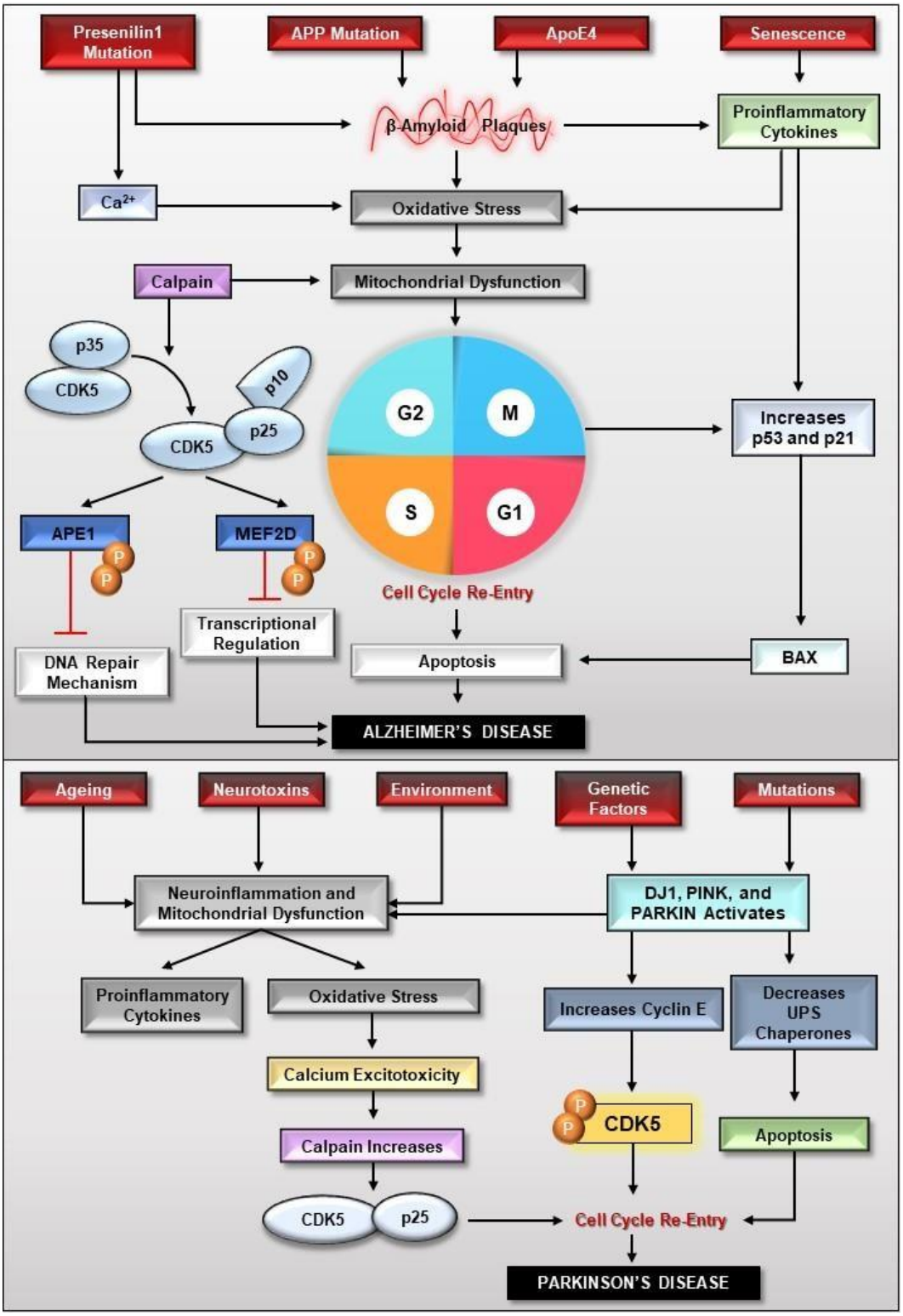

Fig 2.4. Pathophysiological consequences of Alzheimer's disease and Parkinson disease. Various factors like mutation in Presenilin 1 and APP upregulates the Aβ formation and pro-inflammatory cytokines. Calcium excitotoxicity is an important factor that activates enzyme calpain which is responsible for the disintegration of p35 into p25 and p10. p25 can phosphorylate APE1,

MEF2D, and CDK5. Inactivation of MEF2D by CDK5-dependent phosphorylation mechanism represents CDK5 mediates cell cycle re-entry and apoptosis, events such as Aβ formation, tau hyperphosphorylation, synaptic plasticity, neuronal cell apoptosis, aberrant cell cycle re-entry, mitochondrial dysfunction, and oxidative stress ultimately lead to neuronal death. Mitochondrial dysfunction, oxidative stress, aberrant autophagy, and defective UPS pathways are all factors that contribute to the death of dopaminergic neurons in Parkinson's disease. CDK5 contributes to the pathogenesis of PD by phosphorylating important proteins involved in the aforementioned processes, such as Parkin and MEF2 upregulates Cyclin E all the mentioned mechanisms lead toward the pathogenesis of PD. APE-1- AP (apurine/apirimidine) endonuclease 1, MEF2D- Myocyte Enhancer Factor 2D, CDK5- Cyclin-dependent kinase 5.

2.7 Pharmacological approaches

Cell cycle regulation is crucial for neuronal apoptosis, signifying the importance of cell cycle proteins targeting drugs as a promising area of research to develop protective therapies for neurons [105]. Hence compounds that regulate the cell cycle are antiproliferative and act to cease the cell cycle. For example, natural and synthetic compounds that slow down the G0 to G1 phase transition in the cell cycle is evident to be neuroprotective in animal model induced with NDDs [151]. In a study, it has been demonstrated that in TBI, inhibitors of cell cycle such as Roscovitine, Olomoucine, and Flavopiridol, downregulate the cell cycle proteins and inhibit neuronal apoptosis after etoposide-induced DNA damage, cell cycle inhibitors downregulate Cyclin D1 expression using different PTMs like phosphorylation and acetylation [156]. Natural inhibitors like Rivastigmine, Donepezil, and Galantamine are Acetylcholinesterase inhibitors, whereas Memantine is a glutamate receptor antagonist, which is capable of retracting the cell cycle at the G0 and G1 interphase as demonstrated in experimental studies [157]. It is a fact that upregulated Cyclins cause cell cycle re-entry and reduce the activity of CKIs eventually leading to neuronal apoptosis. Roscovitine, a purine analog, downregulates CDK2 and CDK5 and suppresses the signaling cascade ERK1 and ERK2 [158], [159]. Olomoucine arrests the cells at G1/S, G2/M transition and inhibits ERK/MAPK p38 pathway [160]. A study has demonstrated that ibuprofen (a non-steroidal anti-inflammatory drug) arrests cell cycle at S phase and apigenin affects cell cycle by the methylation of cell cycle regulators at G2/M phase [161]. Epigallocatechin-gallate (ECGG), a natural product obtained from

green tea extract (GTE), activates the GSK-3β signalling pathway and reduces Aβ production, and arrests cell cycle at G0 and G1 [162]. Indirubin-3'-monoxime suppresses CDK5 and GSK-3β and ultimately reduces tau phosphorylation [163]. Butyrolactone-I, an inhibitor of cdc2 and CDK2 kinases, inhibits cell cycle progression at G1[164]. The importance of several natural and synthetic compounds involved in therapeutics of NDDs is illustrated in **Table 2.2**

Table 2.2. Natural and Synthetic compounds targeting CDKs in the treatment of NDDs

Compound	PTM Mechanisms	Disease Model	Targets	Mechanism	Signalling affected	References
Curcumin	Phosphorylation	AD APP/PS1 mice	Gab2, K-Ras, TGF-β1, Cyclin D	Restoration of Aβ induced suppression of TGF-β, upregulation of caspase-3 alleviation of the downregulation of Cyclin D	Ras/ERK	[165]
Panax ginseng	Methylation Acetylation	AD Neuron	PPARγ, CDK5, Aβ42	Reduction of Aβ levels	p38/MAPK	[166]
Nobiletin	Phosphorylation	AD APP/PS1 mice	Aβ42, HMGB1, p34 inflammation cytokines, Cyclin-A, Cyclin-E, and E2f8	Down-regulation of expression of HMGB-1 Reduced genes level, including cell cycle-regulating genes Cyclin A and E	MEK/ERK	[167]
Luteolin	Acetylation	AD Mouse model	CDK5, NF-κB, p38, JNK, MAPK and Akt	TLR-4 expression suppression inhibits the activation of JNK, MAPK and Akt.	JNK/p38	[168]
Bilobalide	Acetylation	AD PC12 cells	c-Myc and p53	Reduced ROS-induced Bax	JAK/STAT	[169], [170]

				elevation and caspase-3 activation		
Olomoucine	Phosphorylation	AD, PD Npc Mice	G1 /S and G2/M	Inhibition of ERK/MAPK p38 pathway and arresting cell cycle at G1 to S and G2 to M phase	ERK/ GSK3β	[171]
Butyrolactone I	-	AD, PD AβPP/PS1 Mouse	G1 phase	Inhibitors of cdc2 and CDK2 kinases inhibit cell cycle progression at G1	mTOR	[172]
Roscovitine	Acetylation Phosphorylation	AD SH-SY5Y cells	CDK2 and CDK5	Roscovitine a purine analogue downregulates CDK2 and CDK5 and suppresses signalling cascade ERK1 and ERK2	ERK1 and ERK2	[158], [159], [173]
Flavopiridol	Acetylation Phosphorylation	AD PD CD1 mice	Cyclin D1	Reduced Expression of Cyclin D1 and CDKs activity.	NF-κB / PI3K/Akt	[174]
Quercetin	Phosphorylation Acetylation Methylation	AD PD Adult Mouse Brain	Caspase-3, PPARγ PI3K/AKT/ ROS-protective, metabolic p53/p21/ HIF-1α	Inducing TLR-4 which consequently mediates NF-κB cascade activation, plays an important role in neurodegeneration processes	NF-κB / PI3K/Akt/ mTOR	[175]
Apigenin		AD	CDK5, p38	Apigenin reduces	MAPK/ERK/JNK/p38	[176]

	Methylation	Cortex of newborn and embryonic Wistar rats		microglial activation, characterized by inhibition of proliferation		
Ibuprofen	-	AD PD BV-2 cells	S phase	A non-steroidal anti-inflammatory drug) arrest cell cycle at S phase	-	[177]
Epigallocatechin-gallate (EGCG)	Glycation	AD PD Mouse model	G0, G1 CDK5 and p38	(EGCG) is a natural product obtained from green tea extract (GTE) activates (GSK-3β) signalling pathway and reduces Aβ production and arrests cell cycle at G0 and G1	NF-κβ/MAPK/ JNK/p38	[178], [179]
Indirubin-3'-monoxime	Glycation Phosphorylation	AD APP and PS1 Mice	CDK5	Act as an antioxidant, Anti-inflammatory	GSK3 β	[163]

Various studies have pointed towards different therapeutic approaches that suppress aberrant cell cycle events through different mechanisms like UPS dysfunction and PTMs. The cell cycle is regulated by UPS through the degradation of CDK subunits and their regulators. During the cell cycle, when neurons are in S phase transition, CDK5 is translocated to cytoplasm and ubiquitinated by the E3 ligase APC-Cdh1 complex which provides neuroprotection. APC-Cdh1 complex degrades Cyclin B to maintain post mitotic state of the neuron [180]. As a regulator of glucose metabolism and a suppressor of neuronal apoptosis, Cdh1 has shown an important therapeutic role [180]. Further, in a study, it has been shown that Aβ

oligomer suppresses Cdh1 which is formed due to CDK5, p10, and N terminal of p35, thus acting as an armor against the neurotoxicity induced by CDK5/p25 [181]. Similarly, SKP1 upregulation protects the impairment caused by E3 ligase APC-Cdh1 complex in PD [182]. A complex F-box/WD repeat protein hSel-10 and Cullin-1 is formed by Parkin, another E3, ligase, that protects Cyclin E accumulation [183]. CKIs such as p16, p18, p21and p27 have been reported to inhibit the kinase activity of CDK4/CDK6, therefore, demonstrating a neuroprotective role. Inhibition of CDK4 and Cyclin D is due to various activators such as JNK, AKT kinase, transcription factors (c-Fos and c-Jun), caspases, and Bcl-2 [184]. Kainic acid treatment causes neuronal apoptosis by Notch signaling, which upregulates CDK4 and Cyclin D through PI3K/Akt pathway, resulting in aberrant cell cycle re-entry through activation of CyclinD1-Rb-E2F1 axis [184], [185]. In PS1 mutation, β-catenin is translocated to the nucleus and causes aberrant cell cycle re-entry via upregulation of Cyclin D. Quercetin acts as a β-catenin disruptor and suppresses Cyclin D and neuronal apoptosis [186].

AZD0530 (NCT02167256), also known as Saracatinib, is an inhibitor of FYN kinase family and was earlier used as an anticancer agent. It is an inhibitor of Src family developed in the year 2006 by AstraZeneca. Saracatinib was repurposed as a promising CNS agent for AD treatment due to its excellent pharmacokinetic properties and high BBB permeability [187]. Various clinical studies have revealed that a molecular pathway in Aβ damages neurons and Fyn kinase plays an important part in that pathway. In clinical trials, AZD0530 administration is well tolerated in humans. The outcome of these studies has been a change in cognition in NDDs and related markers. However, the studies have several limitations such as the availability of cerebrospinal fluid (CSF) in a limited percentage of trial participants which limits the potential to evaluate the treatment effects on the change in CSF tau and to assess the adequacy of dose concerning CSF drug levels [188]. Memantine (NCT03858270), is an inhibitor of the NMDA (N-Methyl-D- Aspartate)-receptor also known as glutamate receptor. Memantine blocks the glutamate receptor and prevents the neurotoxicity caused by the glutamate pathway and its effect such as dizziness, headache, confusion, diarrhea, and constipation has

been seen in clinical trials [189]. Trichostatin, an inhibitor of histone deacetylase increases the histone hyperacetylation and p21 (WAF1) expression which ultimately arrests the cell cycle at G1 phase [164]. Valproic acid (VPA) a HDAC inhibitor used as an anti-epileptic drug has also shown inhibitory action on GSK3β and rescue behavioral phenotypes in AD mice [190], [191]. Preclinical studies in animal models of PD have suggested that VPA may have neuroprotective effects. This implies that, in these experimental settings, VPA appeared to show protective action against the degeneration of neurons associated with PD [192]. Sodium butyrate is well known for its role as HDAC inhibitor, which can influence epigenetic modifications, leading to changes in gene expression patterns. In the 5xFAD mouse model of AD Sodium butyrate supplementation for 12 weeks significantly reduces brain Aβ levels by 40% and improves associative learning and memory, as indicated by a 25% increase in fear response during behavioral tests. The findings suggest that Sodium butyrate could be a potential therapeutic agent for early-stage Alzheimer's cognitive deficits [193]. Proteasome inhibitors such as bortezomib, aims to block protein degradation, allowing the buildup of misfolded proteins and triggering apoptosis in aberrant cells. Bortezomib reversibly binds to the chymotrypsin-like subunit of the 26S proteasome, resulting in its inhibition and preventing the degradation of various pro-apoptotic factors [194].

Further, numerous drugs are under clinical trial, which may play an important role in the treatment and control of NDDs by targeting CDKs and their inhibitors through PTM mechanisms as illustrated in **Table 2.3**

Table 2.3. Drugs under clinical trials that targets CDKs, their inhibitors through PTMs in NDDs.

Drugs	NCT number	PTM mechanisms	Phase	Disease	Targets	Status	Outcome Measures
APH-1105	NCT03806478	Glycation Ubiquitination	2	AD	α secretase	Not yet recruiting	Change in Cognitive Functioning
MW150	NCT05194163	Glycation	2	AD	CDK 5	Not yet recruiting	Drug Safety- Blood tests/ Electrocardiographic
Donepezil	NCT00190021	Acetylation	3	AD	CDK2, SIRT1, FOXO, PGC-1α	-	Positive and Negative Syndrome Scale

Baricitinib	NCT05189106	Acetylation	2	AD ALS	CDKs and JAK	Not yet recruiting	Evaluation of CSF Concentration of baricitinib
Dasatinib + Quercetin	NCT04685590	Phosphorylation Acetylation SUMOylation	2	AD	CDK 2,5 and CDK 6, SENP3, SENP1/2, SIRT1	Recruiting	Serious Adverse Events and Adverse Events in the treatment group as compared to placebo group
Memantine Hydrochloride	NCT05063851	Phosphorylation	2	AD	NMDAR, CDK5	Recruiting	Assessing the feasibility of the use of memantine hydrochloride for prevention of AD
Biological: SNK01	NCT0467853	-	1	AD	-	Recruiting	Alzheimer's Disease by monitoring for adverse events.
Dastinib and Quercetin	NCT04063124	Phosphorylation Acetylation SUMOylation	1/2	AD	CDK 2,5 and CDK 6, SENP3, SENP1/2, SIRT1	Recruiting	Brain penetrance of Dasatinib. Brain penetrance of Quercetin
ALZT-OP1 (ibuprofen +cromolyn) ALZT-OP1b (ibuprofen) and ALZT-OP1a (cromolyn)	NCT04570644	-	1	AD	CDK 2, cyclin E	Completed	Part A Non-compartmental PK parameters to be calculated and reported for ALZT-OP1b and ALZT-OP1a
Genistein	NCT01982578	Methylation	-	AD	Cyclin E and A and CDK 2	Completed	Changes in Amyloid beta concentration in cerebrospinal fluid
Simvastatin	NCT01439555	Phosphorylation	2	AD	CDK inhibitors p21	Completed	Alteration in Cerebral Blood Flow determined in MRI (by labelling Arterial Spin)
Resveratrol (BDPP Treatment for Mild Cognitive Impairment (MCI))	NCT02502253	Acetylation	1	AD	Cyclin D and CDK 2,4 and 6, p21, SIRT, p53,	Completed	Adverse Events Assessment and Serious Adverse Events Confirm brain penetrance of BDPP
VX-745	NCT02423122	-	2	AD	CDK 5 and p38 MAPK	Completed	Change from Baseline in Aβ Plaque by 11C-PiB PET
AZD0530	NCT02167256	-	2	AD	p27, cyclin E and CDK 2	Completed	Brain Glucose Uptake Variation Measured Using 18F-FDG PET Imaging
Curcumin + aerobic yoga	NCT01811381		2	AD	CDK 2 SIRT1, p53,	Active, not recruiting	Effects of curcumin effects on

		Acetylation Glycation Phosphorylation			NFκβ, AP-1, STAT		Neuropsychological aspects in comparison to placebo (In early 6 months in combination with aerobic yoga and non-aerobic yoga with curcumin and supplement) and baseline
Saracatinib	NCT01864655	Phosphorylation	1	AD	p27, cyclin E and CDK 2	Completed	CNS availability of AZD0530 after oral dosing. AZD0530 Effect on brain glucose metabolism in patients with AD
Dimebon	NCT01584440	Acetylation	2	AD	SIRT 1, PGC-1α	Completed	Change in the Neuropsychiatric Inventory Agitation/Aggression Domain Score
Naproxen	NCT02702817	Phosphorylation	2	AD	CDK2 and cyclin E	Completed	Trajectory of composite Alzheimer's Progression Score from multiple cognitive and biomarker measures of pre-clinical Alzheimer's Disease
Fligrastim	NCT03656072	-	2	AD	HIF-1α, myc, p21, p27, p53, cyclinD, A and E	Completed	Mini-mental State Examination
Resveratrol with Glucose and Malate	NCT00678431	Methylation, Acetylation	3	AD	Cyclin D and CDK 2,4 and 6, p21, SIRT1, p53	Completed	Alzheimer Disease Assessment Scale (ADAScog)
Memantine	NCT00505167	Ubiquitination	4	AD	NMDAR, CDK5	Completed	Variations in Levels of metabolite N-acetyl-aspartate in various areas of the brain
Naproxen Sodium (Aleve)	NCT00007189	Ubiquitination Phosphorylation	3	AD	CDK2 and cyclin E	Completed	-
Anle138b	NCT04685265	-	1	PD	HSP70	Recruiting	Incidence of treatment-with multiple ascending doses of anle138b taken in the fasted state - emergent adverse events in PD patients

Memantine	NCT03858270	Ubiquitination	3	PD	NMDAR, CDK 5	Recruiting	Variations in RAVLT (Rey Auditory Verbal Learning Test) Scores
Combination injection of EPO and G-CSF	NCT02018406	-	1/2	PD	HIF-1α, myc, p21, p27, p53, cyclin D, A, and E	Recruiting	Haematological Test
Bilobalide	NCT03475823	Acetylation	-	Cognitive Change	Cyclin E and CDK2	Completed	Changes in cognition. Cerebral Blood Flow
Palmitoylethanolamide Combined with Luteoline (PEA-LUT)	NCT04489017	-	-	FTD	CDK 2 and 5, p53, AP-1, p15, p16 and p21	Recruiting	Neuropsychiatric Inventory (NPI). Screening for aphasia in Neurodegeneration
Luteolin	NCT05204407	Acetylation	-	Schizoph-renia	CDK 2 and 5, p53, AP-1	Not yet recruiting	Cognitive impairments. Global oxidative stress
Neflamapimod	NCT04001517	Phosphorylation	2	Dementia With Lewy Bodies (DLB)	CDK 5 and p38 MAPK	Completed	Changes in cognition determined by Letter fluency test
Tamoxifen	NCT01257581	-	2	ALS	CDK 5, cyclin E KLF4, p53, p21	Completed	Variations in ALS Functional Rating Scale – Revised
Biological: Cellavita-HD	NCT04219241	Acetylation Phosphorylation Ubiquitination	2/3	HD	SIRT 1, PGC-1α and FBXW2	Active not Recruiting	Maintenance of effectiveness on clinical progression of the disease
Dimebon	NCT00387270	Acetylation	1/2	HD	SIRT 1, PGC-1α	Completed	Dose-limiting toxicities
Memantine	NCT00652457	Ubiquitination	4	HD	CDK 5, cyclin E	Completed	Variations in the HVLT-R (Hopkins Verbal Learning Test-Revised) for Delayed Recall

2.8 Computation-based drug repurposing (CBDR) approach

The CBDR approach is sometimes called the ‘in-silico’ drug repurposing (ISDR) approach which makes the best utilization of computational tools to discover the novel uses of already existing drugs. The overarching CBDR approach encompasses a drug-centric and disease-centric approach. The former approach studies the properties of existing drugs and finds similarities between the drugs.

Researchers seek to match the properties of drugs and their potential to target the dysregulated pathways in specific diseases. The latter approach involves studying medical data such as multi-omics and phenotypic data associated with a disease condition and then screening drugs that could interfere with the underlying mechanism of that disease. The growth of the CBDR approach has been possible because of two major reasons, first availability of large-scale high-throughput multi-omics data related to disease. The abundance of data allows researchers to study the phenotypes associated with various diseases as well as the potential interactions between the drug and the disease. Second, significant advancements in computational biology and data sciences involve the creation of intricate algorithms for drug reprofiling. The sophisticated algorithms are based on various tools of ML and network analysis and enable researchers to predict drug-disease interactions. Various databases housing enormous data coming from the labs are maintained to validate the predictions made by these algorithms. The CBDR approach includes methods like data mining and analysis, chemical structure matching, adverse effect profile matching, molecular docking, GWAS, pathway mapping and network model-based methods, literature mining and machine learning. The data mining method is the fundamental step in the process of drug reprofiling. It involves creating speculations about potential drug-disease interaction by understanding the medical data present in the EHRs, multi-omics and gene activity data from the experiments and chemical structure data as well. Chemical structures of the drugs are compared to implicate structural similarities. If two drugs are similar structurally then it may be possible that they are similar functionally. The adverse effect profile matching compares the side effects of drugs, if drugs show similar adverse side effects, then they may act on the same molecular pathways and could have similar therapeutic effects. Molecular docking utilizes supercomputers to scrutinize millions of drugs (ligands) against a specific target molecule, disease-causing protein (receptor). The Ensemble docking enables more genuine simulations as it accounts for the dynamic motion of proteins. The decreasing costs of genotyping and better knowledge of the genome have made GWAS more valuable in the current era. Although GWAS are predominantly used for unravelling genetic factors associated with the disease they also help researchers to

comprehend the disease biology and pinpoint potential drug target(s). If the target identified from the GWAS is incompatible with repurposing then, a pathway-based approach is utilized to find out genes that are upstream (UST) and downstream (DST) from the target to search for an alternative. The network-based method is based on an authenticated 'guilt-by-association' principle which states that if drugs similarly affect gene activity, then they may be used to treat similar diseases as they may have similar modes of action. The network represents the relationships between drugs, diseases and gene products and helps to identify closely connected drugs within a heterogeneous network as well as drugs that might have a therapeutic effect for a specific disease. Literature mining involves extracting valuable information from medical texts and establishing new connections between existing studies to explore drug repurposing opportunities. NLP and other information retrieval methodologies are utilized to extract relevant data from the wealth of textual data. Literature data mining also involves semantic inference which represents the links between drugs and disease in an organized way to find hidden connections in the textual data and identify a drug that could be repurposed. The CBDR approach has tremendous benefits including an accelerated and cost-effective drug discovery process, analysis of complex datasets to discover drug targets, especially for rare disorders, reduced risk of unforeseen adverse effects of a drug, and improved patient outcomes by best utilization of pharmaceutical and medical knowledge. [195] In the contemporary world, ML and AI have also gained huge popularity and adoption in the field of drug discovery and development. Steve et. al presented DRIAD (Drug Repurposing in AD) which is an ML-based framework that measures the association between the molecular mechanisms and physiology of AD. Jacek et. al [196] utilized supervised learning to reprofile drugs for PD based on the knowledge about PINK1 expression levels. Zhaobin et. al [197] utilized a baseline regularization algorithm for CBDR using the EHRs. Gottlieb et. al presented 'PREDICT' for predicting similar drugs that could be reprofiled for similar diseases. [198] Recently, HNNDTA (Hybrid Neural Network for Drug-Target Affinity) has been proposed by Xialin et. al to predict the affinity between a drug and its target. A study by Aliper and Plis suggests that Deep Learning Neural Networks (DNNs) can outperform Support Vector Machines (SVM) for predicting

the therapeutic activities of the drug. The gist of different computational methods used in de-novo drug designing and drug reprofiling are summarized in Table 2. There exists a plethora of web-based tools and databases that have utility in drug discovery and reprofiling. PubChem for small biomolecules and their properties, ChEMBL for manually extracted pharmaceutical chemistry literature, BindingDB for binding affinities of potential drug targets (proteins), DrugBank for drugs and their target information, Therapeutic Target Database for data about protein-based drugs and nucleic acid-based drugs, ChemBank for information regarding tiny molecules obtained from biomedical assays, STITCH to explore existing and predicted interactions of chemical ligands and proteins based on invitro experiments and literature, VNP for disease-drug target interaction, and ToxCast and Tox21 for high-throughput data about toxicity of chemicals. Several web-based tools like DINIES for predicting drug-target interaction, SuperPred web server to classify drugs, MANTRA 2.0 to infer similarities between pharmacologically influenced gene expression profiles, TargetHunter to explore possible targets of a compound, and Similarity Ensemble Approach (SEA) to construct multi-target similarity map can be utilized for drug discovery and reprofiling, reducing the time and cost for developing therapies for rare diseases.

CHAPTER 3

MATERIALS AND METHODS

Chapter 3

MATERIALS AND METHODS

3.1 Research objective 1: To identify the cell cycle related biomarkers and their therapeutic role in NDDs

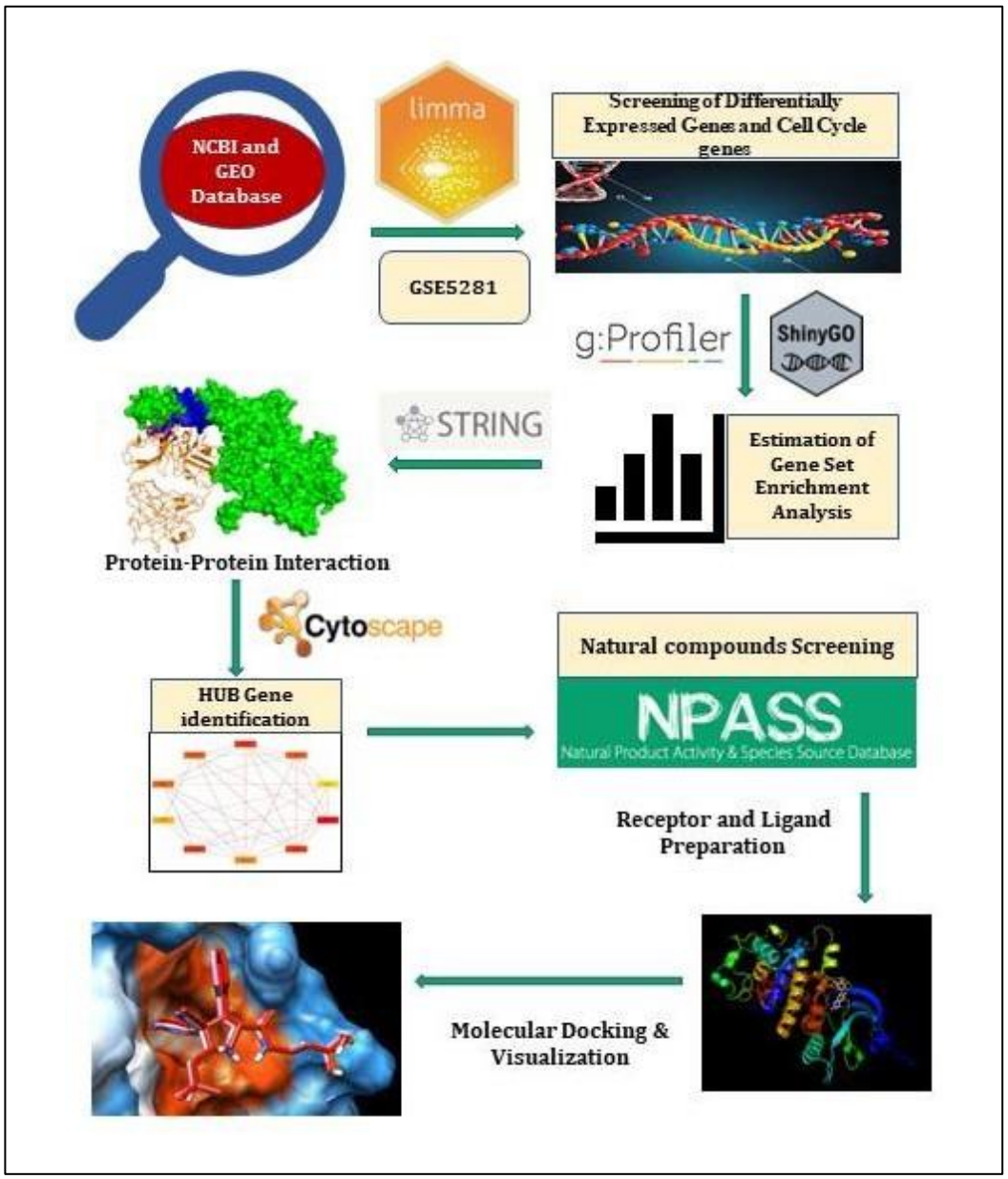

Fig 3.1. Steps involved in the identification of cell cycle related biomarkers and their therapeutics in NDDs.

3.1.1 Microdata acquisition and pre-processing

The National Center for Biotechnology Information (NCBI) managed many databases like Gene Expression Omnibus (GEO) is one of them. The screened GSE5281 AD dataset was extracted from the NCBI database. Specifically, the gene expression profile with the accession number GSE5281 was selected for this study consisting of 161 samples including 44 samples belonging to the diseased category and 61 to healthy category, serving as a critical resource for identifying differentially expressed genes (DEGs) associated with AD.

3.1.2 Screening of Differentially Expressed Genes (DEGs)

The selected dataset was analyzed using the GEO2R web-based tool, which facilitates the comparison of gene expression levels between multiple groups of samples. GEO2R utilizes the limma package in R programming (https://www.ncbi.nlm.nih.gov/ geo/geo2r/?acc=GSE5281) to identify DEGs by applying various filters, including an adjusted p-value threshold of < 0.05 and a Log Fold Change (Log FC) threshold. Genes with a Log FC value between 0 and 0.9 were classified as upregulated, while those with a Log FC value between 0 and -0.9 were identified as downregulated. In addition, a list of Cell cycle related genes (CCR) was extracted from the KEGG (databasehttps://esbl.nhlbi.nih.gov/Signaling-Pathways/Cell-Cycle/,) and overlapping genes between DEGs and CCR were identified through Venn analysis to focus on genes potentially involved in AD pathogenesis.

3.1.3 Functional enrichment analysis of cell cycle genes in AD

The common genes identified from the Venn analysis were subjected to functional enrichment analysis to explore their biological processes, cellular components, and molecular functions. This analysis was conducted using web-based bioinformatics tools such as ShinyGO (http://bioinformatics.sdstate.edu/go/) and gprofiler, (https://biit.cs.ut.ee/gprofiler/gost) which are designed to perform comprehensive

functional enrichment analysis of DEGs. Additionally, the Kyoto Encyclopedia of Genes and Genomes (KEGG) pathway analysis was performed to predict the involvement of these genes in specific biochemical pathways, particularly those related to cell cycle regulation in AD.

3.1.4 Protein-Protein interaction analysis

The common genes were then exported to the Search Tool for the Retrieval of Interacting Genes/Proteins (STRING) (https://string-db.org/) database to construct a protein-protein interaction (PPI) network [199]. A confidence score threshold of 0.4 was used to filter the interactions, ensuring a reliable network of interactions. The resulting PPI network was further analyzed using Cytoscape v3.9.1, a powerful software platform for visualizing molecular interaction networks and integrating these networks with gene expression profiles [200].

3.1.5 Drug screening through NPASS database

For the identification of potential therapeutic compounds, the NPASS Natural Product Activity and Species Source (NPASS) (https://bidd.group/NPASS/) library was employed [201]. This extensive repository contains data on natural compounds, including their biological activities and pharmacological properties. Fisetin is known inhibitor of CDK6, well established for their neuroprotective properties, were selected as a reference drug in this study on the basis tanimoto similarity the NPASS library and their chemical structures were retrieved in the form of canonical SMILES. The ligands (.sdf) files were extracted from the NPASS database and prepared using the Discovery Studio tool for further analysis.

3.1.6 Pharmacokinetics profiling

SWISSADME is a web-based computational tool that was used for pharmacokinetics profiling (Absorption, Distribution, Metabolism, and Excretion) ADME and

medicinal properties of natural compounds used as ligands [202]. Drug likeness of ligands was predicted by the SWISSADME tools, which follow Lipinski's rule of 5 [203], [204], [205], [206]. Rule of five was proposed by Lipinski and co-workers, which is a well-established filter for the drug-likeliness of a ligand [207]. The criteria used for filtering to determine whether a ligand can be absorbed orally or not, are that the molecular weight should be less than or equal to 500, the water partition coefficient (AlogP) should be less than or equal to 5, a number of hydrogen bond acceptors (HBAs) ≤ 10.6 and number of hydrogen bond donors (HBDs) ≤ 5. Several other chemical characteristics such as topological polar surface area (TPSA), % ABS absorption percentage (ABS) and rotatable bond count are also considered in this analysis. According to Lipinski's rule of five, for a compound to be orally active, the TPSA value should be less than 140 $Å^2$ [208], [209], [210], [211]. A few other factors, such as the blood-brain barrier and skin permeability (log Kp), were also considered.

3.1.7 Molecular Docking

The molecular docking studies were performed to evaluate the binding affinity of the selected natural compounds towards CDK6, the target protein implicated in AD. The receptor structure of CDK6 was retrieved from the RCSB Protein Data Bank (PDB) (https://www.rcsb.org/,) specifically the structure with PDB ID 1XO2 which have a resolution of 2.90 Å, protein preparation included the removal of water molecules and heteroatoms, whereas hydrogen atoms were added, and total charges were generated. The ligands .sdf files were extracted and prepared in discovery studio (https://discover.3ds.com/discovery-studio-visualizer-download) The docking was carried out using the Webina online server (https://durrantlab.pitt.edu/Webina/), which allows for efficient and accurate molecular docking studies. The receptor and ligand are prepared in pdbqt format for docking by the Webina. The docking results were visualized and analyzed using BIOVIA Discovery Studio, a software that provides advanced tools for the interpretation of molecular interactions and binding affinities between the compounds and the CDK6 receptor.

3.1.8 Molecular Dynamics Simulation

Molecular dynamic (MD) simulation was assessed to reveal the dynamic behavioral changes of phytochemical and CDK6 binding. The protein-ligand complex structure obtained from docking analysis was retrieved in Gromacs 2023.3 [212]. Charmm36 forcefield was selected for MD simulation for 100 ns. The entire system (phytochemicals and CDK6) was first solvated with a three-point transferable intermolecular potential (TIP3P) orthorhombic box, and their charges were neutralized by adding counter ions, Na and Cl [213]. The Velocity Verlet integrator, known for its stability and energy conservation, was used in MD simulation. Bond lengths are restricted by the LINCS algorithm, thereby setting the time step at 0.002 ps. Energy minimization was carried out using the steepest descent approach prior to the MD simulations to rule out high-energy configurations and ensure a stable starting point. Positional constraints with a force constant of 1000 kJ/mol/nm were placed on the solute's heavy atoms during the first equilibration phase, enabling the solvent and ions to equilibrate around a fixed solute structure. The solvated protein-ligand complex systems were then subjected to 50,000 nsteps of energy minimization followed by 300 K for 100 ps. An equilibration step for pressure was executed for a further 100 ps. Finally, the MD runs were performed for 100 ns, and post-MD simulations were performed for Root Mean Square Deviation (RMSD), Root Mean Square Fluctuation (RMSF), Radius of gyration (Rg), hydrogen bond and minimum distance calculation.

3.2 Research objective 2: To develop the novel therapeutic agents that target CDK4 to control NDDs.

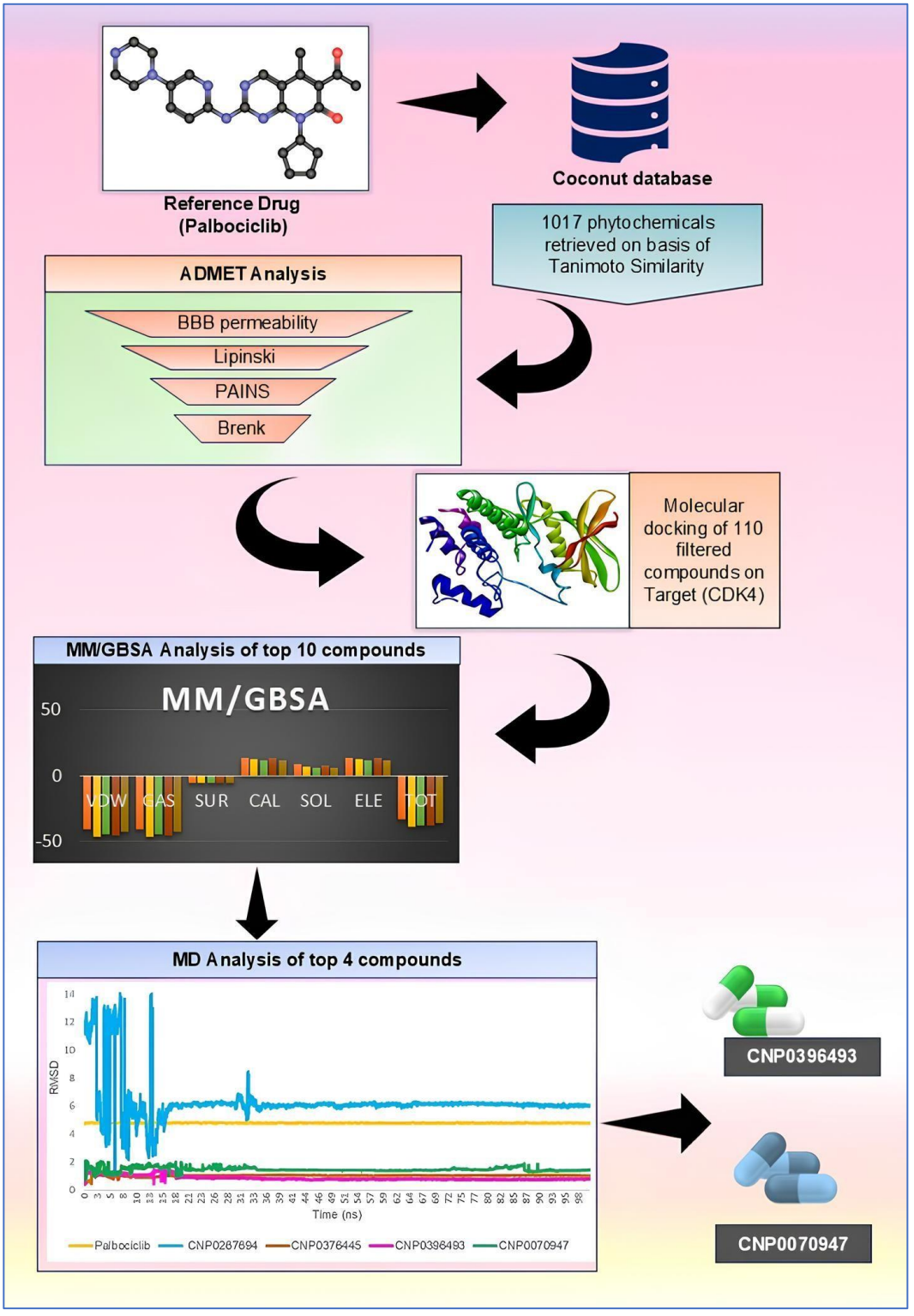

Fig 3.2. Overall steps involved in virtual screening of natural compounds targeting CDK4.

3.2.1 Structure retrieval

In this study, the structure of CDK4 was retrieved from the protein PDB database, maintained by RCSB (http://www.rcsb.org) [214], [215], [216]. The X-ray crystal structure of CDK4 (PDB ID: 2W96) with 2.30 Å resolution was visualized and prepared by web-based server discovery studio (https://discover.3ds.com/discovery-studio-visualizer-download) [217]. The steps followed for protein preparation included the removal of water molecules and heteroatoms, whereas hydrogen atoms were added, and total charges were generated. The protein was then optimized and energy-minimized using the CHARMM force field to achieve the structural integrity of the final proteins. After the structure was fully prepared, saved and then converted to the pdbqt format required for AutoDock Vina docking studies. This conversion was performed using the Webina web-based tool.

3.2.2 Ligand screening for palbociclib analogue

Palbociclib is a well-established drug for suppressing CDK4 and has an inhibitory role in cell proliferation. The COCONUT database is a freely available web-based server (https://coconut.naturalproducts.net/) for the storage, search, and analysis of natural products (NP), gathers information of NP from 50 different open sources [218]. The COCONUT database repository was used to retrieve natural products as ligands for the target protein CDK4 (PDB ID-2W96) based on a 75 percent similarity-based approach considering palbociclib as the reference drug [219].

3.2.3 Ligand preparation

The COCONUT database is a repository of 4,07,270 natural compounds. Based on the Tanimoto similarity algorithm, we extracted 1017 investigational natural products for their prospective role as ligands against CDK4 [218], [220]. The ligands (.sdf) files were extracted from the COCONUT database and prepared using the Discovery Studio tool for further analysis where hydrogen atoms were added, any solvent molecules, counter ions, or other extraneous entities were removed from the ligand

structures to ensure that only the relevant ligand atoms were retained [221]. Hydrogen atoms were added to the ligand structures to ensure correct valence states. This step is crucial for accurate charge assignment and interaction analysis. Appropriate charges were assigned to the ligand atoms using the CHARMM force field available in Discovery Studio. This step ensures that the electronic properties of the ligands are accurately represented. The geometry of the ligands was optimized to relieve any steric clashes and to place the ligands in their lowest energy conformations. This step was performed using the minimization tools available in Discovery Studio. Further, the ligands were fully prepared, saved, and then converted to the pdbqt format required for AutoDock Vina docking studies. This conversion was performed using the Webina web-based tool.

3.2.4 Pharmacokinetics profiling using SWISSADME

These compounds were then subjected to ADMET (Absorption, Distribution, Metabolism, Excretion, and Toxicity) analysis using the SwissADME web tool [222], which evaluates the pharmacokinetic properties and drug-likeness of the compounds. This step was crucial for identifying natural compounds with favorable ADMET profiles for further drug development.

3.2.5 Molecular docking

Molecular docking is a computational technique used in the field of structural biology and drug discovery to predict the preferred orientation of the ligand when bound to the receptor to form a stable complex. In this study, we used Webina (https://durrantlab.pitt.edu/Webina/), a web-based docking tool available for molecular docking, and fastDRH (http://cadd.zju.edu.cn/fastdrh/) to perform docking and analyze the result [223], [224]. The input files of receptor and ligands were prepared in the pdbqt format [225], which were uploaded on Webina, followed by the preparation of a docking box using the grid center x (0) y (-2) z (75) and grid size center x (59), y (42) z (50), while grid space was 0.375[226].

3.2.6 MM/GBSA analysis

In this study for Molecular Mechanics /Generalized Born Surface Area (MM/GBSA) analysis, we have assessed the fastDRH tool [226], [227]. This server predicted the best ligand binding mode and hot spot residue for ligand binding with high speed and accuracy using the Autodock vina docking engine followed by MM/GBSA calculations on an AMBER backend, [228]. The molecular docking study was performed by uploading the CDK4 structure in pdb format and ligand structures in .sdf format. Further, we opted for the Autodock vina docking engine and uploaded the receptor pose file in pdb format for molecular docking, with up to 10 poses selected for further analysis. For rescoring, the forcefield selected for receptor ff99SB with TIP3P water model and ligand were GAFF2, respectively [229], [230]. The hotspot prediction was performed using the MM/GBSA method, along with the other parameters applied for rescoring, and the available default parameter was also chosen for the truncation radius. The results were extracted and used for final analysis.

3.2.7 Molecular Dynamics simulation

Molecular dynamic (MD) simulation was performed to reveal the dynamic behavioral changes of phytochemical binding with CDK4. The protein-ligand complex structure obtained from docking analysis was retrieved in Gromacs 2023.3 [212] and Charmm27 forcefield was selected for 100 ns. The entire complex was first solvated with a TIP3P orthorhombic box, with charges neutralized by adding counter ions, Na and Cl [230]. Bond lengths were restricted by the LINCS algorithm, thereby setting the time step at 0.002 ps. To rule out high-energy configurations and ensure a stable starting point, energy minimization was carried out using the steepest descent approach prior to the MD simulations. During the first equilibration phase, the solute’s heavy atoms were subjected to positional constraints with a force constant of 1000 kJ/mol/nm, enabling the solvent and ions to equilibrate around a fixed solute structure. The solvated protein-ligand complex systems were further subjected to

50,000 nsteps of energy minimization followed by 300 K for 100 ps and an equilibration step for pressure was executed for a further 100 ps. Finally, the MD run was performed for 100 ns, and post-MD simulations were performed for RMSD, RMSF, Rg, hydrogen bond and minimum distance calculation.

3.3 Research objective 3: To identify the novel UPS molecular signatures implemented in NDDs for prospective novel therapeutics.

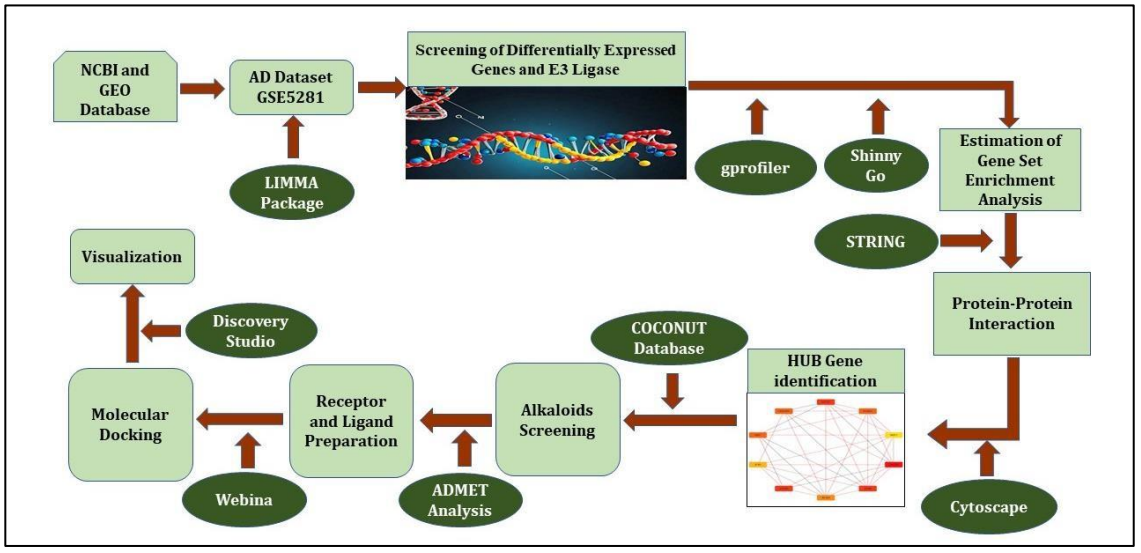

Fig 3.3. Steps involved in the identification of E3 ligases related biomarkers and their therapeutic role in NDDs.

3.3.1 Microdata retrieval

We have extracted the AD dataset from NCBI and GEO database (https://www.ncbi.nlm.nih.gov/geo/query/acc.cgi?acc=gse5281). The gene expression of AD with GSE5281 was selected for our study consisting of 161 samples in which 44 samples belongs to Diseased category and 61 to healthy category.

3.3.2 Screening of differentially expressed genes and E3 Ligases

GEO2R, a web-based tool available on NCBI website (https://www.ncbi.nlm.nih.gov/geo/geo2r/?acc=GSE5281), was used to analyse the dataset utilized in the present study.

Genes with Log Fc value between 0 and 0.9 were considered as upregulated and those with value between 0 and -0.9 were screened as downregulated. Further, the E3 ligases lists are extracted from KSBP2 database available on NHLBI (https://esbl.nhlbi.nih.gov/Databases/KSBP2/Targets/Lists/E3-ligases/) and common genes are extracted through venn analysis (http://www.bioinformatics.com.cn/static/others/jvenn/example.html)

3.3.3 Estimation of gene set enrichment analysis

The common genes were further analysed for their biological, cellular, molecular function and KEGG pathway were predicted using web-based bioinformatics tool such as shiny go (http://bioinformatics.sdstate.edu/go/), Enricher (https://www.google.com/ search?client=firefox-b-d&q=ENRICHER) and gprofiler.

3.3.4 Protein-Protein interaction analysis

The common genes were exported to STRING database (https://string-db.org/) and screened network with confidence score of 0.4 was exported for further analysis through cytoscape v3.9.1[200].

3.3.5 Drugs screening through ADMET analysis

Coconut database (https://coconut.naturalproducts.net/) was used for extraction of natural compounds (Alkaloids) which were further screened through exporting the canonical smiles to SwissADME for ADMET analysis [218], [222].

3.3.6 Molecular Docking

The receptor structure of UBE3A (PDB ID: 6TGK) with resolution of 1.30 Å was extracted from RCBSPDB (https://www.rcsb.org/) molecular docking was executed on an online web server Webina (https://durrantlab.pitt.edu/Webina/) and visualized on the software BIOVIA Discovery Studio Visualizer.

3.3.7 Molecular Dynamics simulation

MD simulation was assessed to reveal the dynamic behavioral changes of UBE3A and Leuconoxine. The protein-ligand complex structure obtained from docking analysis was retrieved in Gromacs 2023.3 [212].

Charmm36 forcefield was selected for MD simulation for 100 ns. The entire system was first solvated with a TIP3P orthorhombic box, and their charges were neutralized by adding counter ions, Na and Cl [213]. The Velocity Verlet integrator, known for its stability and energy conservation, was used in MD simulation. Energy minimization was carried out using the steepest descent approach prior to the MD simulations to rule out high-energy configurations and ensure a stable starting point with a positional constraints of 1000 kJ/mol/nm. The solvated complex systems were then subjected to 50,000 nsteps of energy minimization followed by 300 K for 100 ps. An equilibration step for pressure was executed for a further 100 ps. Finally, the MD runs were performed for 100 ns, and post-MD simulations were performed for RMSD, RMSF, and Rg.

CHAPTER 4

RESULT AND DISCUSSION

Chapter 4

RESULT AND DISCUSSION

4.1 Research objective 1: To identify Cell Cycle Related Biomarker and Their Therapeutics Role in NDDs

4.1.1 Common CCR genes in AD

In this study, for profiling of gene expression of GSE5281, a total 161 sample were selected out of which 44 were AD samples and 61 were control samples. This study is based on GPL570 Affymetrix human genomeU133 Plus Array. Based on applied filters i.e., adj p value and Log Fc, we extracted the significant differentially expressed genes (DEGs) wherein 1799 were downregulated and 1511 were found to be upregulated. In this study we also screened 104 CCR genes from the KEGG database. Further we exported the DEGs and CCR genes to the Venn analysis software for the analysis of common genes and in this process, we screened 24 CCR genes. The Venn analysis and DEGs are elaborated in **Fig 4.1.** The common CCR genes were further analyzed for protein-protein network and function analysis through STRING database. The network was exported to the cytoscape tool where different plugin like Cytohubba, Centiscape performed the topological interpretation of common CCR genes, on the basis of various parameters like betweenness, bottleneck, closeness, eccentricity, degree, radiality and stress method, top 10 hub genes were identified, namely **CDC20, CDC27, CDK6, EP300, CDC25C, RB1, CCNA1, MCM4, ATR, and SKP1**.On the basis of betweenness nodes were characterized, whereas red and yellow specified about the degree score high to low respectively.

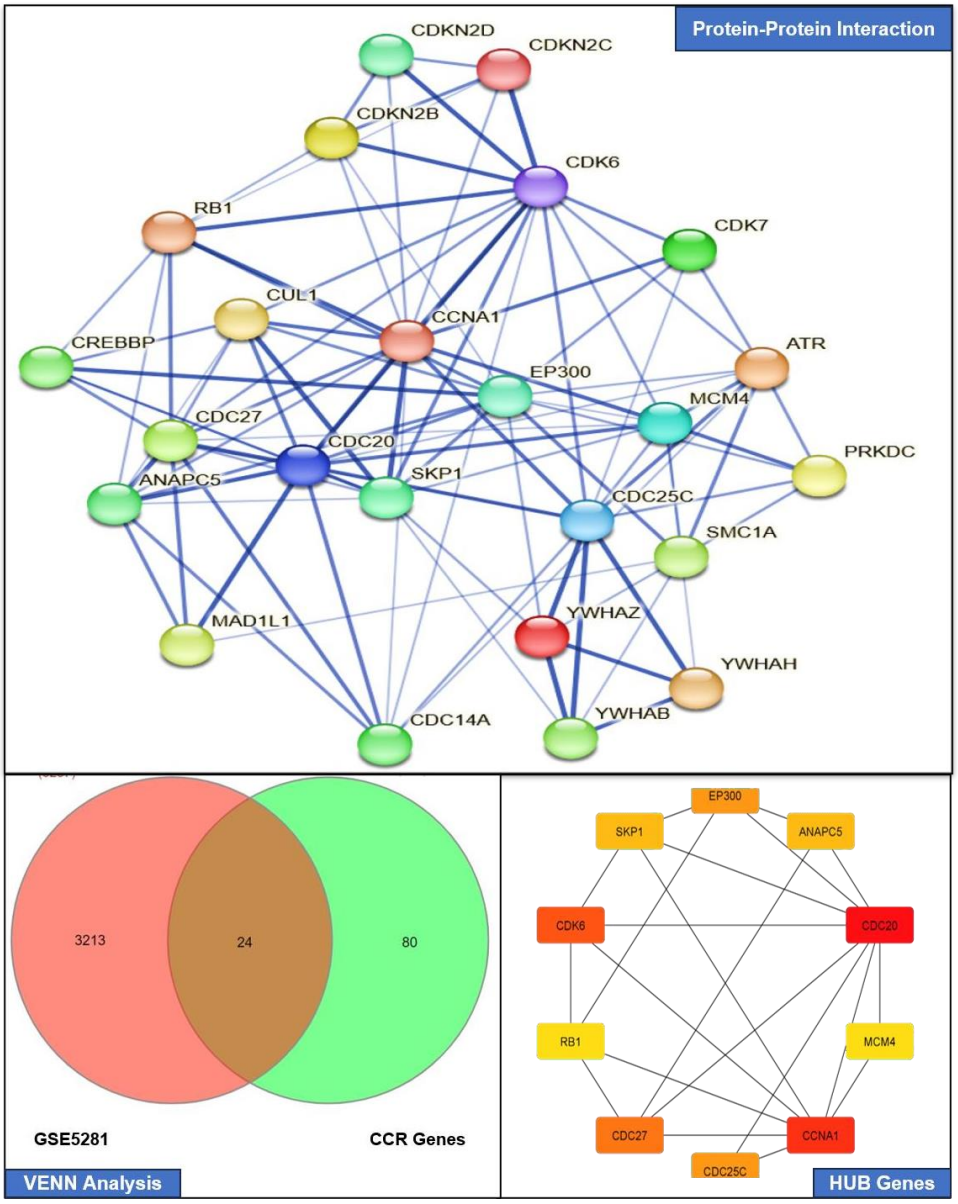

Fig 4.1. Protein-Protein interaction analysis of 24 CCR genes, further through cytoscape tool hub genes identified

4.1.2 functional enrichment analysis of CCR genes in AD

Gene set enrichment analysis of DEGs was performed using gprofiler and ShinyGO, with pathways analysis through KEGG database. In the study we identified significant pathways using a fold enrichment threshold of 1.5 and adj P value < 0.05. Cell cycle pathway showed the highest fold enrichment (150), with

involvement of 20 genes (**Fig 4.2**). This implicates a strong association between cell cycle dysregulation and other pathways, like “Oocyte meiosis” with 15 genes and fold enrichment 130 and Ubiquitin mediated proteolysis with 12 genes and fold enrichment 80, were also indicated the significant enrichment. These results interpreted the potential role of cell cycle and UPS in the AD progression. Gene ontology was performed to determine the significant biological process with CCR genes. As depicted in **Fig 4.3**, cell cycle revealed significant enrichment, the top biological processes namely mitotic cell phase transition and regulation of mitotic cell cycle phase transition, both had fold enrichment of 30 involving 19 genes. Other biological processes also showed substantial fold enrichment namely negative regulation of cell cycle, cell cycle phase transition and mitotic cell cycle processes related to cell cycle indicating about the role CCR genes. Molecular processes of CCR genes showed that cyclin-dependent protein serine/threonine kinase inhibitor activity with highest fold enrichment value approximately 150 indicating the importance of CDK regulation within the CCR genes. Other substantially enriched molecular processes with fold enrichment 100 includes protein kinase inhibitor activity and kinase regulator activity, and kinase inhibitor activity. whereas per cellular process, all genes were observed in Nucleoplasm (GO:0005654) and nucleus (GO:0005634) with adj P value 6.0×10^{-6} and 4.0×10^{-2}, respectively**.**

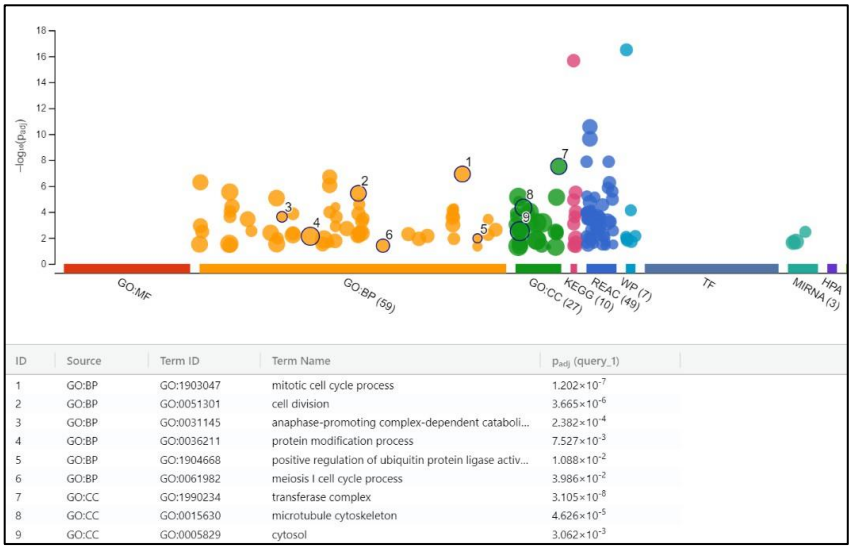

ID	Source	Term ID	Term Name	p_{adj} (query_1)
1	GO:BP	GO:1903047	mitotic cell cycle process	1.202×10^{-7}
2	GO:BP	GO:0051301	cell division	3.665×10^{-6}
3	GO:BP	GO:0031145	anaphase-promoting complex-dependent cataboli...	2.382×10^{-4}
4	GO:BP	GO:0036211	protein modification process	7.527×10^{-3}
5	GO:BP	GO:1904668	positive regulation of ubiquitin protein ligase activ...	1.088×10^{-2}
6	GO:BP	GO:0061982	meiosis I cell cycle process	3.986×10^{-2}
7	GO:CC	GO:1990234	transferase complex	3.105×10^{-8}
8	GO:CC	GO:0015630	microtubule cytoskeleton	4.626×10^{-5}
9	GO:CC	GO:0005829	cytosol	3.062×10^{-3}

Fig 4.2. Gene ontology prediction using gprofiler

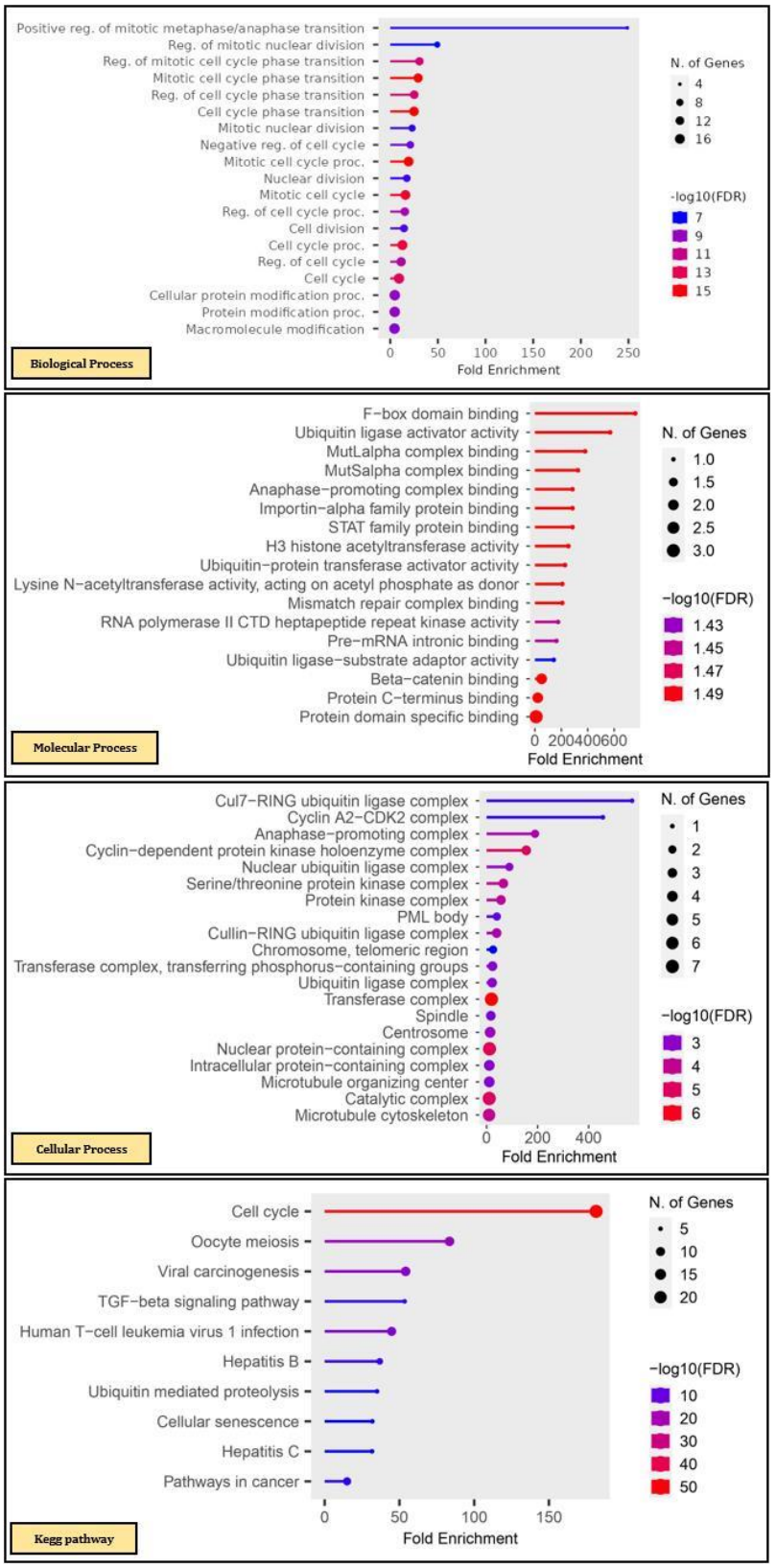

Fig 4.3. Gene ontology validation by ShinyGO

4.1.3 NPASS library screening

The NPASS is a library of 43,825 natural compounds, which was explored for the natural products with quantitative concentration data. The reference compound used in this study was fisetin and tanimoto algorithm was used for the database mining. In filtering the NPASS database, the Tanimoto method measures the similarity between a reference drug, and natural compounds. We can filter out compounds that are dissimilar to the fisetin by setting a threshold Tanimoto coefficient, retaining those with a high degree of similarity. This approach is essential for narrowing down large datasets to a manageable number of relevant compounds for further analysis. We uploaded the smile of fisetin in the NPASS database at structure search and selected a 0.7 threshold of Tanimoto similarity, which is a measure of similarity between two sets, which often helps in data mining, informatics retrieval, and bioinformatics [231]. After application of threshold tanimoto algorithm we screened and retrieved the .sdf file 191 natural compound and further filtered for pharmacokinetics profiling through SWISSADME database.

4.1.4 Pharmacokinetics profiling

In this study, physiochemical and pharmacokinetics evaluation of the selected 191 natural compounds retrieved from NPASS database were done for further analysis. Drug-likeness was assessed to determine whether the natural products have favorable ADME properties [232]. Drug likeness of natural products depends on Lipinski's rule of five, which was an established filter to determine whether a compound can be absorbed orally, the efficiency of drug absorption from the bloodstream, and factors influencing absorption such as molecular size, lipophilicity, and the presence of efflux transporters. The BBB permeability determines whether a compound can cross the blood-brain barrier and affect the CNS. The P-glycoprotein (Pgp), an efflux transporter belonging to the ATP-binding cassette (ABC) transporters, recognizes several different xenobiotics, and many of them are CYP3A4 substrates. The pan-Assay Interference Compounds

(PAINS) filter was assessed to investigate and filter out compounds that may interpret false positive results in various bioassays. These compounds are often found to interfere with a wide range of biological assays and can lead to misleading conclusions during drug discovery. The Brenk filter was used to identify potentially problematic chemical structures. These filters are designed to recognize sub-structures that may lead to false positives. Subsequently, we filtered 154 natural compounds from 191 previously retrieved natural compounds on the basis molecular weight further applied various parameters namely Lipinski rule of 5, PAINS, and Brenk rule based on them we extracted 11 compounds. The pharmacokinetic profile of filtered compounds with high GI absorption and BBB permeability along with binding affinity scores obtained through molecular docking is further represented in **Table 4.1**.

Table 4.1. ADME Analysis with Binding score of selected natural compounds

Natural compound ID	TPSA	iLOGP	XLOGP3	WLOGP	MLOGP	GI absorption	BBB permeant	Binding Affinity Score	Lipinski violations/ PAINS/ Brenks alerts	Bioavailability Score
NPC209560	59.67	2.49	2.8	3.17	1.33	High	Yes	-8.177	0	0.55
NPC201284	30.21	2.51	3.18	3.46	2.27	High	Yes	-8.035	0	0.55
NPC314329	26.3	2.41	3.14	3.07	2.47	High	Yes	-8.544	0	0.55
NPC172262	70.67	1.97	3.56	2.8	1.33	High	Yes	-8.477	0	0.55
NPC234560	70.67	1.77	2.47	2.87	1.08	High	Yes	-8.099	0	0.55
NPC222342	75.99	2.41	2.85	2.49	0.96	High	Yes	-7.448	0	0.55
NPC20287	66.76	3.48	2.76	3.23	2.14	High	Yes	-6.784	0	0.55
NPC108455	67.13	3.43	3.07	3.49	0.94	High	Yes	-7.087	0	0.55
NPC215932	76.36	3.66	3.5	3.5	0.63	High	Yes	-7.377	0	0.55
NPC40818	76.36	3.71	3.04	3.5	0.63	High	Yes	-7.322	0	0.55
NPC176814	74.22	2.8	3.59	2.99	2.12	High	Yes	-7.240	0	0.55

4.1.5 Interpretation of interaction of lead compound and CDK6

The molecular docking of filtered natural compounds with CDK6 (PDB ID-1XO2), was performed for studying their molecular similarity with the reference drug fisetin. In the present study, Webina tool was used, which involves computational algorithms to identify the natural compounds that bind specifically to CDK6. The interpretation of this study gave the binding energy, which is crucial for understanding the interaction. The strength of binding is often quantified by the binding energy; a high negative binding energy score corresponds to a strong interaction. The filtered 11 drugs were screened for their ability to bind to the CDK6, and the binding score was determined. The reference compound fisetin showing the binding score of (-7.589 Kcal/mol). The natural compounds having docking score more than that of fisetin were selected as potential compound, amongst which NPC314329 had the highest binding affinity as compared to the reference compound. The interaction of NPC314329 with CDK6 is represented in **Fig 4.4**.

The information about the active site of CDK6 was collected, and the ATP-binding site was deeply analyzed, which was occupied by **Lys43, Phe98, His100, Asp104, Thr107, and Asp163** [233]. The interactive active site residues in CDK6-Fisetin complex are **ILE12, GLY13, GLY15, GLY18, VAL20, ALA33, LYS35, HIS95, VAL96, PHE98, ASP99, ARG101, THR102, LEU147, ASP158.** These residues are primarily involved in the ATP binding and the kinase activity of CDK6. This complex was stabilized by a Conventional Hydrogen Bond at **HIS100, VAL101, GLN149 and ASP163** position, and several hydrophobic interactions at positions **VAL20, ALA33, and LEU147**. **CDK6-NPC314329** was stabilized by Conventional Hydrogen Bond at **HIS100, VAL101, ASP104, ASP163** Carbon Hydrogen Bond at **GLN103** and several other hydrophobic interactions at position **ILE19, VAL27, ALA41, VAL77, LEU152, and ALA162.**The common hydrogen bonds at following residues **HIS100, VAL101, ASP163** are found in both ligands The distances in NPC314329 are generally shorter, indicating potentially stronger hydrogen bonding compared to Fisetin. NPC314329 has a slightly better binding affinity (-8.544 kcal/mol) compared to

Fisetin (-7.589 kcal/mol), suggesting that NPC314329 may bind more tightly to the target. NPC314329 engages in hydrophobic interactions with residues that are involved in hydrogen bonding as well. This could enhance the stability of NPC314329's binding due to overlapping interaction types.

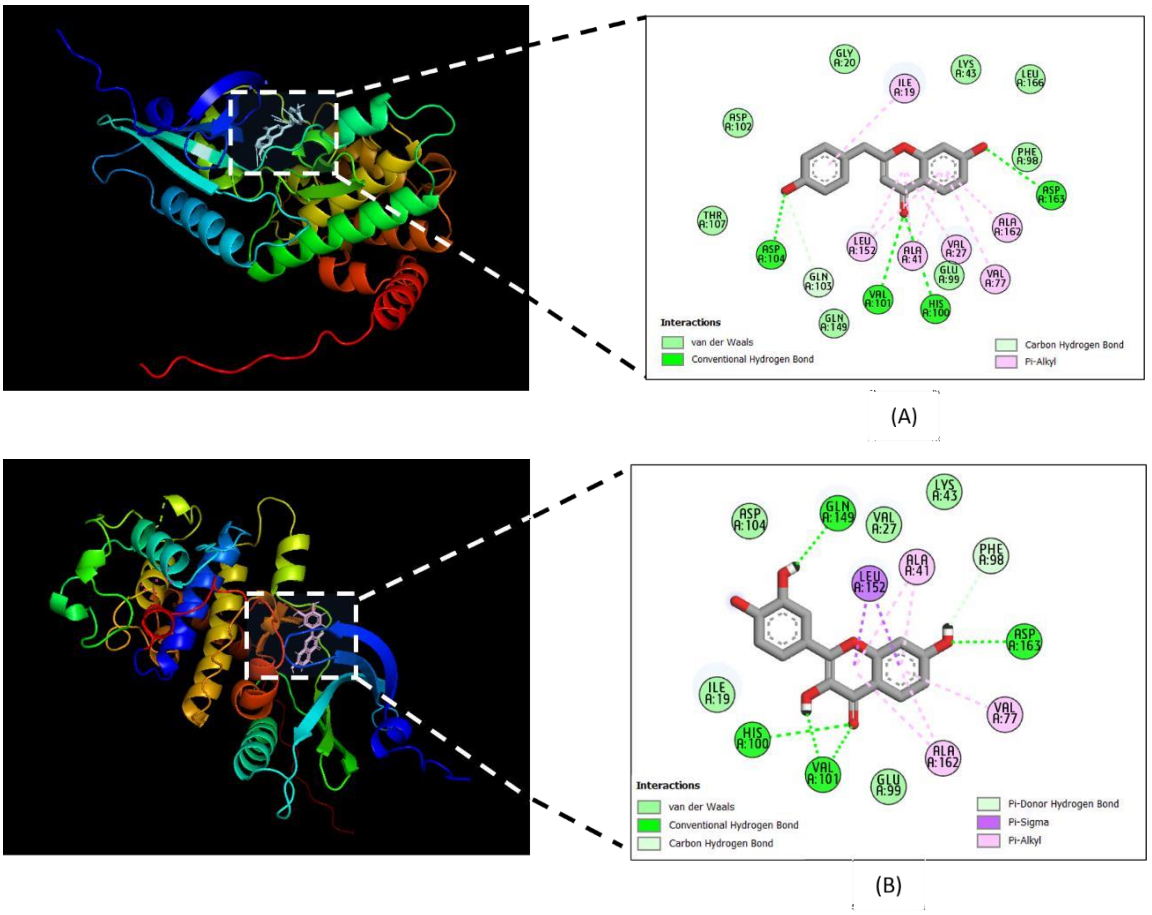

Fig 4.4. Interaction analysis of CDK6 ligand complexes A) CDK6-NPC314329 B) CDK6-Fisetin

4.1.6 CDK6 - NPC314329 Dynamic Stability Interpretation

To enhance the accuracy of the study, the reliability and stability of the result, we performed the MD simulation. This helped us to analyzed the changes in the CDK6 - NPC314329 complex confirmation during the period of MD simulation. The exact movement of each atom during the entire time duration was predicted

by the MD simulation, which helped us to implicate the fluctuation and changes in the CDK6 structure. The simulation was performed for 100 ns and post MD simulation result was assessed based on RMSD, Rg, RMSF, Hydrogen bond, and distance.

4.1.6.1 Root Mean Square Deviation (RMSD)

The RMSD analysis of the APO protein (CDK6) as depicted in **Fig 4.5** shows that during the first 10 ns, RMSD of APO protein reached at a peak of 1.2 nm, indicating conformational changes at the start of simulation. After 10 ns, the system demonstrated significant fluctuations, with RMSD lying between 0.6 nm to 1.2 nm. This shows that APO protein remains unstable during the entire period of simulation, whereas CDK6-NPC314329 complex RMSD demonstrates a more stable conformation. The RMSD of this complex rises during the initial 10 ns, but the system stabilized after the 10 ns time, maintaining RMSD value in the range 0f 0.4 nm to 0.8 nm. This result interpreted that CDK6-NPC314329 complex exhibits a higher stability as compared to APO protein, during the entire duration of 100 ns of the simulation.

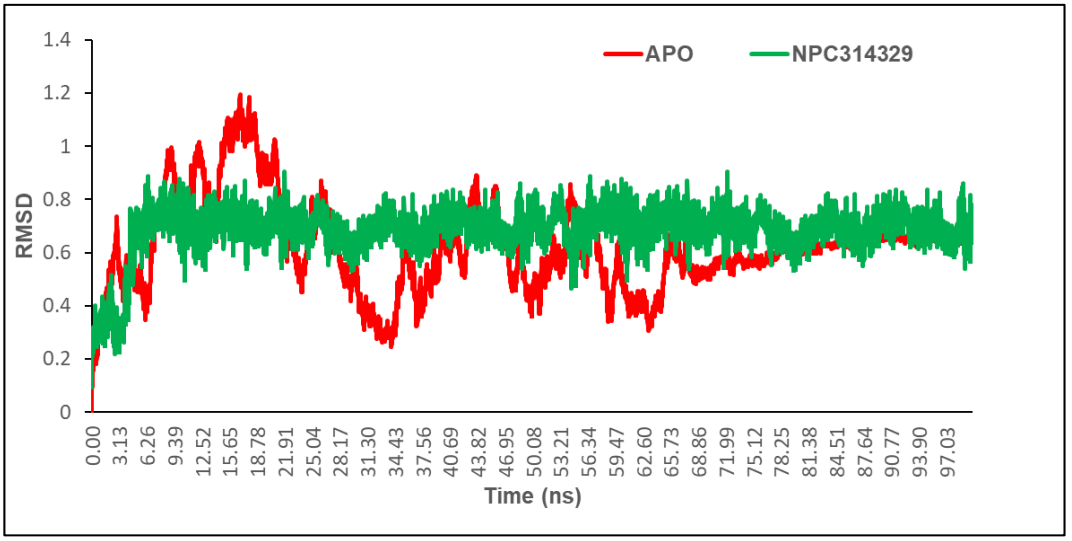

Fig 4.5. RMSD representation of CDK6-NPC314329 complex

4.1.6.2 Root Mean Square Fluctuation (RMSF)

To evaluate the flexibility of APO protein and CDK6 - NPC314329 complex, RMSF was performed for each residue during the simulation (**Fig 4.6**). The value of RMSF for most residues showed minor fluctuations indicating a high stability in both forms. Most of the residues showed fluctuations below 0.5 nm, indicating the stability of protein core in both - APO protein and the ligand complex. The residues (1-30), showed a marginal increase in the flexibility with RMSF values approaching 1.0 nm in which CDK6-NPC314329 complex demonstrated higher fluctuation than the APO form. In central region both the forms are showing RMSF value around 0.5 nm. Whereas residues (300-321) located near the C-terminal showed a sharp rise in the RMSF value of approximately 2 nm, indicating about the flexibility of the protein which was more than the rest of the area of protein. Ligand complex indicated a higher fluctuation than the APO form. Further, overall value of RMSF interpretation shows that both the protein forms maintain stability throughout its length, but binding of NPC314329 to the CDK6 induces the localized flexibility at the C- terminal.

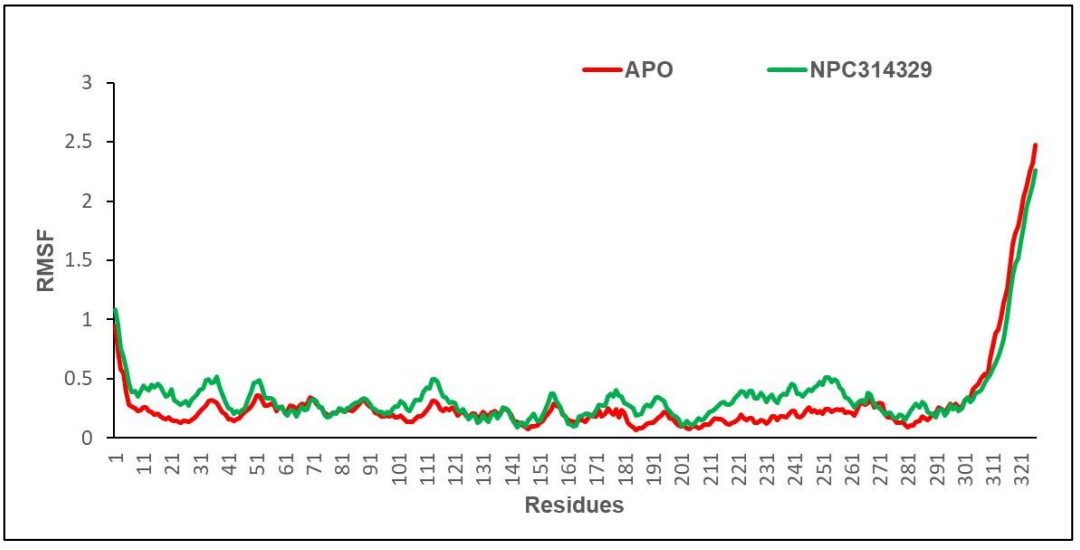

Fig 4.6. RMSF representation of CDK6-NPC314329 complex

4.1.6.3 Radius of Gyration (Rg)

The Rg depicts the distribution of mass of the molecules around its Centre of mass. It gives an insight about the compactness of the structure, lower Rg value indicates a more compact and stable structure. In the graph (**Fig 4.7**), it is seen that NPC314329 stabilizes at a lower Rg value, particularly after around 20 ns, suggesting a more compact and stable molecular structure. This consistent lower Rg indicates that NPC314329 takes a more stable arrangement in comparison to the APO state, likely due to favorable interactions or binding. Overall, NPC314329 exhibits greater structural stability and compactness throughout the simulation, potentially strengthening its biological relevance and functional efficiency as compared to the APO form.

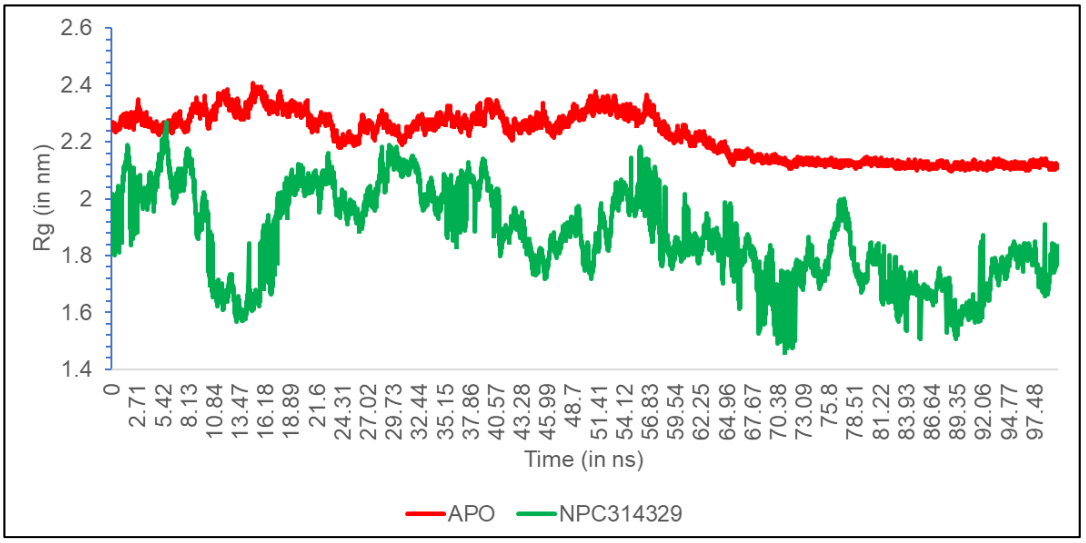

Fig 4.7. Radius of Gyration representation of CDK6-NPC314329 complex.

4.1.6.4 Hydrogen bond and minimum distance analysis

Furthermore, the NPC314329 formed the hydrogen bonds with the CDK6, and the survival time of these H-bonds and the number of H-bonds reflected the degree of binding between the complex till the 100 ns simulation. The main aim was to analyse both the stability as well as the number of hydrogen bonds formed within

a 0.35 nm threshold (**Fig 4.8**). The number of H-bonds were between 2-6 for the most of duration during the simulation. Maximum number of H-bonds formed during 55-90 ns reached a significant rise in peak of 9 H-bonds approximately. The overall minimum distance ranged between 0.16 to 0.22 nm for the entire duration of the simulation (**Fig 4.9**).

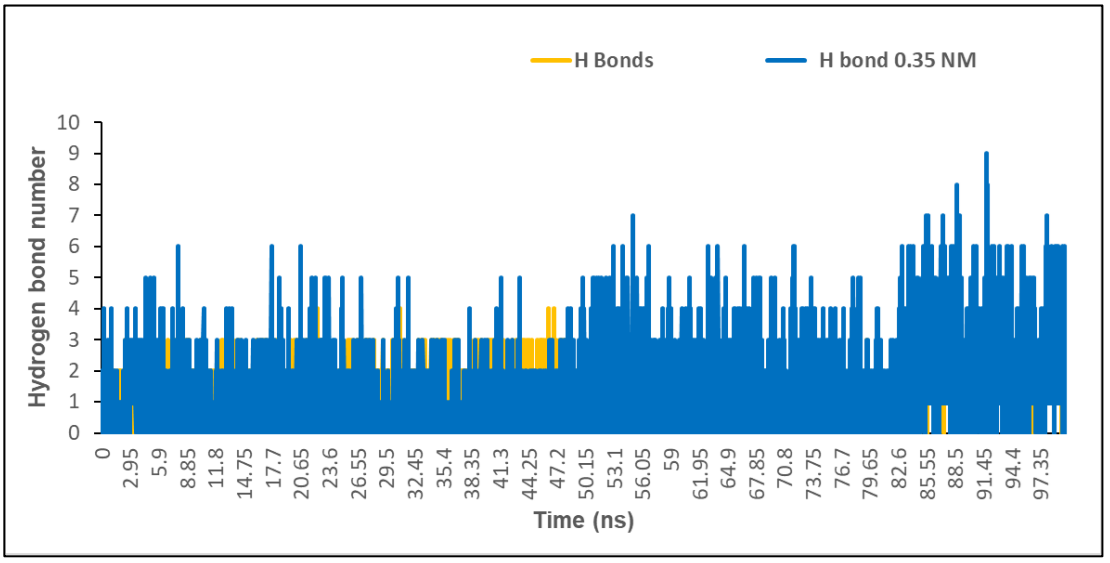

Fig 4.8. Number of Hydrogen bonds formed by NPC314329 with the CDK6 within 0.35 nm threshold

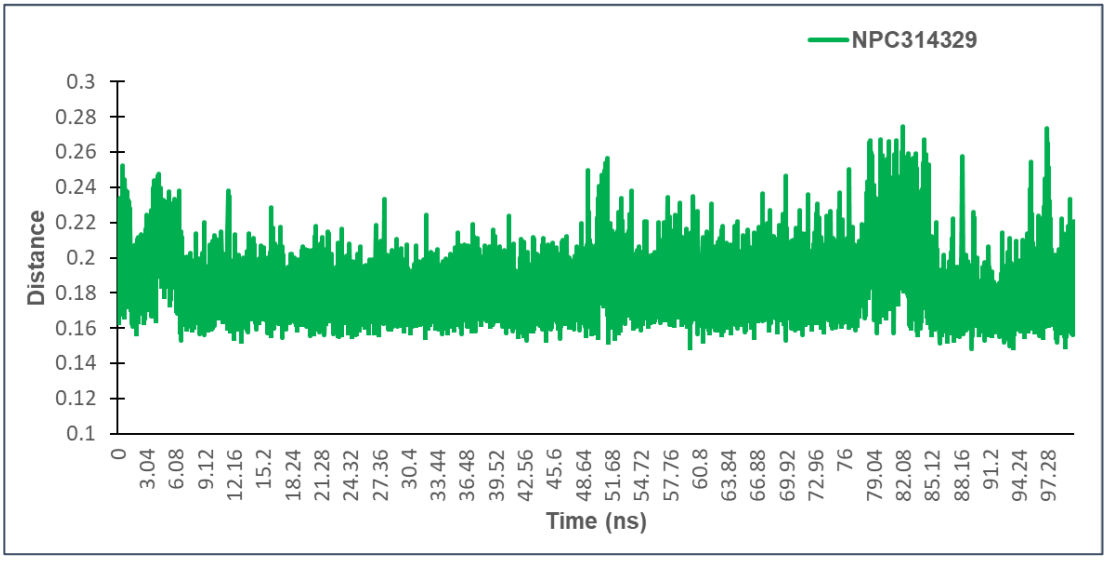

Fig 4.9. Minimum distance between the H-bonds formed by NPC314329

4.2 Research objective 2: To develop the novel therapeutic agents that target CDK4 to control NDDs.

4.2.1 Natural Compounds as Potential CDK4 Inhibitors in NDDs

Developing effective therapies for NDDs remain offer cost-effective means to generate preliminary data a formidable challenge. Recognizing the potential of natural products, traditionally acknowledged for their therapeutic benefits and safety, researchers are increasingly turning to computational studies to screen and predict the potential of these compounds as drug candidates. These computational approaches, employing methods like molecular docking and molecular dynamic simulation, offer a cost-effective means to generate preliminary data, guiding the selection of promising natural products for further in vitro and in vivo studies, facilitating the identification of lead compounds, and expediting the drug discovery process in the quest for safer and more efficacious treatments for NDDs. Our quest is not only to unravel the mysteries of CDK4 but also to pioneer innovative therapeutic modalities that may redefine the landscape of NDDs research and treatment.

4.2.2 Structural Analysis for Predicting Key Residues and Binding Sites of CDK4

Understanding the three-dimensional structure of CDK4 is crucial for unraveling its functional dynamics and identifying potential points of interaction with Palbociclib-like natural products. CDK4 consists of distinct structural domains that confer its specific functions. In this study, we retrieved the CDK4 (2W96) structure from the RCBS database, a complex of chain A, i.e., cyclin, and chain B belonging to CDK4. We selected chain B for our study with a sequence length of 303 amino acids in which the PISTVRE-like cyclin binding domain is present at the 50th-56th position, the protein kinase domain is situated from the 3^{rd}-267^{th} position, and the ATP binding site is at the 12^{th} -35^{th}, as per the data available from Interpro database [234]. According to literature analysis, Lys35 is an

important residue in the catalytic domain, and Phe93 acts as a gatekeeper residue and their active site is located at 133rd -145th position as per Interpro result [234]. When we assessed the PDBSUM database for motif analysis of 3rd -267th position, we found that 2W96 consists of N-lobe and C-lobe with 2β sheets A and B, antiparallel in nature with 5β strand in sheet A and 2β strand in sheet 2, 4β hairpins are situated at strand 1 and 2. Locations of β hairpins are as follows, 1 at (Glu7 -Gly13) – (Val20-Arg24), 2 at (Val20-Arg24)-(Phe31-Pro40), 3 at (Leu74 -Arg82)-(Glu86-Glu94) and 4 at (Ile146-Val148)-(Val154-Leu156). The location of β strands is denoted as 1st (Glu7-Gly13), 2nd (Val20-Arg24), 3rd (Phe31-Pro40), 4th (Leu74 -Arg82) ,5th (Glu86-Glu94), 6th (Ile146-Val148), 7th (Val154-Leu156) [235]. Studies on CDK4 have also shown that certain specific residues are more frequently engaged in binding naturally in the ATP cleft e.g. Ile12, Val20, Ala33, Val77, Phe93, Glu94, His95, Val96, Gln98, Asp99, Thr102, Glu144, Leu147, Ala157, Asp158 whereas Glu144 interacts with the terminal phosphates of ATP as depicted in **Fig 4.10** where it can be seen that CDK4-Palbociclib binding at the active site in which hydrogen bond interaction at GLY15, LYS35 [236].

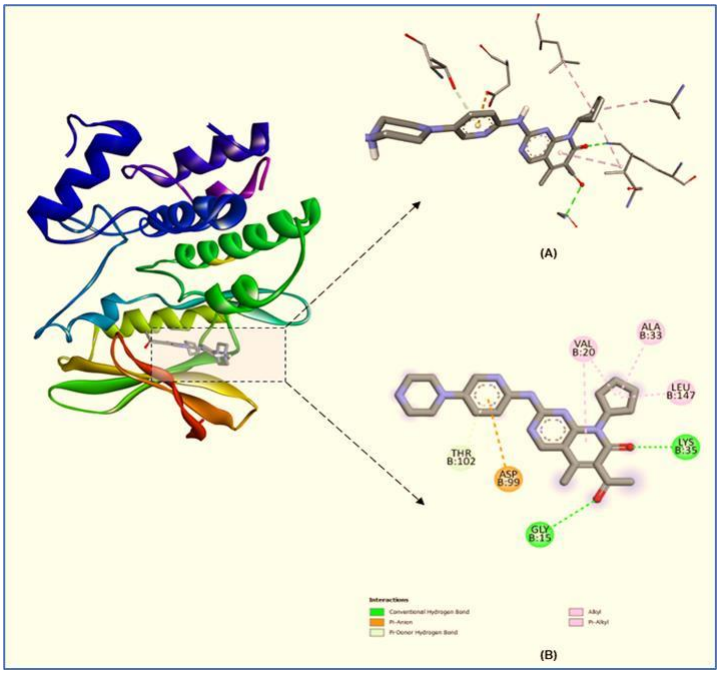

Fig 4.10. CDK4-Palbociclib binding at the active site depicting Hydrogen bond interaction at GLY15, LYS35, and hydrophobic interaction at VAL20, ALA33, ASP99, THR102, LEU147.

4.2.3 Database mining

The current study selected Palbociclib, a CDK 4/6 inhibitor molecule, as the reference drug. Palbociclib can split CDK4/6-cyclin-D complexes, inhibiting pRb phosphorylation and E2F1 release, which results in G1 phase arrest and cell growth reduction, even though CDK4/6 can bind cyclin D and cause pRb hyperphosphorylation [237]. Palbociclib has an elimination half-life of more than 29 hours. The liver is the main metabolic area, where SULT2A1 and CYP3A are involved in metabolism; the kidneys and feces account for 17.5% and 74.1% of excretion, respectively. In the present study, we used the Tanimoto similarity method, which is a widely used metric in cheminformatics for comparing the similarity between two molecular structures [231]. This method calculates the similarity between two sets of binary data, typically representing the presence or absence of certain features in the molecules (such as chemical substructures or fingerprints) [219], [238]. A threshold of 75% has been found to provide a good compromise between sensitivity and specificity and minimize the false positive and false negative rate. This threshold is often chosen because it is high enough to ensure meaningful similarity. As a result, we extracted 1017 natural compounds and retrieved (.sdf) files for further analysis.

4.2.4 ADME prediction

In this research, we assessed compounds denoted by their CNP identifiers to evaluate their suitability as potential pharmaceutical agents, filtered the compounds on the basis of SWISSADME parameters like Lipinski rule of 5, PAINS, and brenk and we identified 110 natural compounds. Among these compounds, CNP0070947 stood out as a highly promising candidate owing to its favorable molecular attributes and pharmacological properties. With a molecular weight (MW) of 322.36, CNP0070947 demonstrated exceptional solubility and notable lipophilicity, as confirmed by its logP values of 2.54 (iLOGP) and 1.14 (XLOGP3), respectively. Additionally, CNP0070947 exhibited favorable ADME characteristics, including permeability across the BBB and its status as a substrate

for P-glycoprotein (Pgp), suggesting its potential for efficient delivery and distribution throughout the organism. Despite CNP0070947 presenting the most promising profile, other compounds also displayed significant attributes worthy of consideration. For example, CNP0346604 exhibited moderate to high solubility and favorable lipophilicity (with logP values of 2.74 (iLOGP) and 1.7 (XLOGP3), respectively), in addition to interactions with cytochrome P450 enzymes (CYPs) as depicted in **Table 4.2**. In the same way, CNP0396493 has displayed high solubility and lipophilicity, making it another compound worthy of further examination. Overall, this study showcases valuable insights into the drug-likeliness of these natural compounds forming a base for future research endeavours to utilize their therapeutic potential.

Table 4.2. Drug likeliness of selected compounds

Compound ID	GI Absorption	BBB	Lipinski violations	PAINS alerts	Brenk alerts	Log $P_{o/w}$	Log S	Log Kp	Synthetic Bioavailability
CNP0376445	High	Yes	0	0	2	2.46	-3.83	-6.83	2.16
CNP0352050	High	Yes	0	0	0	3.10	-4.17	-5.90	2.78
CNP0267694	High	Yes	0	0	0	2.27	-3.63	-6.80	2.61
CNP0346604	High	Yes	0	0	0	2.39	-3.26	-7.22	2.85
CNP0396493	High	Yes	0	0	0	2.84	-3.53	-6.74	3.12
CNP0070947	High	Yes	0	0	0	1.80	-2.76	-7.46	3.34
CNP0319774	High	Yes	0	0	1	3.18	-4.29	-5.82	2.18
CNP0396034	High	Yes	0	0	0	2.55	-3.21	-6.94	2.58
CNP0162466	High	Yes	0	0	0	2.50	-3.25	-6.81	2.48
CNP0438514	High	Yes	0	0	0	3.30	-4.43	-5.92	2.63

4.2.5 Molecular docking analysis

The molecular docking of 110 filtered natural compounds with CDK4 (2W96), was performed for studying their molecular similarity with the reference drug palbociclib. In the present study, Webina tool was used, which involves computational algorithms to interpret the natural compounds that bind specifically to CDK4 (PDB: 2W96). The interpretation of this study gave the binding energy, which is crucial for understanding the interaction between CDK4 and natural compounds. The strength of binding is often quantified by the binding energy; a

high negative binding energy score corresponds to a strong interaction. The filtered 110 drugs were screened for their ability to bind to the CDK4 (2W96), and the binding score was determined. The top 10 natural compounds were determined based on the highest negative binding energy scores, as depicted in **Table 4.3**. The molecular docking studies revealed that palbociclib bound with CDK4 with binding energy (or the affinity score) of -8.988 kcal/mol. Based on affinity scores, 37 compounds with affinity score more than palbociclib were observed and we selected top 10 compounds with COCONUT ID: CNP0376445, CNP0352050, C N P 0267694, C N P 0346604, C N P 0438514, C N P 0396493, CNP0070947, CNP0319774, CNP0396034, and CNP0162466 for further analysis and the interpretation is represented in **Table 4.3**. In this study, we also used FastDRH for docking study validation. Finally, we filtered the top 4 natural compounds CNP0376445, CNP0267694, CNP0396493, and CNP0070947 as hit compounds for further evaluation.

Table 4.3. 2D structure and binding free energy in Kcal/mol of selected natural compounds

Compound ID	Structure	Affinity score (Kcal/mol)	fastDRH score (Kcal/mol)
CNP0376445	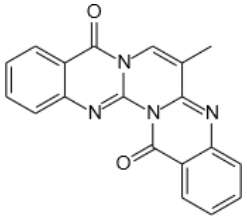	-9.99	-9.90
CNP0162466	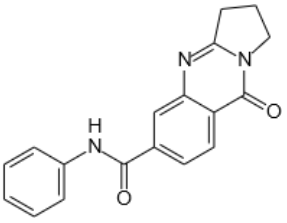	-9.83	-8.69
CNP0396493	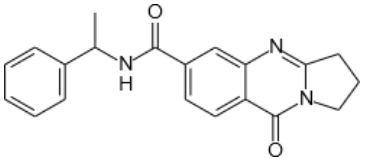	-9.79	-8.84

CNP0352050	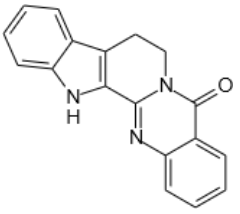	-9.74	-9.46
CNP0346604	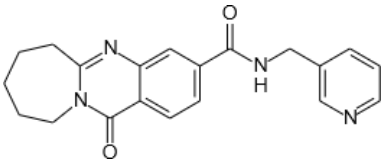	-9.72	-8.88
CNP0319774	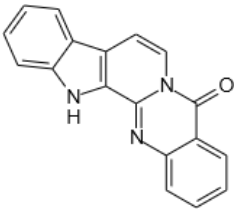	-9.67	-8.77
CNP0267694	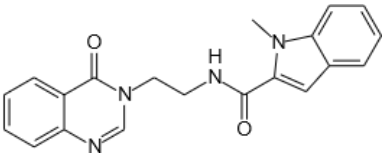	-9.64	-9.09
CNP0070947	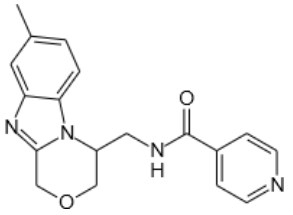	-9.55	-8.78
CNP0396034	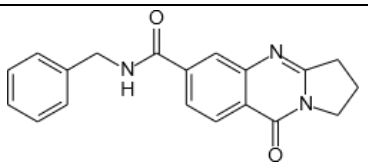	-9.32	-8.74
CNP0438514	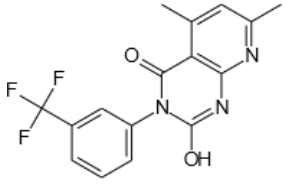	-9.00	-8.44

4.2.6. Interpretation of interaction of hit compounds with CDK4

The top hit compounds retrieved through molecular docking studies have a comparatively higher negative binding affinity as well as key residue interaction with CDK4. In this study, we opted for compounds that have a negative binding

score of more than -8.988 kcal/mol from Webina. Further, fastDRH was also utilized as a criterion for the selection of hit compounds on the basis of a docking score of more than -8.57 kcal/mol and a GB1 score of more than -32.5 kcal/mol. Accordingly, taking into consideration the score obtained from Webina and fastDRH, the four natural compounds selected were CNP0070947, CNP0376445, CNP0267694, and CNP0396493 as depicted in **Fig 4.11.**

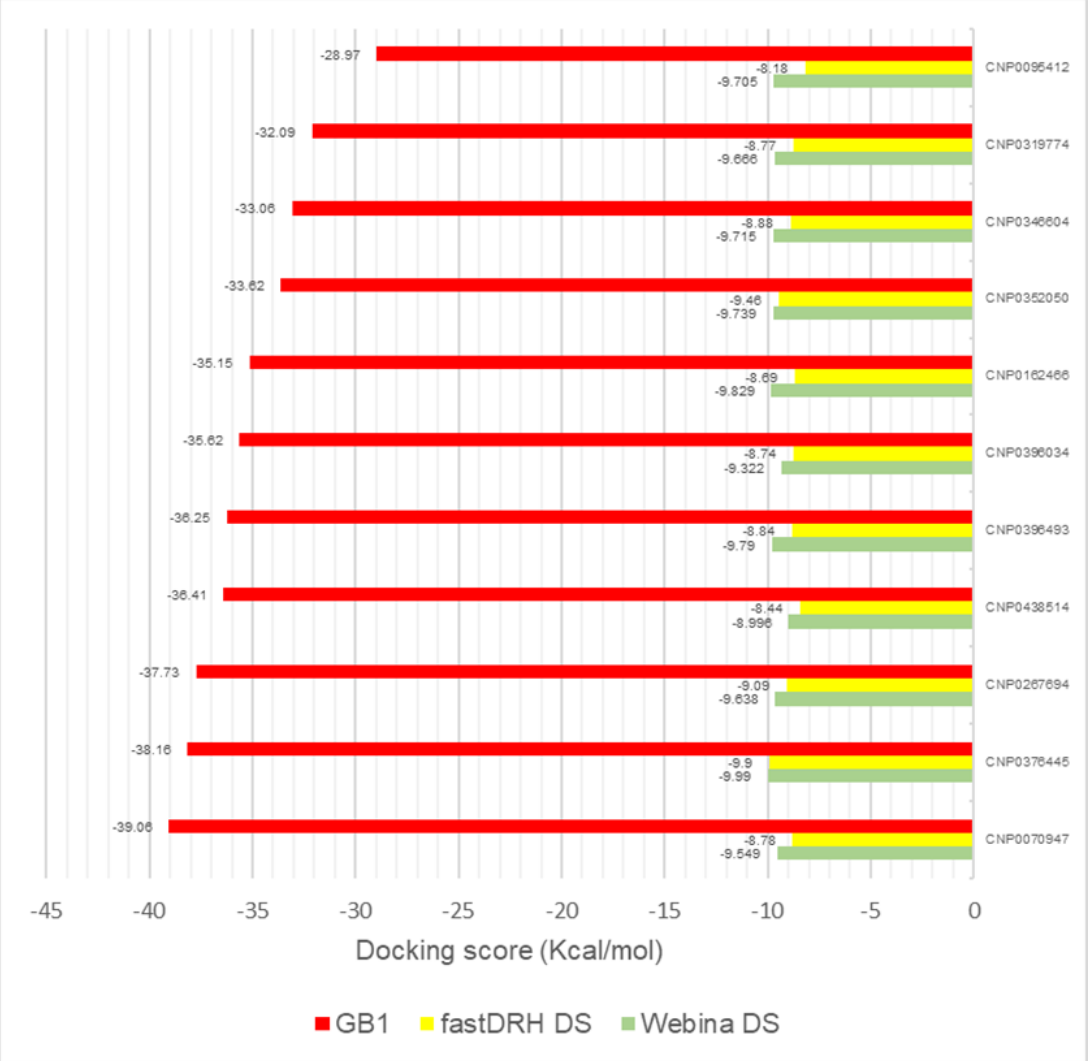

Fig 4.11. Docking score interpretation illustrating the selected compounds' binding affinity after filtration through the SWISSADME tool. Top ten compounds (CNP0376445, CNP0352050, CNP0267694, CNP0346604, CNP0438514, CNP0396493, CNP0070947, CNP0319774, CNP0396034, and CNP0162466) with the

highest negative binding energy after molecular docking by different tools such as fastDRH, Webina and arranged on the basis of GB1 total binding energy.

The interactive active site residues in CDK4-Palbociclib complex are ILE12, GLY13, GLY15, GLY18, VAL20, ALA33, LYS35, HIS95, VAL96, GLY98, ASP99, ARG101, THR102, LEU147, ASP158. These residues are primarily involved in the ATP binding and the kinase activity of CDK4. This complex was stabilized by a Conventional Hydrogen Bond at GLY15, LYS35 position, and several hydrophobic interactions at positions VAL20, ALA33, and LEU147. This palbociclib complex interferes with substrate accessibility and this interferes with its kinase activity. The amino acid residues among hit compounds analysis were with different types of interactions, namely hydrogen bonds, hydrophobic contacts, π-stacks, π alkyl, and alkyl contact. CNP0376445 forms two hydrogen bonds with LYS35, ARG101 while CNP0267694 forms four hydrogen bonds with ILE12, ALA16, ARG101, ASP158. CNP0396493 forms Hydrogen Bond at LYS35, GLU94, HIS95, VAL96, ARG101 and CNP0070947 forms Hydrogen Bond at GLY15, TYR17, LYS35, GLU144. LYS35 is the common residue involved in the Hydrogen bond formation in all hit compounds except CNP0267694. Hydrophobic interaction at LEU147 is common in all the hit compounds, whereas ALA33 is also involved in all hit compounds in hydrophobic contacts except CNP0267694. The ligand binding sites and hydrogen bonds formed by these hit compounds are shown in **Table 4.4.** and **Fig 4.12**.

Table 4.4. Ligand binding interactive residue sites of CDK4 and hit selected compounds

Compound ID	Ligand binding sites	Residues involved in hydrogen bond formation (Distance in Å)	Number of Hydrogen bonds formed	Residues involved in hydrophobic Interactions	Binding Affinity (Kcal/mol)
CNP0267694	ARG101, ASP158, ILE12, ALA16, LEU147, ALA33	ARG101 (3.30) ASP158 (3.63) ILE12 (3.67) ALA16 (3.72)	04	LEU147, ALA33	-9.63
CNP0376445	LYS35, ARG101, LEU147, LYS142, ILE12, VAL20, ALA33	LYS35 (3.02) ARG101 (3.25)	02	LEU147, LYS142 ILE12, VAL20, ALA33	-9.99
CNP0396493	LYS35, HIS95, ARG101, GLU94, ASP158LEU147, ALA33, VAL72, ALA157,ALA16, PHE93,VAL96	LYS35 (3.42) HIS95 (3.36) VAL96 (3.82) ARG101 (3.07) GLU94 (3.32)	05	LEU147, ALA33, VAL72, ALA157, ALA16, PHE93, ASP158	-9.79
CNP0070947	GLY15, TYR17 GLU144, LYS35 ASP158, EU147, ALA33, ALA157, ALA16, PHE93	GLY15 (3.29) TYR17 (3.19) GLU144 (3.21) LYS35 (4.00)	04	ASP158, LEU147 ALA33, ALA157 ALA16, PHE93	-9.55

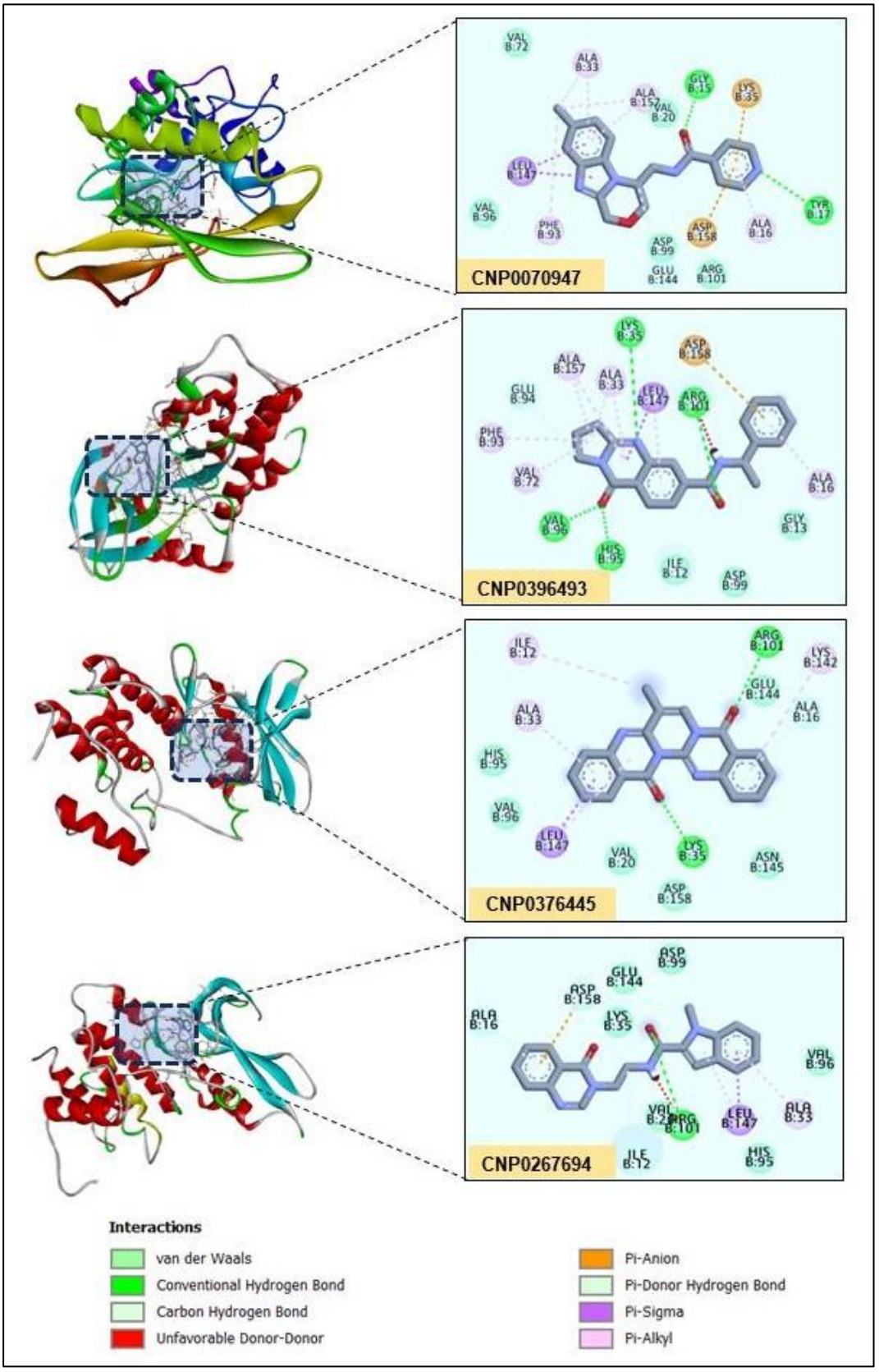

Fig 4.12. Two-dimensional interaction between CDK4 and selected hit compounds- depicting different types of interactions such as van der Waals,

conventional hydrogen bond, carbon-hydrogen bond, pi anion, pi -donor hydrogen bond, pi sigma, pi alkyl bond. In CNP0070947, active residues involved in an interaction

To further validate the ligand molecule complex, MM/GBSA and MM/PBSA were used for the calculation of free energy, which was performed by the fastDRH tool. This tool determines the electrostatic energy (ELE), van der Waals (VDW), and internal energy (INT) as calculated by the MM forcefield; total gas phase energy (GAS) sum of ELE, VDW, and INT, PBSUR/GBSUR, based on empirical model to calculate solvation free energy contributed by non-polar solvation; PBCAL/GB solvation free energy contributed by electrostatic; PBSOL/GB/SOL, solvation based on the sum of polar and non-polar; PBTOT/GBTOT, and the final binding energy (Kcal/mol). In the present study, we assessed fastDRH for determining the decomposition energy of Palbociclib, CNP0070947, CNP0376445, CNP0267694, and CNP0396493 with CDK4 and the result is depicted in **Table 4.5**. Based on the data provided by fastDRH, ΔEVDW was considered as important parameter for molecular complex formation, and it was observed that CDK4 molecular complex with palbociclib has ΔEVDW value of -41.21 Kcal/mol and with the natural compounds CNP0070947, CNP0376445, CNP0267694, and CNP0396493 this value of ΔEVDW (Kcal/mol) have been found to be -46.09, -44.21, -45.29, and -42.54, respectively. The result interpretated that total binding energy (TOT) (Kcal/mol) for Palbociclib, CNP0070947, CNP0376445, CNP0267694, CNP0396493 with CDK4 was -32.72, -39.16, -38.16, -37.73, and -36.25 respectively. Decomposition Energy per residue of CDK4 with reference and selected phytochemicals is depicted in **Fig 4.13**.

Table 4.5. MM/GBSA score (Kcal/mol) of CDK4-selected compounds complex and the reference drug

Complex formed with CDK4 (2W96)	VDW	GAS	PBSUR/ GBSUR	PBCAL/ GBCAL	PBSOL/ GBSOL	PBELE/ GBELE	PBTOT/ GBTOT
Palbociclib	-41.21	-41.21	-5.32	13.81	8.49	13.81	-32.72
CNP0070947	-46.09	-46.09	-5.6	12.64	7.04	12.64	-39.06
CNP0376445	-44.21	-44.21	-5.19	11.25	6.05	11.25	-38.16
CNP0267694	-45.29	-45.29	-5.67	13.23	7.56	13.23	-37.73
CNP0396493	-42.54	-42.54	-5.7	11.98	6.28	11.98	-36.25

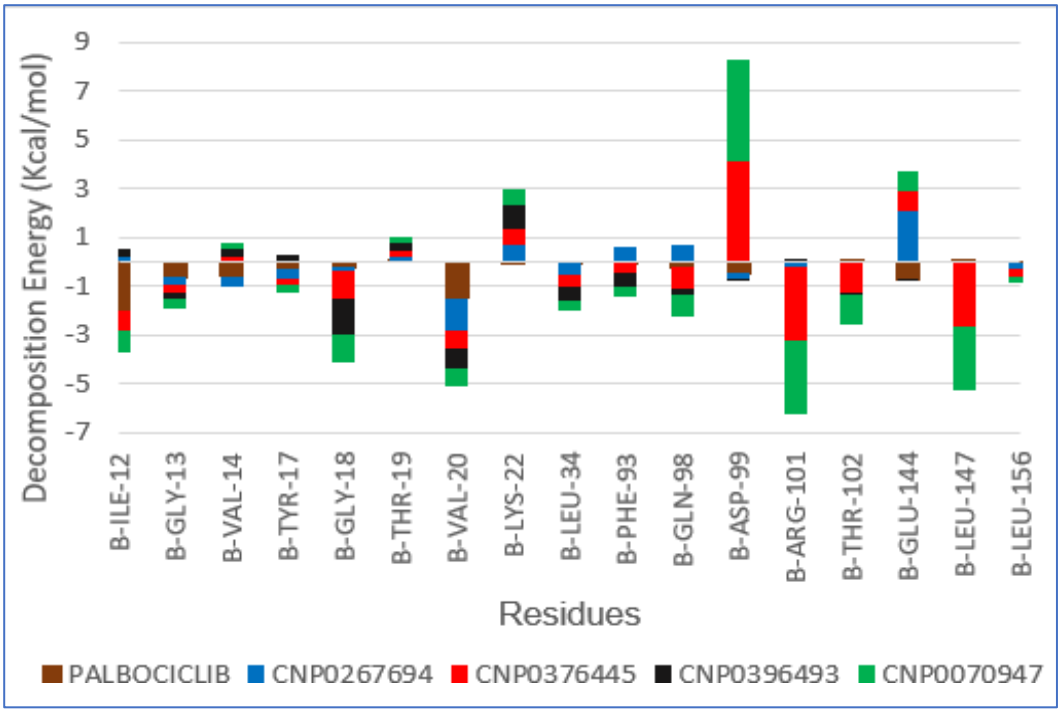

Fig 4.13. Decomposition energy per residue of CDK4 with reference and selected phytochemicals. Val 20 and ARG 101 are the best hotspot residues involved in active site binding in each complex.

4.2.7. Molecular Dynamics simulation

The use of molecular dynamics simulation enables the computation and prediction of compound stability. As a fundamental computational tool, molecular dynamics is highly effective in capturing molecular and atomistic changes. It plays a vital role in understanding the stability of protein-ligand complexes by analyzing deviations and fluctuations, as well as examining intermolecular interactions. Using conventional methods like molecular docking and virtual screening, the design of drugs based on structure provided a list of selected compounds. MD simulation is crucial for gaining insights into the dynamic properties of the ligand and its interaction with the protein. The CDK4 and hit compounds like CNP0070947, CNP0376445, CNP0267694, and CNP0396493 complex were

analyzed after MDS for 100 ns, and post MDS analysis result has interpreted based on RMSD, RMSF, and Rg, minimum distance and hydrogen bond.

4.2.7.1. Root Mean Square Deviation (RMSD)

To determine the difference between the backbone and final position of a protein, one can use the RMSD by analyzing the deviations generated during that simulation, one can determine whether the protein remains stable in terms of its shape. The less deviation there are, the more stable the protein structure. To check the stability of both systems, the RMSD value of the C-α backbone was determined for 100 ns. The protein C-α backbone RMSD of control, along with reference and other hit compounds, were analyzed as displayed in **Fig 4.14**. The RMSD of the control protein was approximately 0.27 nm, and Palbociclib represented stability with an average RMSD value of 0.52 nm and maintained stability in the entire simulation. It was observed that control, CNP0267694, and CNP0070947 compounds showed stability throughout the entire simulation process at an average RMSD value of 0.37 and 0.32 nm, while CNP0396493 showed RMSD value of 0.4 nm till 15 ns after that, it stabilized at the average RMSD fluctuation till 20 ns after that, it remained stable till the end of the simulation and showed an average RMSD value of 0.85 nm. CNP0376445 showed consistent stability from the starting point till 100 ns with an average RMSD of 0.52 nm.

The ligand RMSD for Palbociclib, CNP0070947, CNP0376445, CNP0267694, and CNP0396493 represented; these simulated systems displayed steady state stability after 10 ns of MD run [239]. Palbociclib represented stability with an average RMSD value of 4.79 nm and remained constant throughout the entire simulation. CNP0396493 represented an average RMSD value of 0.85 nm till 100 ns simulation whereas CNP0376445 and CNP0070947 indicated an average RMSD value of 1.03 and 1.47 nm, respectively till 100 ns, whereas, a slight unstability was observed for CNP0267694 till around 32 ns, afterwards it attained stability till 100 ns MD run. However, after 32 ns, the RMSD values of all the

complexes remained unchanged until the final MD run. Broadly, the entire simulated complex displayed an RMSD value of more than 0.74 nm. The results interpret that all hit compounds are tightly bound and not affected by the protein topology. The stability of CNP0396493 and CNP0070947 is significantly higher than that of CNP0376445 and CNP0267694, which had very minor deviations and were somewhat like Palbociclib.

4.2.7.2. Root Mean Square Fluctuation (RMSF)

RMSF is one of the essential parameters for the characterization of rigid and flexible areas of protein and is used for assessing the flexibility of the protein structure. The Control protein showed an average RMSF value of 0.11 nm. The RMSF was calculated for the four-hit compounds and reference drug palbociclib. The average RMSF value of the reference drug was 0.15 nm. CNP0267694, CNP0376445, CNP0070947, and CNP0396493 represented the average RMSF value of 0.12, 0.14, 0.14, and 0.11 nm, respectively, as illustrated in **Fig 4.15**.

4.2.7.3. Radius of Gyration (Rg)

In MD simulation studies, Rg depicts the compactness and flexibility of a protein inside the biological environment. The control protein showed an average Rg value of 1.95 nm. The lower the value of Rg, the more firmly packed and stable the structure is during the simulation. The control protein showed an average Rg value of 1.95 nm, while the reference palbociclib average Rg value was observed at 2.03 nm, whereas CNP0376445, CNP0267694, CNP0070947, and CNP0396493 had an average Rg value recorded as 2.06, 2.00, 1.98, and 1.95 nm respectively as represented in **Fig 4.15**. CNP0376445 results indicated considerable bumps during the simulation. However, the graph of CNP0267694, CNP0070947 and CNP0396493 was considerably stabilized.

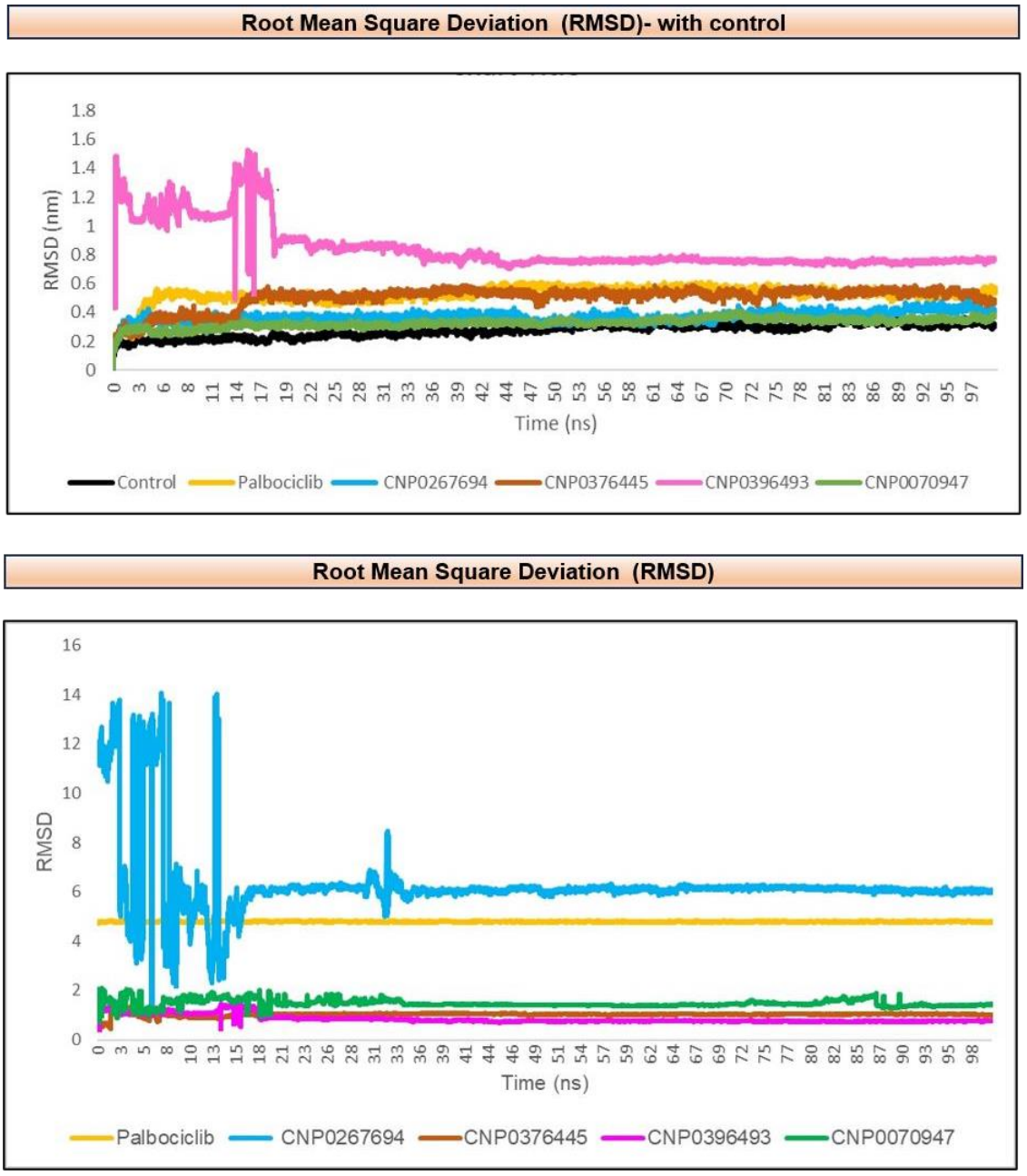

Fig 4.14. Graphical representation of RMSD (with and without control) obtained through MD Simulation analyses of the reference drug (Palbociclib) and the selected compounds.

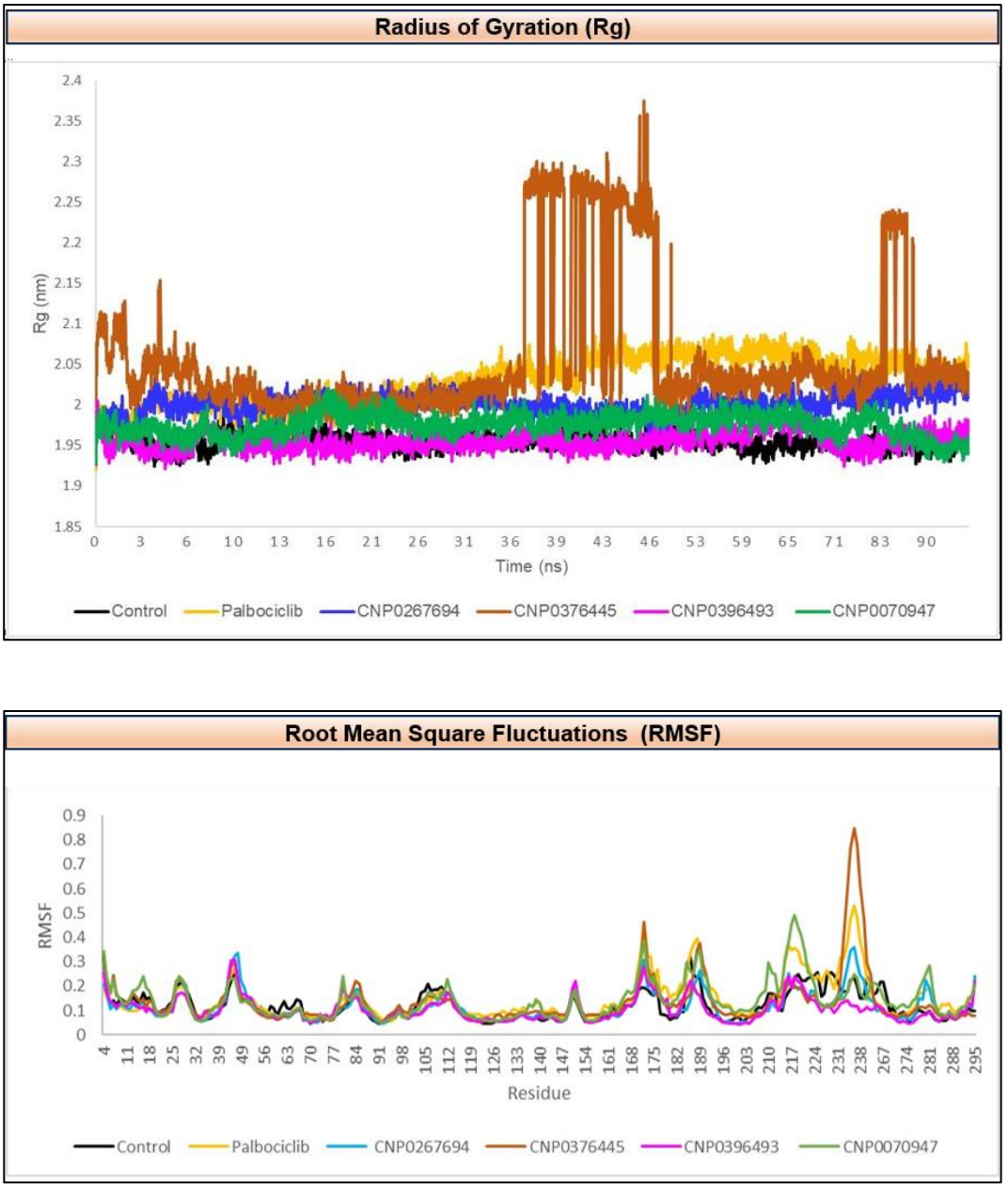

Fig 4.15. Graphical representation of Radius of Gyration and RMSF obtained through MD simulation analyses for the reference drug (Palbociclib) and the selected compounds.

4.2.7.4. Hydrogen bond and minimum distance analysis

Furthermore, the hit compounds formed the hydrogen bonds with the CDK4, and the survival time of these H-bonds and the number of H-bonds reflected the degree of binding between the ligand and CDK4. As indicated in **Fig 4.16(A),** palbociclib had four H- bonds for a longer period in the MD simulation, while the compound CNP0267694 made two H bonds for a short period, which are lesser in comparison to the reference, CNP0376445 represented 3 H-bond. On further analysis, as evident from **Fig 4.16(A)**, compounds CNP0396493 and CNP0070947 formed 3 and 7 H bonds in the simulation with a longer survival rate. Further, the minimum distance of ligand from the CDK4 binding site was also analyzed as an important post-MDS analysis interpretation, and it was seen that except CNP0267694, all other hit compounds show distance below the range of 0.35 nm throughout the simulation after 20 ns as illustrated in **Fig 4.16(B)**. CNP0396493, CNP0070947, and CNP0376445 indicated minimum distance in the range of 0.23 and 0.24 nm.

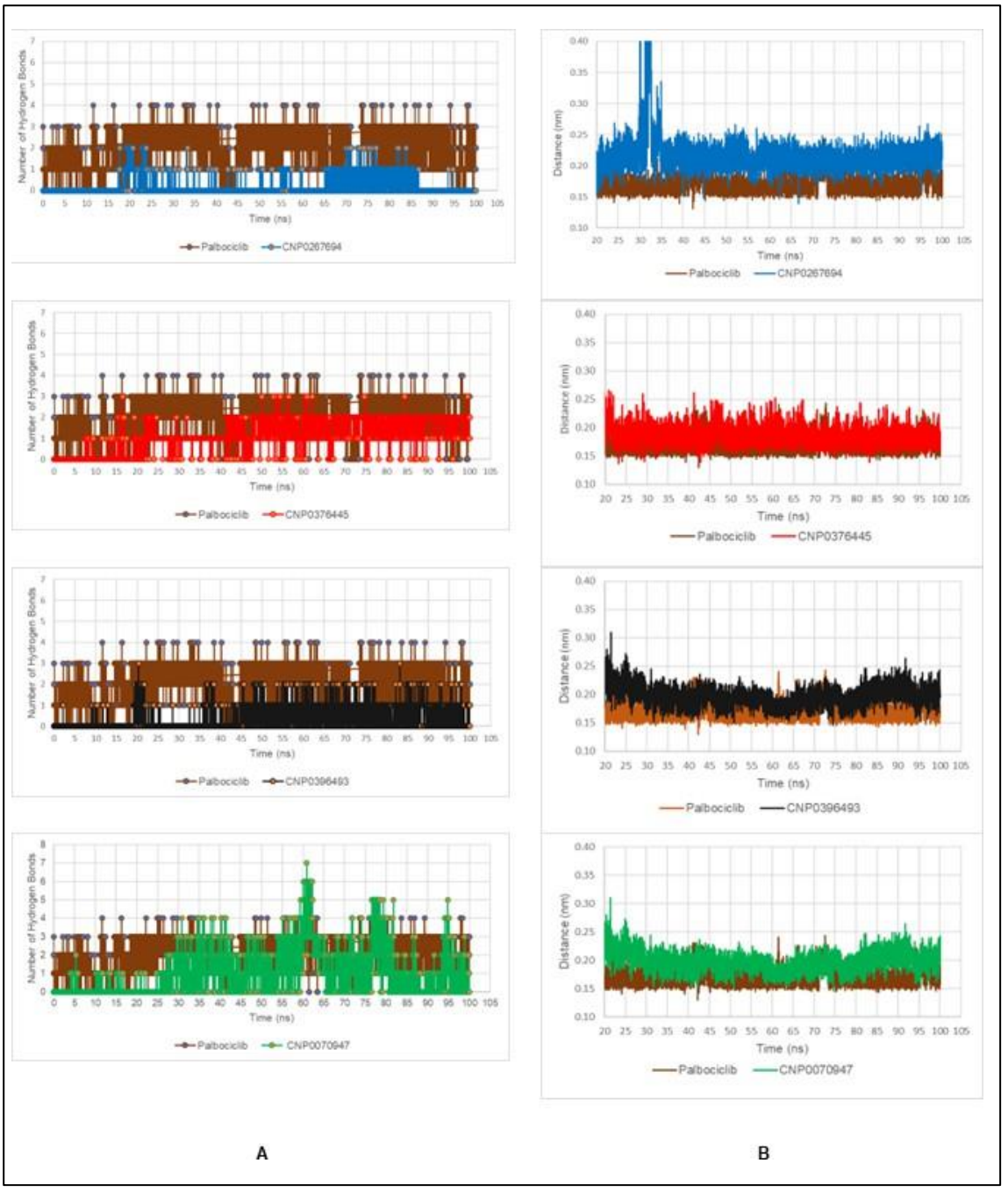

Fig 4.16. (A) Graphical representation of number of Hydrogen bonds formed between the ligand and the reference drug (Palbociclib) in comparison to each of the selected compounds. (B) Graphical representation of minimum distance between the Hydrogen bonds formed between the ligand and the reference drug (Palbociclib) in comparison to each of the selected compounds.

Overall, the results suggest that the hit compounds, particularly CNP0396493 and CNP0070947, exhibit promising binding affinities and stability within the CDK4 protein active site.

4.3 Research objective 3: To identify the novel UPS molecular signatures implemented in NDDs for prospective novel therapeutics.

4.3.1. Data extraction and analysis of differential expressed genes

In this study, for profiling of gene expression of GSE5281, a total 161 sample were selected out of which 44 were AD samples and 61 were control samples. This study is based on GPL570 Affymetrix human genomeU133 Plus Array. Based on applied filters i.e., adjp value and Log Fc, we extracted the significant differentially expressed genes (DEGs) 3247 wherein 1799 were downregulated and 1511 were found to be upregulated. In this study we also screened 377 E3 ligases genes from the KSBP2 database. Further we exported the DEGs and E3 ligases lists to the Venn analysis software for the analysis of common genes and in this process, we screened 55 E3 ligase related genes. The Venn and DEGs analysis are elaborated in **Fig 4.17** and **Table 4.6**, respectively.

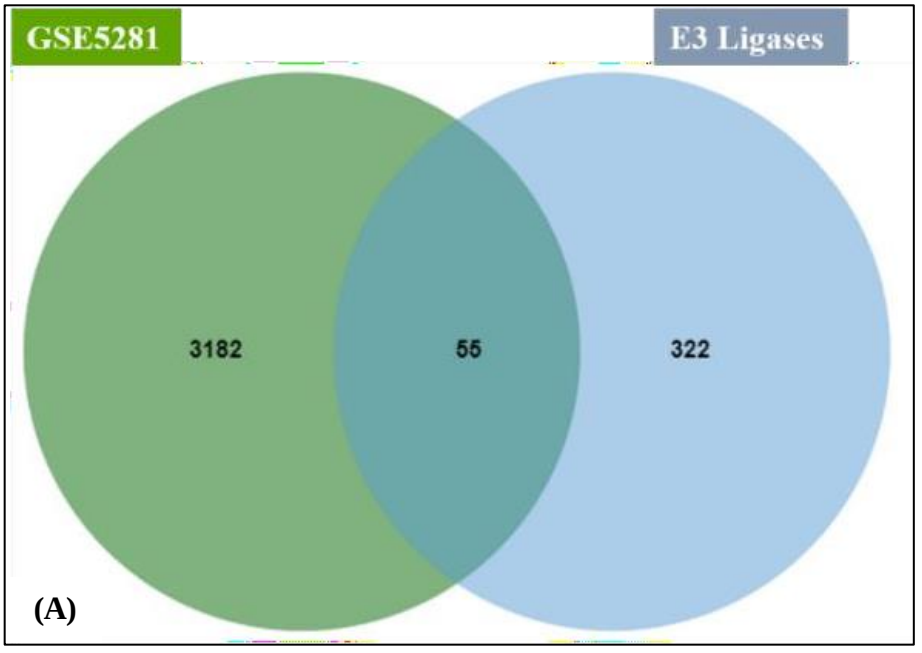

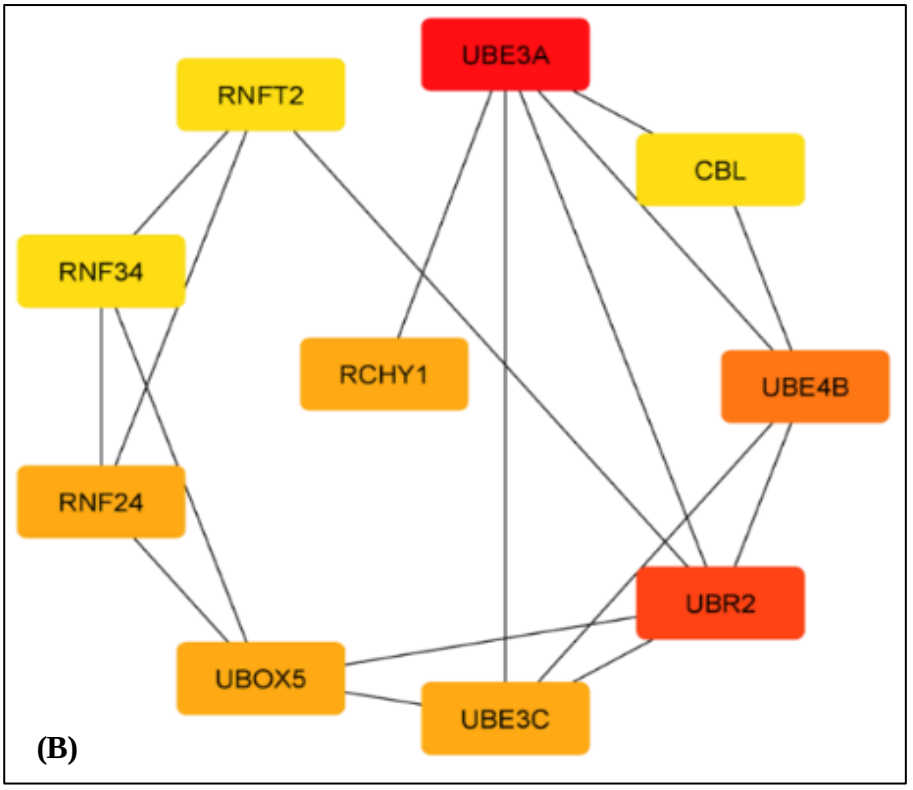

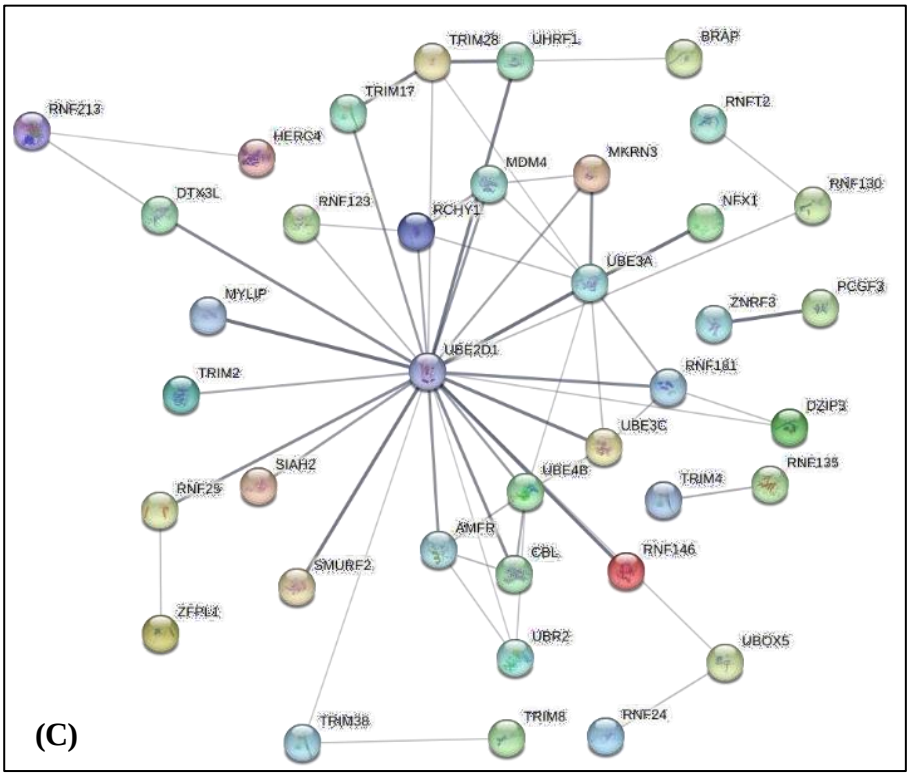

Fig 4.17. Analysis of DEGs – (A) VENN Analysis, (B) HUB Genes, (C) Protein-Protein Interactions

Table 4.6. DEG Analysis- Upregulated and Downregulated Hub Genes.

ID	adj.P.Val	P.Value	logFC	Gene.symbol
234163_at	4.31E-09	1.47E-11	2.072064	UBE3A
221884_at	1.06E-04	5.50E-06	1.63125	MECOM
210268_at	1.02E-05	3.12E-07	1.534697	NFX1
213850_s_at	1.46E-09	3.89E-12	1.481695	SCAF11
225742_at	1.58E-05	5.42E-07	1.420985	MDM4
203567_s_at	5.87E-05	2.67E-06	1.392411	TRIM38
1554287_at	2.32E-07	2.64E-09	1.360553	MIB1
224569_s_at	4.96E-09	1.77E-11	1.304518	IRF2BP2
1561130_at	8.30E-04	6.86E-05	1.258541	HECTD4
1563975_at	1.42E-04	7.86E-06	1.158613	RNF130
225415_at	2.90E-07	3.54E-09	1.132288	ZNRF3
1554287_at	1.16E-05	3.69E-07	1.130516	TRIM4
229413_s_at	1.04E-06	1.76E-08	1.129073	DTX3L
228098_s_at	4.19E-04	2.97E-05	1.12566	MYLIP
1569262_x_at	5.49E-05	2.47E-06	1.096432	PCGF3
1569262_x_at	1.41E-03	1.31E-04	1.081822	UBE3D
225655_at	4.50E-03	5.44E-04	1.057214	UHRF1
232593_at	1.25E-04	6.75E-06	1.050047	NEURL3
231956_at	2.79E-03	3.01E-04	1.026187	RNF213
206585_at	3.69E-04	2.53E-05	1.017283	MKRN3
205596_s_at	1.23E-06	2.18E-08	1.01085	SMURF2
234991_at	1.16E-06	2.02E-08	0.97639	ZXDC
223132_s_at	1.02E-06	1.70E-08	0.958693	TRIM8
208054_at	1.38E-02	2.21E-03	0.942466	HERC4
225234_at	2.65E-07	3.17E-09	0.918963	CBL
223592_s_at	4.97E-03	6.16E-04	0.914298	RNF135
236556_s_at	9.18E-03	1.33E-03	0.912586	LONRF1
1559500_at	1.52E-02	2.50E-03	0.900898	VPS8
229855_at	5.61E-03	7.15E-04	-0.933195	RNF34
221909_at	9.00E-04	7.58E-05	-0.948741	RNFT2
209339_at	2.31E-03	2.38E-04	-0.959992	SIAH2
212749_s_at	2.61E-03	2.78E-04	-0.964588	RCHY1
221430_s_at	3.25E-03	3.63E-04	-0.965556	RNF146
209565_at	2.07E-04	1.24E-05	-0.992273	RNF113A
202203_s_at	9.99E-04	8.60E-05	-0.99785	AMFR
202585_s_at	8.67E-04	7.23E-05	-1.004779	NFX1
214310_s_at	2.26E-03	2.33E-04	-1.02088	ZFPL1
224186_s_at	3.61E-04	2.47E-05	-1.020921	RNF123
200990_at	1.89E-04	1.11E-05	-1.022855	TRIM28
215544_s_at	1.56E-03	1.47E-04	-1.042953	UBOX5
231123_at	3.31E-02	6.79E-03	-1.046936	TRIM36
223064_at	2.12E-04	1.28E-05	-1.051096	RNF181
214249_at	1.39E-03	1.29E-04	-1.055119	TRIM2
233362_at	1.02E-03	8.79E-05	-1.087882	ZNF341
230662_at	2.37E-03	2.47E-04	-1.114156	RNF187
218564_at	8.26E-04	6.82E-05	-1.188006	RFWD3
1554793_at	7.02E-03	9.46E-04	-1.199709	UBE3C
210706_s_at	8.70E-06	2.57E-07	-1.202279	RNF24
219104_at	3.83E-04	2.65E-05	-1.250898	RNF141
202316_x_at	3.73E-04	2.57E-05	-1.293395	UBE4B
209922_at	2.01E-03	2.01E-04	-1.322269	BRAP
1569140_at	1.27E-04	6.87E-06	-1.329741	UBR2
220279_at	1.78E-05	6.30E-07	-1.390208	TRIM17
218861_at	5.57E-05	2.51E-06	-1.402079	RNF25
207232_s_at	6.12E-09	2.37E-11	-2.032542	DZIP3

Hub Genes

4.3.2 Gene set enrichment analysis

To predict the biological, cellular and molecular function and the pathway analysis related to AD, E3 ligases genes were uploaded to web-based tools such as Shinygo, Enricher and gprofiler. At biological level, E3 ligases genes are found to be involved in various pathways like protein ubiquitination, auto and mono ubiquitination, protein catabolic process and cellular catabolic process. Molecular level results indicated that the key E3 ligases genes are involved in ubiquitin ligase, ubiquitin-ubiquitin ligase, ubiquitin protease transferase, Zn binding domain, p53 binding domain, transcription co-activator and coregulator activity. At cellular level all these genes are found to be involved in ubiquitin ligase complex and catalytic complex. KEGG pathway analysis predicted that the key E3 ligases are involved in ubiquitination proteasome system. All the above explained enrichment analysis are represented in **Fig 4.18** and **Table 4.7.**

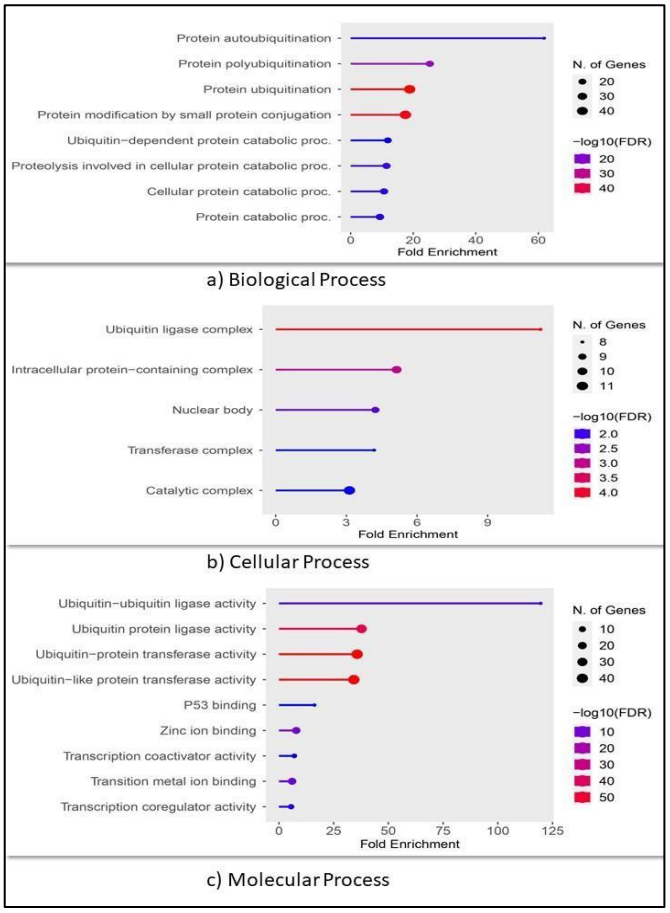

Fig 4.18. Gene Ontology Study.

Table 4.7. Gene Set Enrichment Analysis

Source	Term Name	Term ID	Adjusted P Value	Negative Log of Adjusted P Value	Intersections									
					UBE3A	UBR2	UBE4B	RNF24	RCHY1	UBOX5	UBE3C	RNFT2	RNF34	CBL
GO:MF	ubiquitin protein ligase activity	GO:0061630	1.99E-16	15.7014	✓	✓	✓	✓	✓	✓	✓	✓	✓	✓
GO:MF	ubiquitin-like protein ligase activity	GO:0061659	2.86E-16	15.5437	✓	✓	✓	✓	✓	✓	✓	✓	✓	✓
GO:MF	ubiquitin-protein transferase activity	GO:0004842	4.13E-15	14.3839	✓	✓	✓	✓	✓	✓	✓	✓	✓	✓
GO:MF	ubiquitin-like protein transferase activity	GO:0019787	7.34E-15	14.1343	✓	✓	✓	✓	✓	✓	✓	✓	✓	✓
GO:MF	aminoacyltransferase activity	GO:0016755	1.05E-14	13.9785	✓	✓	✓	✓	✓	✓	✓	✓	✓	✓
GO:MF	acyltransferase activity	GO:0016746	5.56E-13	12.2552	✓	✓	✓	✓	✓	✓	✓	✓	✓	✓
GO:MF	transferase activity	GO:0016740	7.45E-08	7.12774	✓	✓	✓	✓	✓	✓	✓	✓	✓	✓
GO:MF	catalytic activity, acting on a protein	GO:0140096	7.71E-08	7.1129	✓	✓	✓	✓	✓	✓	✓	✓	✓	✓
GO:MF	catalytic activity	GO:0003824	0.000611	3.21408	✓	✓	✓	✓	✓	✓	✓	✓	✓	✓
GO:MF	ubiquitin-ubiquitin ligase activity	GO:0034450	0.002969	2.52732			✓			✓				
GO:MF	metal ion binding	GO:0046872	0.022188	1.65388	✓	✓		✓	✓	✓		✓	✓	✓
GO:MF	cation binding	GO:0043169	0.026052	1.58415	✓	✓		✓	✓	✓		✓	✓	✓
GO:BP	protein ubiquitination	GO:0016567	1.02E-11	10.9906	✓	✓	✓	✓	✓	✓	✓	✓	✓	✓
GO:BP	protein modification by small protein conjugation	GO:0032446	2.44E-11	10.613	✓	✓	✓	✓	✓	✓	✓	✓	✓	✓
GO:BP	protein modification by small protein conjugation or removal	GO:0070647	1.12E-10	9.9521	✓	✓	✓	✓	✓	✓	✓	✓	✓	✓
GO:BP	proteolysis involved in protein catabolic process	GO:0051603	2.19E-07	6.65867	✓	✓	✓		✓		✓	✓	✓	✓
GO:BP	protein polyubiquitination	GO:0000209	6.40E-07	6.19412	✓		✓			✓	✓		✓	✓
GO:BP	protein catabolic process	GO:0030163	1.71E-06	5.76667	✓	✓	✓		✓		✓	✓	✓	✓
GO:BP	ubiquitin-dependent protein catabolic process	GO:0006511	5.52E-06	5.25824	✓	✓	✓		✓		✓		✓	✓
GO:BP	modification-dependent protein catabolic process	GO:0019941	6.09E-06	5.21525	✓	✓	✓		✓		✓		✓	✓
GO:BP	modification-dependent macromolecule catabolic process	GO:0043632	6.85E-06	5.16446	✓	✓	✓		✓		✓		✓	✓
GO:BP	organonitrogen compound catabolic process	GO:1901565	1.62E-05	4.78997	✓	✓	✓		✓		✓	✓	✓	✓
GO:BP	macromolecule catabolic process	GO:0009057	1.76E-05	4.75543	✓	✓	✓		✓		✓	✓	✓	✓
GO:BP	protein modification process	GO:0036211	2.63E-05	4.57969	✓	✓	✓	✓	✓	✓	✓	✓	✓	✓
GO:BP	macromolecule modification	GO:0043412	4.79E-05	4.31955	✓	✓	✓	✓	✓	✓	✓	✓	✓	✓
GO:BP	proteolysis	GO:0006508	0.000118	3.92676	✓	✓	✓		✓		✓	✓	✓	✓
GO:BP	organic substance catabolic process	GO:1901575	0.000533	3.27314	✓	✓	✓		✓		✓	✓	✓	✓
GO:BP	protein metabolic process	GO:0019538	0.001592	2.79819	✓	✓	✓	✓	✓	✓	✓	✓	✓	✓
GO:BP	catabolic process	GO:0009056	0.002292	2.63987	✓	✓	✓		✓		✓	✓	✓	✓
GO:BP	proteasomal protein catabolic process	GO:0010498	0.002636	2.57903		✓	✓		✓			✓	✓	
GO:BP	protein K48-linked ubiquitination	GO:0070936	0.004811	2.31774	✓						✓		✓	
GO:BP	protein autoubiquitination	GO:0051865	0.008106	2.09119	✓				✓					✓
GO:BP	organonitrogen compound metabolic process	GO:1901564	0.008486	2.07127	✓	✓	✓	✓	✓	✓	✓	✓	✓	✓
GO:CC	intracellular protein-containing complex	GO:0140535	0.003238	2.48968	✓	✓	✓		✓		✓			
GO:CC	ubiquitin ligase complex	GO:0000151	0.035828	1.44578		✓	✓		✓					
GO:CC	proteasome complex	GO:0000502	0.044184	1.35473	✓						✓			
KEGG	Ubiquitin mediated proteolysis	KEGG:04120	1.10E-09	8.95811	✓		✓		✓	✓	✓			✓
REAC	Antigen processing: Ubiquitination & Proteasome degradation	REAC:R-HSA-	8.20E-07	6.08642	✓	✓			✓	✓	✓		✓	
REAC	Class I MHC mediated antigen processing & presentation	REAC:R-HSA-	2.90E-06	5.53753	✓	✓			✓	✓	✓		✓	
REAC	Adaptive Immune System	REAC:R-HSA-	0.00027	3.56854	✓	✓			✓	✓	✓		✓	
REAC	Immune System	REAC:R-HSA-	0.002054	2.68744	✓	✓			✓	✓	✓		✓	✓

4.3.3. Protein-Protein interaction analysis

The screened E3 ligases were further analysed through string database with confidence score of 0.4 and network file was exported to cytoscape tool in cytohubba and centiscape plugin and the top 15 E3 ligases UBE3A, UBR2, UBE4B, RNF24, UBE3C, UBOX5, RCHY1, CBL, RNFT2, RNF34, UHRF1, TRIM38, AMFR, RNF146 and SMURF2 were extracted based on their rank and

score. All the above results are explained in **Fig 4.17(C)**. On the basis Gene set enrichment and pathway analysis, **UBE3A, UBE4B, RCHY1, UBOX5, UBE3C and CBL** were identified as novel E3 ligase biomarkers. UBE3A has been selected for further analysis due to its highest Log Fc value among selected biomarker and its active involvement in biological, cellular, and molecular processes.

4.3.4. Natural compound selection and ADMET analysis

In this study we extracted the natural compounds (Alkaloids) from coconut database (https://coconut.naturalproducts.net/). Further we filtered the extracted natural compounds (Alkaloids) based on BBB permeability and ADMET analysis. For further analysis, 43 most appropriate compounds were selected.

4.3.5. Docking analysis

Interpretation of docking of UBE3A (PDB id-6TGK) and 43 selected alkaloids were performed through Webina web-based tool and visualization were assessed through BIOVIA Discovery Studio Visualizer software. Receptor UBE3A and alkaloid structures were prepared for the docking analysis in PDBQT format. After completion of docking, 11 alkaloids with the best binding score of -10 Kcal/mol and above were selected as shown in **Table 4.8**. The top 3 alkaloids, leuconoxine, Jamine and panamine with maximum binding affinity score of -11.54, -11.34, and -11.06 Kcal/mol respectively, were further visualised by discovery studio, as illustrated in **Table 4.9** and **Fig 4.19**.

Table 4.8. Molecular Docking Interpretation of selected natural compounds

Natural compound	Binding affinity	Molecular Weight	Bood Brain Permeability	SwissADME
Leuconoxine	-11.54	310.39	YES	YES
Jamine	-11.31	328.52	YES	YES
Panamine	-11.06	315.5	YES	YES
Erysonine	-10.69	285.34	YES	YES
Herquline	-10.5	314.42	YES	YES
Cularicine	-10.37	311.33	YES	YES
Ibogaine	-10.13	310.43	YES	YES
Ormosanine	-10.09	317.51	YES	YES
Ulenine	-10.06	266.38	YES	YES
Nantenine	-10.05	339.39	YES	YES
Groelandicine	-9.925	324.35	YES	YES
Pallidine	-9.891	327.37	YES	YES
Epiberberine	-9.864	338.38	YES	YES
Oxymatrine	-9.697	264.36	YES	YES
Galantamine	-9.688	287.35	YES	YES
Lobeline	-9.49	337.46	YES	YES
Piperine	-9.46	285.34	YES	YES
Eserine	-9.418	275.35	YES	YES
Spinosine	-9.353	327.37	YES	YES
Coramine	-9.193	327.37	YES	YES
Rotundine	-9.113	355.43	YES	YES
Aegeline	-9.02	311.37	YES	YES
Aloperine	-8.975	232.36	YES	YES
Xylopinine	-8.968	355.43	YES	YES
Atropine	-8.875	289.37	YES	YES
Tinctorine	-8.459	244.33	YES	YES
Harmine	-8.203	212.25	YES	YES
Nigragillin	-8.001	222.33	YES	YES
Ismine	-7.626	257.28	YES	YES

Table 4.9. Ligand binding sites and type of interactive residues

Alkaloids	**Types**	**From**	**To**	**From chemistry**	**To chemistry**	**Distance**
Leuconoxine	Conventional Hydrogen Bond	:UNL1:O	H-Donor	C:THR786:O	H-Acceptor	3.30714
	Conventional Hydrogen Bond	:UNL1:O	H-Donor	C:HIS818:O	H-Acceptor	3.58584
	Conventional Hydrogen Bond	:UNL1:O	H-Donor	C:THR819:O	H-Acceptor	3.32497
	Conventional Hydrogen Bond	C:THR786:N	H-Donor	C:PHE782:O	H-Acceptor	3.03098
	Conventional Hydrogen Bond	C:THR786:N	H-Donor	C:LEU783:O	H-Acceptor	3.364

	Conventional Hydrogen Bond	C:THR786:OG1	H-Donor	C:PHE782:O	H-Acceptor	2.97435
	Conventional Hydrogen Bond	C:THR786:OG1	H-Donor	C:LEU783:O	H-Acceptor	3.76236
	Conventional Hydrogen Bond	C:LEU800:N	H-Donor	C:LEU797:O	H-Acceptor	3.02244
	Carbon Hydrogen Bond	C:THR819:CA:B	H-Donor	:UNL1:O	H-Acceptor	3.62863
	Pi-Donor Hydrogen Bond	C:THR786:OG1	H-Donor	C:PHE782	Pi-Orbitals	4.14136
	Pi-Sigma	C:THR786:CG2	C-H	C:PHE782	Pi-Orbitals	3.91299
	Alkyl	C:LEU747	Alkyl	C:LEU800	Alkyl	5.47348
	Alkyl	C:PRO793	Alkyl	C:LEU800	Alkyl	4.54802
	Alkyl	C:LEU797	Alkyl	C:LEU800	Alkyl	5.35053
	Alkyl	C:LYS801	Alkyl	:UNL1	Alkyl	4.40868
	Pi-Alkyl	:UNL1	Pi-Orbitals	C:LEU800	Alkyl	5.49053
Jamine	Carbon Hydrogen Bond	:UNL1:C	H-Donor	C:THR786:O	H-Acceptor	3.38498
	Alkyl	C:LYS801	Alkyl	:UNL1	Alkyl	4.26663
	Alkyl	C:ILE803	Alkyl	:UNL1	Alkyl	5.35836
	Pi-Alkyl	:UNL1	Pi-Orbitals	C:LYS801	Alkyl	4.45558
Panamine	Carbon Hydrogen Bond	:UNL1:C	H-Donor	C:HIS818:O	H-Acceptor	3.78028
	Pi-Sigma	C:MET802:CA	C-H	:UNL1	Pi-Orbitals	3.9916
	Alkyl	C:LYS801	Alkyl	:UNL1	Alkyl	5.06304
	Pi-Alkyl	:UNL1	Pi-Orbitals	C:ILE803	Alkyl	5.44745

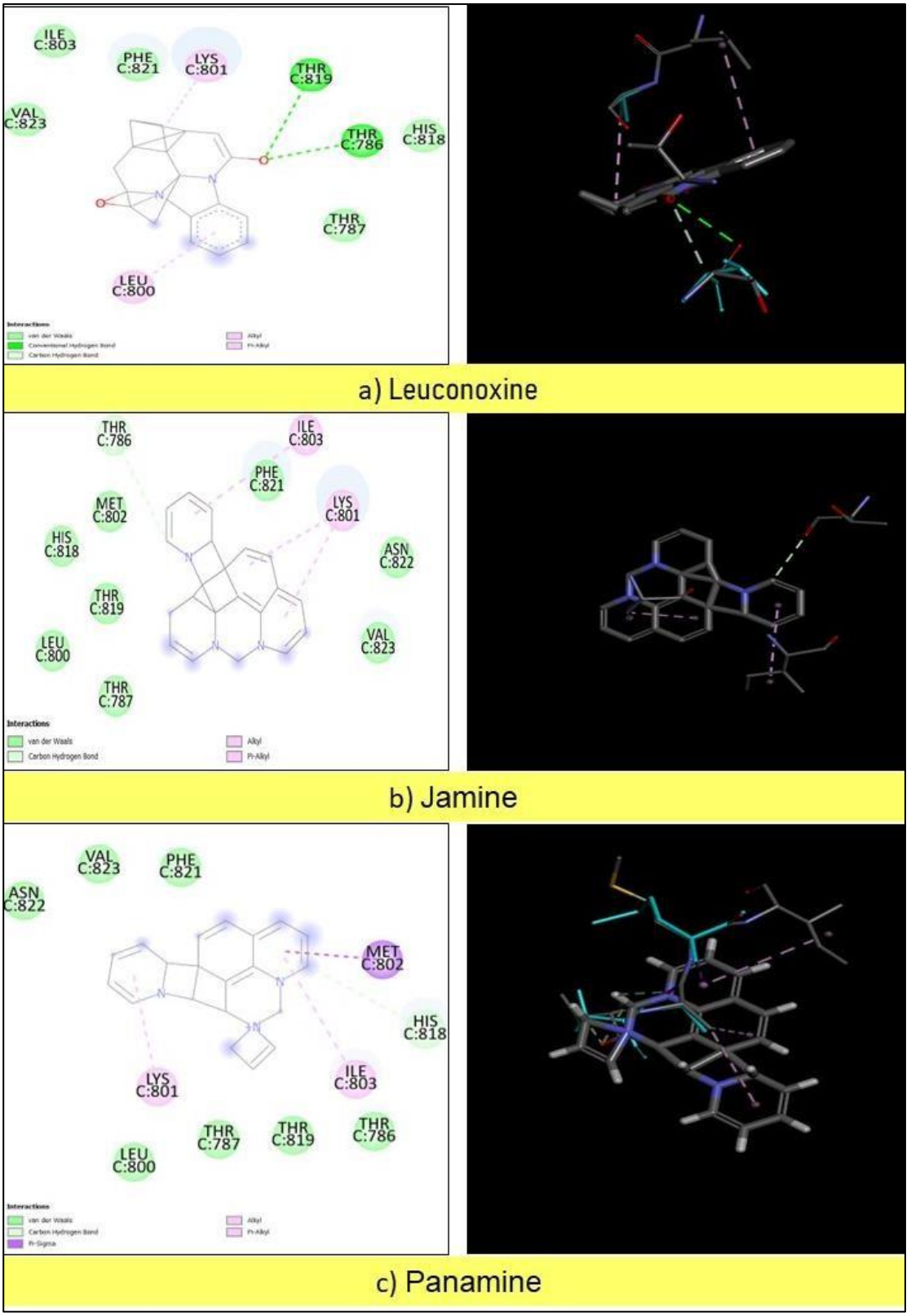

Fig 4.19. Molecular docking visualization of Leuconoxine, Jamine and Panamine.

4.3.6. UBE3A-Leuconoxine Dynamic stability interpretation

The MD simulation was performed to enhance the accuracy of the study, the reliability and stability of the result, that enabled to analyze the changes in the compound with the highest docking score i.e., UBE3A-Leuconoxine complex confirmation during the period of MD simulation. The exact movement of each atom during the entire time duration was predicted by the MD simulation, which helped us to implicate the fluctuation and changes in the CDK6 structure. The simulation was performed for 100 ns and post MD simulation result was assessed based on RMSD, RMSF, and Rg.

4.3.6.1 Root Mean Square Deviation (RMSD)

The RMSD analysis of the APO protein (UBE3A) as depicted in **Fig 4.20** shows that during the first 10 ns, RMSD of APO protein reached at a peak of 1.5 nm, indicating conformational changes at the start of simulation. After 10 ns, RMSD attains values between 1.3 nm to 1.4 nm. Whereas in UBE3A-Leuconoxine complex, RMSD rises during the initial 10-20 ns, and thereafter achieves an average RMSD between 1.0 nm to 1.3 nm as the simulation progresses. This result interpreted that UBE3A-Leuconoxine complex exhibits a lower overall RMSD during the entire duration of 100 ns of the simulation indicating a higher stability as compared to APO protein.

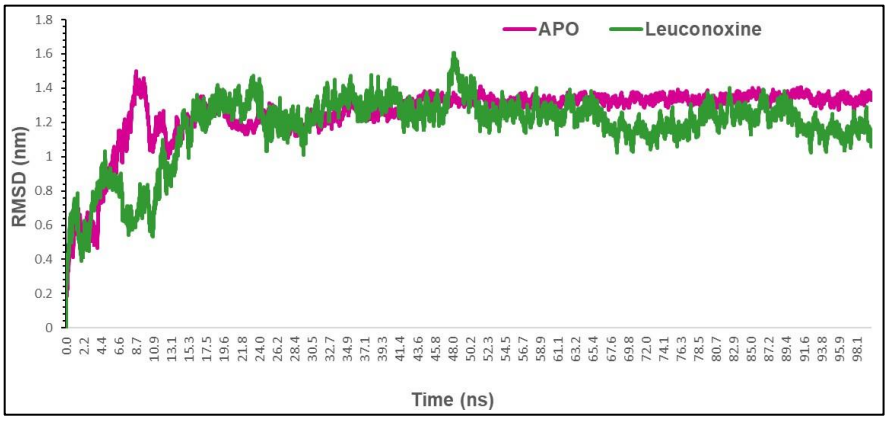

Fig 4.20. Graphical representation of RMSD obtained through MD simulation of APO protein and UBE3A-Leuconoxine complex.

4.3.6.2 Root Mean Square Fluctuation (RMSF)

RMSF was performed for the residues during the simulation, to evaluate the flexibility of UBE3A-Leuconoxine complex and the APO protein (**Fig 4.21**). Minor fluctuations were observed in the value of RMSF for most residues, indicating a high stability in both forms. Both the forms indicated high flexibility at the N-terminus (residues 710-720), with lower fluctuations across most of the protein. However, around residues 740-760, 810-850, and at the C-terminus, Leuconoxine binding slightly increases, suggesting a localized changes in the protein's dynamic behavior and interaction sites or structural changes due to binding.

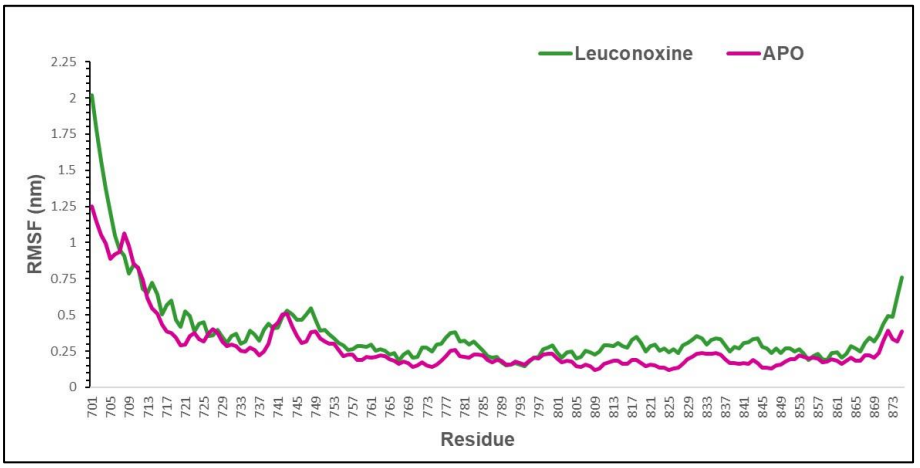

Fig 4.21. Graphical representation of RMSF obtained through MD simulation of APO protein and UBE3A-Leuconoxine complex

4.3.6.3 Radius of Gyration (Rg)

The Rg depicts the distribution of mass of the molecules around its Centre of mass and thus is indicative of the compactness of the structure, a lower Rg value showing a more compact and stable structure. In the graph (**Fig 4.22**), it is observed that after around 10 ns, Leuconoxine stabilizes at a lower Rg value, suggestive of a more compact and stable molecular structure. This consistent lower Rg indicates that Leuconoxine attains a more stable arrangement as compared to the APO state. Overall, Leuconoxine exhibits greater structural

stability and compactness throughout the simulation, likely due to favorable interactions or binding, which potentially strengthens its biological relevance and functional efficiency as compared to the APO form.

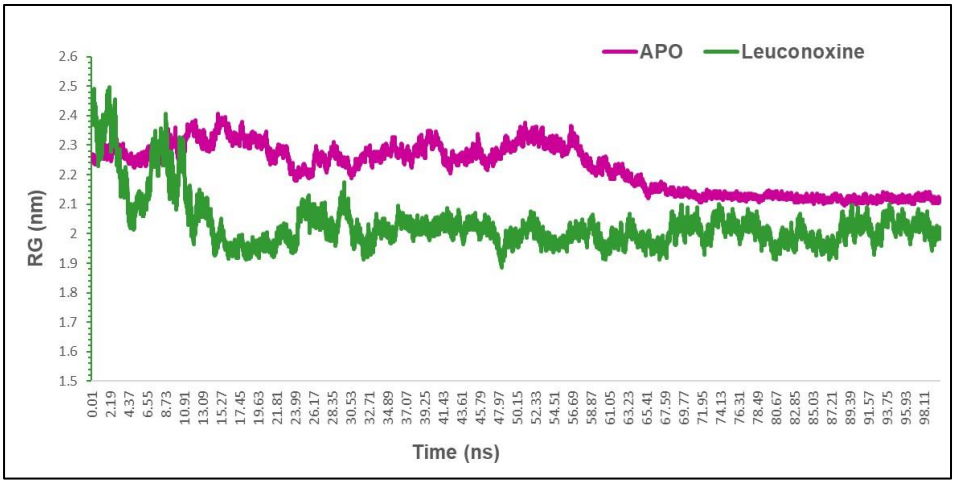

Fig 4.22. Graphical representation of Radius of Gyration (Rg) obtained through MD simulation of APO protein and UBE3A-Leuconoxine complex

UBE3A, UBE4B, RCHY1, UBOX5, UBE3C, CBL were identified as E3 ligase biomarker for AD. With this study, leuconoxine was predicted as protective agents against UBE3A in AD. However further studies are required to determine the efficacy of these inhibitors.

CHAPTER 5

CONCLUSION

LIMITATION OF THE STUDY

FUTURE PROSPECTIVE

Chapter 5

CONCLUSION, LIMITATION OF THE STUDY, AND FUTURE PROSPECTIVE

5.1 Discussion

NDDs consists of several processes such as cell cycle dysregulation, oxidative stress, ER stress, environment toxins and UPS impairment. Cell cycle and UPS dysfunction is different from other processes involved in NDDs and can be a novel biomarker which can have a therapeutic role. In initial steps of study, DEGs from GSE5281 dataset and CCR genes from the KEGG database were screened as potential biomarkers for AD. Further, CDK6, EP300, RB1, ATR and CDC25C were highlighted using gene set enrichment analysis for their role in key biological processes such as cell cycle regulation, neuroinflammation and apoptosis. CDK6 has been selected for further analysis due to higher Log FC value and central role in protein-protein interaction work. The molecular docking analysis of natural compounds and CDK6 showed that NPC314329 is having the highest binding affinity, Further MD simulation analysis of complex also suggesting NPC314329 as a promising therapeutic agent, potentially inhibiting CDK6's kinase activity, thereby regulating abnormal cell cycle progression and reducing overall neurodegenerative effects. The prominent interaction between NPC314329 and CDK6 provides a novel approach for drug development for management of AD, focusing on critical pathways in neuronal protection and inflammation. The docking results also suggest that NPC314329 could offer new treatment strategies in management of neurodegeneration in AD, by restoring cell cycle dynamics. However, pre-clinical validation is required to confirm the findings of this study.

The second part of study focused on the CDK4 inhibitors which have been increasingly used in clinical studies for various NDDs in recent years. Nevertheless, these inhibitors exhibit several drawbacks, including gastrointestinal irritation and drug resistance, which ultimately decrease their

effectiveness. Currently, there is a growing focus on using natural products for therapeutic research and development. The scientific community has shown particular interest in natural products due to their distinct benefits. Hence, our work seeks to evaluate the effect of natural products filtered from the COCONUT database, on CDK4 molecules.

In this study, we have comprehensively explored potential CDK4 inhibitors by employing various computational tools and methodologies. On exploring the COCONUT database for natural compounds exhibiting molecular similarity with the target drug – Palbociclib, having a considerable therapeutic role in the management of NDDs by targeting CDK4, around 1017 natural compounds were retrieved, which were further filtered to 110 natural compounds using the swissADME tool. We further restricted our study to the ten most suitable natural compounds based on molecular docking studies to assess their binding affinity with CDK4. Notably, we employed stringent criteria, including negative binding scores exceeding -8.988 kcal/mol from Webina and -8.57 kcal/mol from FastDRH, along with the GB1 score calculated by FastDRH, to select the top four hit compounds: CNP0070947, CNP0376445, CNP0267694, and CNP0396493.

Our findings revealed promising total binding energies for each compound, indicating their strong binding affinity with CDK4. Further analysis of the decomposition energy profiles has shed light on the contribution of individual energy components, providing insights into the stability and interaction dynamics of the ligand-protein complexes. CNP0070947 and CNP0396493 have the potential to be dominant CDK4 inhibitors due to their chemical interactions with key amino acid residues of CDK4, including LYS35, GLU94, HIS95, VAL96, and ARG101. These hydrogen bonding and hydrophobic interactions are crucial for binding ligands and suppressing CDK4 activity, showing that both these compounds may have therapeutic qualities.

Molecular dynamics and MM/GBSA play a crucial role in verifying the stability of the interaction between hit compounds and CDK4. Following the 100 ns simulation, we obtained the RMSD and RMSF data from the trajectory. This data

was analyzed to verify the stability and flexibility of the interaction between the hit compounds and CDK4. The interaction and stability dynamics of control, CDK4 protein-ligand complexes involving Palbociclib and the hit compounds CNP0376445, CNP0070947, CNP0396493, and CNP0267694 have been demonstrated by the molecular dynamic simulations involving them. RMSD protein backbone analysis showed that control, palbociclib, and all the compounds are stabilized in the entire simulation after 10 - 20 ns. In the RMSD analysis, all these protein-ligand complexes demonstrated steady-state stability after an initial equilibration phase. During the entire simulation, the reference drug Palbociclib kept a stable RMSD, whereas the hit compounds also demonstrated such stability, baring few occasional variances, with CNP0070947 and CNP0396493 having the highest stability levels, whereas CNP0267694 and CNP0376445 having comparatively higher deviations, but maintaining the stability levels following an initial adjustment phase. Secondly, the RMSF analysis highlighted regions of flexibility within the protein structure. While all compounds exhibited comparable average RMSF values,

CNP0376445 showed the highest fluctuation at the 230^{th} residue with 0.84 nm and the 166^{th} residue with 0.45 nm. Whereas, CNP0267694 showed the fluctuation at the 44^{th} residue with 0.33 nm. These residues showed significant fluctuations, suggesting regions of flexibility that could be targeted for further optimization. Further, the Rg analysis indicated the compactness and stability of the protein-ligand complexes. Lower Rg values were observed for CNP0070947, CNP0396493, and CNP0267694, indicating a tighter packing and greater stability than Palbociclib and CNP0376445. Additionally, the analysis of hydrogen bonds, revealing varying degrees of interaction between the ligands and CDK4 and minimum distances between protein binding sites with the ligand, further elucidated the binding interactions between the hit compounds and CDK4. Palbociclib formed four hydrogen bonds consistently throughout the simulation, indicating stable binding interactions. A lower binding affinity is suggested by the fact that CNP0267694 only created two hydrogen bonds for a brief period; this transient nature of hydrogen bonds raises the question about its binding efficiency

with CDK4, while CNP0396493 and CNP0070947 had the greatest number of hydrogen bonds three and seven, respectively CNP0376445 established three hydrogen bonds, indicating robust and long-lasting interactions with CDK4. After the first equilibration phase, all hit compounds aside from CNP0267694 maintained minimum distances below 0.35 nm for the whole duration of the simulation. CNP0396493 and CNP0070947 demonstrated minimum distances between 0.23-0.24 nm, which is a sign of proximity to the active site and robust binding interactions. Additionally, CNP0376445 demonstrated a minimum distance of 0.24 nm, indicating a sustained binding to CDK4. Based on their greater number of hydrogen bonds, minimum distance, and significant binding affinity to CDK4, our results support the stability and viability of CNP0396493 and CNP0070947. Overall, the results suggest that the hit compounds, particularly CNP0396493 and CNP0070947, exhibit promising binding affinities and stability within the CDK4 protein active site.

AD consists of several processes such as oxidative stress, ER stress, environment toxins and UPS impairment. UPS dysfunction is different from other processes involved in AD and can be a novel biomarker which can have a therapeutic role. In this study, common DEGs (i.e. E3 ligase) were screened after comparing DEGs from GSE5281 dataset and the KSB2 E3 ligases dataset, based on the applied filters of adj p value < 0.05 and Log FC value. Further Gene set enrichment analysis was undertaken to assess the biological, cellular and molecular processes of E3 ligase. These E3 ligase were further screened for Protein-protein interaction with the help of STRING and string network exported to cytoscape from where we extracted the 15 E3 ligase. In this study we have identified E3 ligase biomarker (UBE3A, UBE4B, RCHY1, UBOX5, UBE3C, CBL) based on Gene set enrichment analysis and pathway analysis. We have selected UBE3A for further analysis due to its highest Log Fc value among selected biomarker and its active involvement in biological, cellular, and molecular processes. Molecular docking interpretation predicted that leuconoxine, Jamine and panamine have maximum binding affinity score of -11.54, -11.34, and -11.06 Kcal/mol respectively. UBE3A, UBE4B, RCHY1, UBOX5, UBE3C, CBL were identified as E3 ligase

biomarker for AD. With this study, leuconoxine, Jamine and panamine were predicted as protective agents against UBE3A in AD. Further after MD simulation and analyzing the RMSD, RMSF, and Rg data it was observed that Leuconoxine was the most promising candidate in for further studies to determine its role and effectiveness in the management of AD.

The study's methodology and results provide a foundation for future research and optimization in developing efficient CDK6, CDK4, and UBE3A inhibitors, eventually enhancing our knowledge and treatment of NDDs associated with CDK4/6 dysregulation, as demonstrated in **Fig 5.1**. However, further experimental validation such as kinase assay and structural studies may be required to corroborate these computational findings and guide the development of novel CDK4/6 inhibitors with improved efficacy and therapeutic potential.

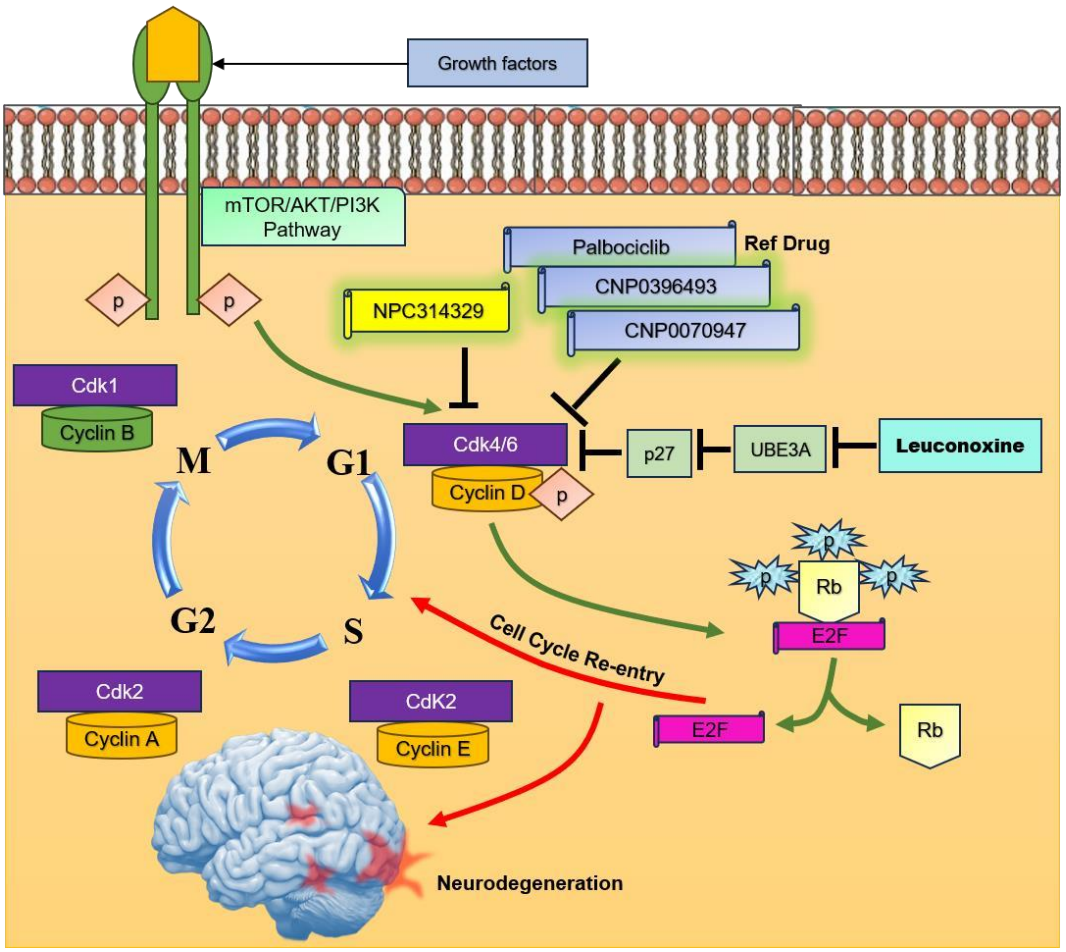

Fig 5.1. Representation of mechanism of identified inhibitors in NDDs. The cell cycle is tightly regulated by various regulators, which can act positively and negatively. Var0ious growth factors initiate different kinds of signaling, such as mTOR/PI3K/AKT, which induces the cyclin-D /CDK4/6 complex formation, an important factor involved in the phosphorylation of Rb protein and the release of E2F transcription factor. E2F allows cell proliferation, which means cell cycle re-entry, ultimately moving toward neurodegeneration. NPC314329 are the promising therapeutic agent targeting CDK6. Palbociclib, the reference drug, inhibits the cyclin-D/CDK4/6 complex. It is hypothesized that palbociclib analog natural compounds CNP0396493 and CNP0070947 are promising candidates as CDK4 inhibitors and have been validated through MM/GBSA and molecular dynamic simulation. Leuconoxine has been identified as UBE3A inhibitors in AD.

5.2 Limitations of the Study

There are certain limitations to the current study. This study's methodology is based on computational analysis, which relies on the application of various tools and filters for analysis and result interpretation. However, depending on the instruments and software used at different phases of the drug screening process, the outcome could alter slightly. Furthermore, for these suggested medications and the genes associated with them to be confirmed *in vivo* or *in vitro*, wet lab validations are required. The effectiveness of these anticipated candidate medications as well as their mechanism of action, BBB permeability variables, and other downstream and upstream targets will be demonstrated by this validation.

5.3 Future prospective

- By targeting cell cycle regulators and E3 ligase inhibitors, the study's findings could lead to a breakthrough in the creation of novel treatment approaches. Additionally, the investigation of interconnected pathways could open new avenues for the therapeutic management of NDDs.
- This study has identified the role of various potential biomarkers CCR biomarkers (CDK6, EP300, RB1, ATR and CDC25C) and E3 ligase biomarkers (UBE3A, UBE4B, RCHY1, UBOX5, UBE3C, CBL) that can be further explored for the development of novel therapeutic avenues in NDDs
- The objectives and the methodology adopted in the study would be extremely useful for identifying the therapeutic potential of new drugs and the use of natural compounds in combating NDDs.

  The societal impact of this work is in healthcare developments this study sheds light on new therapeutic approaches to target the UPS and cell cycle dysregulation in NDDs such as AD and PD. This enables the development of novel drugs that have the potential to stop or slow down the negative

consequences of these diseases, hence improving the quality of life for millions across the globe. Due to the long-term care and treatment that NDDs require, these NDDs tend to have a high economic burden on health care systems. In pursuit of targeted therapies that this study brings, these costs may be reduced which will be beneficial to patients and society in general due to the reduced economic pressure on health care systems, by showing the possibility of using natural compounds for the modulation of the proteins implicated in neurodegeneration. It fosters the advancement of drug development and computational biology by inspiring collaboration between disciplines. With the global population aging, NDDs are unfortunately on the rise, which further adds to the growing awareness of scope in the work. Further, focusing on how these diseases work on a molecular level and how individualized approaches to treatment can assist people's health policies and management of the patient. Current study allows for more precise medicine, meaning that there is less guesswork during prescription and minimal negative repercussions which eventually leads to a better patient experience. This impact has made current research essential in rethinking future therapeutic paradigms for NDDs with prospects for improvement of the world society in general.

REFERENCES

[1] C. Marras *et al.*, “Prevalence of Parkinson’s disease across North America,” *NPJ Parkinsons Dis*, vol. 4, no. 1, Dec. 2018, doi: 10.1038/S41531-018-0058-0.

[2] E. M. J. Jackson *et al.*, “Promoting Healthy Aging: Public Health as a Leader for Reducing Dementia Risk.,” *Public Policy Aging Rep*, vol. 33, no. 2, pp. 92–95, Jul. 2023, doi: 10.1093/ppar/prad011.

[3] A. Katsnelson, B. De Strooper, and H. Y. Zoghbi, “Neurodegeneration: From cellular concepts to clinical applications,” *Sci Transl Med*, vol. 8, no. 364, Nov. 2016, doi: 10.1126/SCITRANSLMED.AAL2074.

[4] J. Correale, M. I. Gaitán, M. C. Ysrraelit, and M. P. Fiol, “Progressive multiple sclerosis: from pathogenic mechanisms to treatment,” *Brain*, vol. 140, no. 3, pp. 527–546, Mar. 2017, doi: 10.1093/BRAIN/AWW258.

[5] S. Kumar, “Overcoming gaps in the treatment of neurodegenerative disease,” *EBioMedicine*, vol. 60, p. 103088, Oct. 2020, doi: 10.1016/j.ebiom.2020.103088.

[6] D. M. Wilson, M. R. Cookson, L. Van Den Bosch, H. Zetterberg, D. M. Holtzman, and I. Dewachter, “Hallmarks of neurodegenerative diseases,” *Cell*, vol. 186, no. 4, pp. 693–714, Feb. 2023, doi: 10.1016/J.CELL.2022.12.032.

[7] J. Busser, D. S. Geldmacher, and K. Herrup, “Ectopic Cell Cycle Proteins Predict the Sites of Neuronal Cell Death in Alzheimer’s Disease Brain,” *The Journal of Neuroscience*, vol. 18, no. 8, pp. 2801–2807, Apr. 1998, doi: 10.1523/JNEUROSCI.18-08-02801.1998.

[8] S. Di Giovanni, S. M. Knoblach, C. Brandoli, S. A. Aden, E. P. Hoffman, and A. I. Faden, “Gene profiling in spinal cord injury shows role of cell cycle in neuronal death,” *Ann Neurol*, vol. 53, no. 4, pp. 454–468, Apr. 2003, doi: 10.1002/ana.10472.

[9] H. Osuga *et al.*, “Cyclin-dependent kinases as a therapeutic target for stroke,” *Proceedings of the National Academy of Sciences*, vol. 97, no. 18, pp. 10254–10259, Aug. 2000, doi: 10.1073/pnas.170144197.

[10] G. U. Höglinger *et al.*, “The pRb/E2F cell-cycle pathway mediates cell death in Parkinson’s disease,” *Proceedings of the National Academy of Sciences*, vol. 104, no. 9, pp. 3585–3590, Feb. 2007, doi: 10.1073/pnas.0611671104.

[11] G. G. Kovacs, “Molecular pathology of neurodegenerative diseases: principles and practice,” *J Clin Pathol*, vol. 72, no. 11, pp. 725–735, Nov. 2019, doi: 10.1136/jclinpath-2019-205952.

[12] J. M. Lee, H. M. Hammarén, M. M. Savitski, and S. H. Baek, “Control of protein stability by post-translational modifications,” *Nature Communications 2023 14:1*, vol. 14, no. 1, pp. 1–16, Jan. 2023, doi: 10.1038/s41467-023-35795-8.

[13] R. Gupta, A. Jha, R. K. Ambasta, and P. Kumar, “Regulatory mechanism of cyclins and cyclin-dependent kinases in post-mitotic neuronal cell division,” *Life Sci*, vol. 285, p. 120006, Nov. 2021, doi: 10.1016/j.lfs.2021.120006.

[14] N. Malhotra, R. Gupta, and P. Kumar, “Pharmacological relevance of CDK inhibitors in Alzheimer’s disease,” *Neurochem Int*, vol. 148, p. 105115, Sep. 2021, doi: 10.1016/j.neuint.2021.105115.

[15] T. Zou and Z. Lin, “The Involvement of Ubiquitination Machinery in Cell Cycle Regulation and Cancer Progression,” *Int J Mol Sci*, vol. 22, no. 11, p. 5754, May 2021, doi: 10.3390/ijms22115754.

[16] C. Norbury and P. Nurse, “ANIMAL CELL CYCLES AND THEIR CONTROL,” *Annu Rev Biochem*, vol. 61, no. 1, pp. 441–468, Jun. 1992, doi: 10.1146/annurev.bi.61.070192.002301.

[17] A. Satyanarayana and P. Kaldis, “Mammalian cell-cycle regulation: several Cdks, numerous cyclins and diverse compensatory mechanisms,” *Oncogene*, vol. 28, no. 33, pp. 2925–2939, Aug. 2009, doi: 10.1038/onc.2009.170.

[18] S. Lim and P. Kaldis, “Cdks, cyclins and CKIs: roles beyond cell cycle regulation,” *Development*, vol. 140, no. 15, pp. 3079–3093, Aug. 2013, doi: 10.1242/dev.091744.

[19] K. J. Barnum and M. J. O’Connell, “Cell Cycle Regulation by Checkpoints,” *Methods Mol Biol*, vol. 1170, p. 29, 2014, doi: 10.1007/978-1-4939-0888-2_2.

[20] A. S. Coutts and L. Weston, Eds., “Cell Cycle Oscillators,” vol. 2329, 2021, doi: 10.1007/978-1-0716-1538-6.

[21] R. Y. C. Poon, “Cell Cycle Control: A System of Interlinking Oscillators,” *Methods in Molecular Biology*, vol. 2329, pp. 1–18, 2021, doi: 10.1007/978-1-0716-1538-6_1/COVER.

[22] L. Ding *et al.*, “The Roles of Cyclin-Dependent Kinases in Cell-Cycle Progression and Therapeutic Strategies in Human Breast Cancer,” *Int J Mol Sci*, vol. 21, no. 6, Mar. 2020, doi: 10.3390/IJMS21061960.

[23] W. Stallaert, K. M. Kedziora, H. X. Chao, and J. E. Purvis, “Bistable switches as integrators and actuators during cell cycle progression,” *FEBS Lett*, vol. 593, no. 20, pp. 2805–2816, Oct. 2019, doi: 10.1002/1873-3468.13628.

[24] P. Łukasik, M. Załuski, and I. Gutowska, “Cyclin-Dependent Kinases (CDK) and Their Role in Diseases Development–Review,” *Int J Mol Sci*, vol. 22, no. 6, pp. 1–33, Mar. 2021, doi: 10.3390/IJMS22062935.

[25] N. Johnson and G. I. Shapiro, “Cyclin-dependent kinases (cdks) and the DNA damage response: rationale for cdk inhibitor–chemotherapy combinations as an anticancer strategy for solid tumors,” *Expert Opin Ther Targets*, vol. 14, no. 11, p. 1199, Nov. 2010, doi: 10.1517/14728222.2010.525221.

[26] L. Cao, F. Chen, X. Yang, W. Xu, J. Xie, and L. Yu, “Phylogenetic analysis of CDK and cyclin proteins in premetazoan lineages,” *BMC Evol Biol*, vol. 14, no. 1, p. 10, 2014, doi: 10.1186/1471-2148-14-10.

[27] J. Cicenas and M. Valius, “The CDK inhibitors in cancer research and therapy,” *J Cancer Res Clin Oncol*, vol. 137, no. 10, p. 1409, 2011, doi: 10.1007/s00432-011-1039-4.

[28] L. Ding *et al.*, “The Roles of Cyclin-Dependent Kinases in Cell-Cycle Progression and Therapeutic Strategies in Human Breast Cancer,” *Int J Mol Sci*, vol. 21, no. 6, Mar. 2020, doi: 10.3390/IJMS21061960.

[29] J. A. Perry and S. Kornbluth, “Cdc25 and Wee1: Analogous opposites?,” *Cell Div*, vol. 2, no. 1, pp. 1–12, May 2007, doi: 10.1186/1747-1028-2-12/FIGS/2.

[30] E. Monaco and M. Lou Vallano, “Role of protein kinases in neurodegenerative disease: Cyclin-dependent kinases in Alzheimer’s disease,” *Front Biosci*, vol. 10, pp. 143–159, Feb. 2005.

[31] V. W. Yang, “The Cell Cycle,” in *Physiology of the Gastrointestinal Tract*, Elsevier, 2018, pp. 197–219. doi: 10.1016/B978-0-12-809954-4.00008-6.

[32] C. J. Sherr and J. M. Roberts, “CDK inhibitors: positive and negative regulators of G1-phase progression,” *Genes Dev*, vol. 13, no. 12, pp. 1501–1512, Jun. 1999, doi: 10.1101/gad.13.12.1501.

[33] C. Bertoli, J. M. Skotheim, and R. A. M. De Bruin, “Control of cell cycle transcription during G1 and S phases,” *Nat Rev Mol Cell Biol*, vol. 14, no. 8, p. 518, Aug. 2013, doi: 10.1038/NRM3629.

[34] J. Chen, “The Cell-Cycle Arrest and Apoptotic Functions of p53 in Tumor Initiation and Progression,” *Cold Spring Harb Perspect Med*, vol. 6, no. 3, Mar. 2016, doi: 10.1101/CSHPERSPECT.A026104.

[35] S. G. Zebell and X. Dong, “Cell-Cycle Regulators and Cell Death in Immunity,” *Cell Host Microbe*, vol. 18, no. 4, pp. 402–407, Oct. 2015, doi: 10.1016/J.CHOM.2015.10.001.

[36] B. Pucci, M. Kasten, and A. Giordano, “Cell Cycle and Apoptosis,” *Neoplasia*, vol. 2, no. 4, p. 291, 2000, doi: 10.1038/SJ.NEO.7900101.

[37] S. Ray, S. K. Panda, S. R. Nayak, S. Behera, S. S. Bhanja, and V. Acharya, “A Review on Cell Cycle Checkpoints in Relation to Cancer,” *The Journal of Medical Sciences*, vol. 5, no. 4, pp. 88–95, Oct. 2020, doi: 10.5005/JP-JOURNALS-10045-00138.

[38] K. J. Barnum and M. J. O’Connell, “Cell cycle regulation by checkpoints,” *Methods in Molecular Biology*, vol. 1170, pp. 29–40, 2014, doi: 10.1007/978-1-4939-0888-2_2.

[39] P. Xia, Y. Liu, J. Chen, and Z. Cheng, “Cell Cycle Proteins as Key Regulators of Postmitotic Cell Death,” *Yale J Biol Med*, vol. 92, no. 4, pp. 641–650, Dec. 2019, [Online]. Available: https://pubmed.ncbi.nlm.nih.gov/31866779

[40] D. S. Park, E. J. Morris, L. A. Greene, and H. M. Geller, “G1/S Cell Cycle Blockers and Inhibitors of Cyclin-Dependent Kinases Suppress Camptothecin-Induced

Neuronal Apoptosis," *The Journal of Neuroscience*, vol. 17, no. 4, pp. 1256–1270, Feb. 1997, doi: 10.1523/JNEUROSCI.17-04-01256.1997.

[41] A. Giovanni, F. Wirtz-Brugger, E. Keramaris, R. Slack, and D. S. Park, "Involvement of Cell Cycle Elements, Cyclin-dependent Kinases, pRb, and E2F·DP, in B-amyloid-induced Neuronal Death," *Journal of Biological Chemistry*, vol. 274, no. 27, pp. 19011–19016, Jul. 1999, doi: 10.1074/jbc.274.27.19011.

[42] H. J. Rideout, Q. Wang, D. S. Park, and L. Stefanis, "Cyclin-Dependent Kinase Activity Is Required for Apoptotic Death But Not Inclusion Formation in Cortical Neurons after Proteasomal Inhibition," *The Journal of Neuroscience*, vol. 23, no. 4, pp. 1237–1245, Feb. 2003, doi: 10.1523/JNEUROSCI.23-04-01237.2003.

[43] J. Wu *et al.*, "Inhibition of E2F1/CDK1 Pathway Attenuates Neuronal Apoptosis In Vitro and Confers Neuroprotection after Spinal Cord Injury In Vivo," *PLoS One*, vol. 7, no. 7, p. e42129, Jul. 2012, doi: 10.1371/journal.pone.0042129.

[44] R. Requejo-Aguilar, "Cdk5 and aberrant cell cycle activation at the core of neurodegeneration," *Neural Regen Res*, vol. 18, no. 6, p. 1186, 2023, doi: 10.4103/1673-5374.360165.

[45] F. Bassermann, R. Eichner, and M. Pagano, "The ubiquitin proteasome system — Implications for cell cycle control and the targeted treatment of cancer," *Biochimica et Biophysica Acta (BBA) - Molecular Cell Research*, vol. 1843, no. 1, pp. 150–162, Jan. 2014, doi: 10.1016/j.bbamcr.2013.02.028.

[46] P. Ebner, G. A. Versteeg, and F. Ikeda, "Ubiquitin enzymes in the regulation of immune responses," *Crit Rev Biochem Mol Biol*, vol. 52, no. 4, p. 425, Jul. 2017, doi: 10.1080/10409238.2017.1325829.

[47] Z. S. Hann *et al.*, "Structural basis for adenylation and thioester bond formation in the ubiquitin E1," *Proceedings of the National Academy of Sciences*, vol. 116, no. 31, pp. 15475–15484, Jul. 2019, doi: 10.1073/pnas.1905488116.

[48] Q. Yang, J. Zhao, D. Chen, and Y. Wang, "E3 ubiquitin ligases: styles, structures and functions," *Molecular Biomedicine*, vol. 2, no. 1, p. 23, Dec. 2021, doi: 10.1186/s43556-021-00043-2.

[49] F. Dang, L. Nie, and W. Wei, “Ubiquitin signaling in cell cycle control and tumorigenesis,” *Cell Death Differ*, vol. 28, no. 2, pp. 427–438, Feb. 2021, doi: 10.1038/s41418-020-00648-0.

[50] L. K. Nguyen, M. Dobrzyński, D. Fey, and B. N. Kholodenko, “Polyubiquitin chain assembly and organization determine the dynamics of protein activation and degradation,” *Front Physiol*, vol. 5, 2014, doi: 10.3389/fphys.2014.00004.

[51] Q. Yang, J. Zhao, D. Chen, and Y. Wang, “E3 ubiquitin ligases: styles, structures and functions,” *Molecular Biomedicine*, vol. 2, no. 1, Dec. 2021, doi: 10.1186/S43556-021-00043-2.

[52] Y. Wang, D. Argiles-Castillo, E. I. Kane, A. Zhou, and D. E. Spratt, “HECT E3 ubiquitin ligases - emerging insights into their biological roles and disease relevance,” *J Cell Sci*, vol. 133, no. 7, Apr. 2020, doi: 10.1242/JCS.228072.

[53] D. Rotin and S. Kumar, “Physiological functions of the HECT family of ubiquitin ligases,” *Nat Rev Mol Cell Biol*, vol. 10, no. 6, pp. 398–409, Jun. 2009, doi: 10.1038/NRM2690.

[54] H. Walden and K. Rittinger, “RBR ligase–mediated ubiquitin transfer: a tale with many twists and turns,” *Nature Structural & Molecular Biology 2018 25:6*, vol. 25, no. 6, pp. 440–445, May 2018, doi: 10.1038/s41594-018-0063-3.

[55] X. S. Wang *et al.*, “The unifying catalytic mechanism of the RING-between-RING E3 ubiquitin ligase family,” *Nature Communications 2023 14:1*, vol. 14, no. 1, pp. 1–17, Jan. 2023, doi: 10.1038/s41467-023-35871-z.

[56] B. Sharma and J. Taganna, “Genome-wide analysis of the U-box E3 ubiquitin ligase enzyme gene family in tomato,” *Scientific Reports 2020 10:1*, vol. 10, no. 1, pp. 1–15, Jun. 2020, doi: 10.1038/s41598-020-66553-1.

[57] D. E. Spratt, H. Walden, and G. S. Shaw, “RBR E3 ubiquitin ligases: new structures, new insights, new questions,” *Biochem J*, vol. 458, no. 3, pp. 421–437, Mar. 2014, doi: 10.1042/BJ20140006.

[58] F. Dang, L. Nie, and W. Wei, “Ubiquitin signaling in cell cycle control and tumorigenesis,” *Cell Death & Differentiation 2020 28:2*, vol. 28, no. 2, pp. 427–438, Oct. 2020, doi: 10.1038/s41418-020-00648-0.

[59] H. C. Vodermaier, “APC/C and SCF: Controlling Each Other and the Cell Cycle,” *Current Biology*, vol. 14, no. 18, pp. R787–R796, Sep. 2004, doi: 10.1016/j.cub.2004.09.020.

[60] E. Eytan, Y. Moshe, I. Braunstein, and A. Hershko, “Roles of the anaphase-promoting complex/cyclosome and of its activator Cdc20 in functional substrate binding,” *Proceedings of the National Academy of Sciences*, vol. 103, no. 7, pp. 2081–2086, Feb. 2006, doi: 10.1073/pnas.0510695103.

[61] J. W. Harper, J. L. Burton, and M. J. Solomon, “The anaphase-promoting complex: it’s not just for mitosis any more,” *Genes Dev*, vol. 16, no. 17, pp. 2179–2206, Sep. 2002, doi: 10.1101/gad.1013102.

[62] J.-M. Peters, “The Anaphase-Promoting Complex,” *Mol Cell*, vol. 9, no. 5, pp. 931–943, May 2002, doi: 10.1016/S1097-2765(02)00540-3.

[63] C. M. Pickart, “Mechanisms Underlying Ubiquitination,” *Annu Rev Biochem*, vol. 70, no. 1, pp. 503–533, Jun. 2001, doi: 10.1146/annurev.biochem.70.1.503.

[64] A. W. Murray, “Recycling the Cell Cycle,” *Cell*, vol. 116, no. 2, pp. 221–234, Jan. 2004, doi: 10.1016/S0092-8674(03)01080-8.

[65] J. Xie, Y. Jin, and G. Wang, “The role of SCF ubiquitin-ligase complex at the beginning of life,” *Reproductive Biology and Endocrinology*, vol. 17, no. 1, p. 101, Dec. 2019, doi: 10.1186/s12958-019-0547-y.

[66] T. Cardozo and M. Pagano, “The SCF ubiquitin ligase: insights into a molecular machine,” *Nat Rev Mol Cell Biol*, vol. 5, no. 9, pp. 739–751, Sep. 2004, doi: 10.1038/nrm1471.

[67] V. P. Ronchi, J. M. Klein, D. J. Edwards, and A. L. Haas, “The Active Form of E6-associated protein (E6AP)/UBE3A Ubiquitin Ligase Is an Oligomer,” *J Biol Chem*, vol. 289, no. 2, p. 1033, Jan. 2014, doi: 10.1074/JBC.M113.517805.

[68] A. Pal and R. Kundu, “Human Papillomavirus E6 and E7: The Cervical Cancer Hallmarks and Targets for Therapy,” *Front Microbiol*, vol. 10, p. 510168, Jan. 2020, doi: 10.3389/FMICB.2019.03116/BIBTEX.

[69] J. C. K. Wang *et al.*, "Structure of the p53 degradation complex from HPV16," *Nature Communications 2024 15:1*, vol. 15, no. 1, pp. 1–18, Feb. 2024, doi: 10.1038/s41467-024-45920-w.

[70] A. L. Talis, J. M. Huibregtse, and P. M. Howley, "The Role of E6AP in the Regulation of p53 Protein Levels in Human Papillomavirus (HPV)-positive and HPV-negative Cells," *Journal of Biological Chemistry*, vol. 273, no. 11, pp. 6439–6445, Mar. 1998, doi: 10.1074/JBC.273.11.6439.

[71] D. Raghu *et al.*, "E6AP promotes prostate cancer by reducing p27 expression," *Oncotarget*, vol. 8, no. 26, p. 42939, Jun. 2017, doi: 10.18632/ONCOTARGET.17224.

[72] A. Montagnoli *et al.*, "Ubiquitination of p27 is regulated by Cdk-dependent phosphorylation and trimeric complex formation," *Genes Dev*, vol. 13, no. 9, p. 1181, May 1999, doi: 10.1101/GAD.13.9.1181.

[73] L. García-Gutiérrez *et al.*, "Myc stimulates cell cycle progression through the activation of Cdk1 and phosphorylation of p27," *Scientific Reports 2019 9:1*, vol. 9, no. 1, pp. 1–17, Dec. 2019, doi: 10.1038/s41598-019-54917-1.

[74] L. K. Ries, A. K. L. Liess, C. G. Feiler, D. E. Spratt, E. D. Lowe, and S. Lorenz, "Crystal structure of the catalytic C-lobe of the HECT-type ubiquitin ligase E6AP," *Protein Sci*, vol. 29, no. 6, p. 1550, Jun. 2020, doi: 10.1002/PRO.3832.

[75] S. A. Beasley, C. E. Kellum, R. J. Orlomoski, F. Idrizi, and D. E. Spratt, "An Angelman syndrome substitution in the HECT E3 ubiquitin ligase C-terminal Lobe of E6AP affects protein stability and activity," *PLoS One*, vol. 15, no. 7, Jul. 2020, doi: 10.1371/JOURNAL.PONE.0235925.

[76] Y. Liu, O. Tavana, and W. Gu, "p53 modifications: exquisite decorations of the powerful guardian," *J Mol Cell Biol*, vol. 11, no. 7, p. 564, Jul. 2019, doi: 10.1093/JMCB/MJZ060.

[77] S. Kook, X. Zhan, K. Thibeault, M. R. Ahmed, V. V. Gurevich, and E. V. Gurevich, "Mdm2 enhances ligase activity of parkin and facilitates mitophagy," *Sci Rep*, vol. 10, no. 1, p. 5028, Mar. 2020, doi: 10.1038/s41598-020-61796-4.

[78] V. P. Ronchi, J. M. Klein, and A. L. Haas, “E6AP/UBE3A Ubiquitin Ligase Harbors Two E2∼ubiquitin Binding Sites,” *Journal of Biological Chemistry*, vol. 288, no. 15, pp. 10349–10360, Apr. 2013, doi: 10.1074/JBC.M113.458059.

[79] F. Mateo *et al.*, “Degradation of cyclin A is regulated by acetylation,” *Oncogene*, vol. 28, no. 29, pp. 2654–2666, Jul. 2009, doi: 10.1038/ONC.2009.127.

[80] S. Bruno, A. Ghelli Luserna di Rorà, R. Napolitano, S. Soverini, G. Martinelli, and G. Simonetti, “CDC20 in and out of mitosis: a prognostic factor and therapeutic target in hematological malignancies,” *Journal of Experimental & Clinical Cancer Research 2022 41:1*, vol. 41, no. 1, pp. 1–16, Apr. 2022, doi: 10.1186/S13046-022-02363-9.

[81] P. Genschik, K. Marrocco, L. Bach, S. Noir, and M. C. Criqui, “Selective protein degradation: a rheostat to modulate cell-cycle phase transitions,” *J Exp Bot*, vol. 65, no. 10, pp. 2603–2615, Jun. 2014, doi: 10.1093/JXB/ERT426.

[82] H. J. Park, R. H. Costa, L. F. Lau, A. L. Tyner, and P. Raychaudhuri, “Anaphase-promoting complex/cyclosome-CDH1-mediated proteolysis of the forkhead box M1 transcription factor is critical for regulated entry into S phase,” *Mol Cell Biol*, vol. 28, no. 17, pp. 5162–5171, Sep. 2008, doi: 10.1128/MCB.00387-08.

[83] C. Lindon, R. Grant, and M. Min, “Ubiquitin-mediated degradation of Aurora kinases,” *Front Oncol*, vol. 5, no. JAN, p. 170413, Jan. 2016, doi: 10.3389/FONC.2015.00307/BIBTEX.

[84] Z. Cai *et al.*, “The Skp2 Pathway: A Critical Target for Cancer Therapy,” *Semin Cancer Biol*, vol. 67, pp. 16–33, Dec. 2020, doi: 10.1016/j.semcancer.2020.01.013.

[85] G. Wang, C. H. Chan, Y. Gao, and H. K. Lin, “Novel roles of Skp2 E3 ligase in cellular senescence, cancer progression, and metastasis,” *Chin J Cancer*, vol. 31, no. 4, pp. 169–177, 2012, doi: 10.5732/cjc.011.10319.

[86] X. Qiao, L. Zhang, A. M. Gamper, T. Fujita, and Y. Wan, “APC/C-Cdh1,” *Cell Cycle*, vol. 9, no. 19, pp. 3904–3912, Oct. 2010, doi: 10.4161/CC.9.19.13585.

[87] L. Jia and Y. Sun, “SCF E3 ubiquitin ligases as anticancer targets,” *Curr Cancer Drug Targets*, vol. 11, no. 3, pp. 347–356, Feb. 2011, doi: 10.2174/156800911794519734.

[88] C. H. Chan, S. W. Lee, J. Wang, and H. K. Lin, “Regulation of Skp2 expression and activity and its role in cancer progression,” *ScientificWorldJournal*, vol. 10, pp. 1001–1015, Jun. 2010, doi: 10.1100/TSW.2010.89.

[89] U. Benary and J. Wolf, “Controlling Nuclear NF-κB Dynamics by β-TrCP—Insights from a Computational Model,” *Biomedicines*, vol. 7, no. 2, p. 40, May 2019, doi: 10.3390/biomedicines7020040.

[90] D. Guardavaccaro *et al.*, “Control of Meiotic and Mitotic Progression by the F Box Protein β-Trcp1 In Vivo,” *Dev Cell*, vol. 4, no. 6, pp. 799–812, Jun. 2003, doi: 10.1016/S1534-5807(03)00154-0.

[91] N. Watanabe *et al.*, “M-phase kinases induce phospho-dependent ubiquitination of somatic Wee1 by SCF $^{\beta\text{-TrCP}}$,” *Proceedings of the National Academy of Sciences*, vol. 101, no. 13, pp. 4419–4424, Mar. 2004, doi: 10.1073/pnas.0307700101.

[92] J. Liu *et al.*, “Wnt/β-catenin signalling: function, biological mechanisms, and therapeutic opportunities,” *Signal Transduct Target Ther*, vol. 7, no. 1, p. 3, Jan. 2022, doi: 10.1038/s41392-021-00762-6.

[93] Y. Kanemori, K. Uto, and N. Sagata, “β-TrCP recognizes a previously undescribed nonphosphorylated destruction motif in Cdc25A and Cdc25B phosphatases,” *Proceedings of the National Academy of Sciences*, vol. 102, no. 18, pp. 6279–6284, May 2005, doi: 10.1073/pnas.0501873102.

[94] F. Dang, L. Nie, and W. Wei, “Ubiquitin signaling in cell cycle control and tumorigenesis,” *Cell Death Differ*, vol. 28, no. 2, pp. 427–438, Feb. 2021, doi: 10.1038/s41418-020-00648-0.

[95] Z. Zhang *et al.*, “Function and regulation of F-box/WD repeat-containing protein 7 (Review),” *Oncol Lett*, vol. 20, no. 2, pp. 1526–1534, Jun. 2020, doi: 10.3892/ol.2020.11728.

[96] D. J. Bonda *et al.*, “Evidence for the progression through S-phase in the ectopic cell cycle re-entry of neurons in Alzheimer disease,” *Aging*, vol. 1, no. 4, pp. 382–388, Apr. 2009, doi: 10.18632/aging.100044.

[97] K. Herrup and Y. Yang, “Cell cycle regulation in the postmitotic neuron: oxymoron or new biology?,” *Nat Rev Neurosci*, vol. 8, no. 5, pp. 368–378, May 2007, doi: 10.1038/nrn2124.

[98] W.-C. Chou, L.-Y. Hu, C.-N. Hsiung, and C.-Y. Shen, “Initiation of the ATM-Chk2 DNA damage response through the base excision repair pathway,” *Carcinogenesis*, vol. 36, no. 8, pp. 832–840, Aug. 2015, doi: 10.1093/carcin/bgv079.

[99] P. A. Do and C. H. Lee, “The Role of CDK5 in Tumours and Tumour Microenvironments,” *Cancers (Basel)*, vol. 13, no. 1, p. 101, Dec. 2020, doi: 10.3390/cancers13010101.

[100] J. Zhang, S. A. Cicero, L. Wang, R. R. Romito-DiGiacomo, Y. Yang, and K. Herrup, “Nuclear localization of Cdk5 is a key determinant in the postmitotic state of neurons,” *Proceedings of the National Academy of Sciences*, vol. 105, no. 25, pp. 8772–8777, Jun. 2008, doi: 10.1073/pnas.0711355105.

[101] M. G. Andrusiak *et al.*, “Rb/E2F Regulates Expression of Neogenin during Neuronal Migration,” *Mol Cell Biol*, vol. 31, no. 2, pp. 238–247, Jan. 2011, doi: 10.1128/MCB.00378-10.

[102] T. Kawauchi, K. Chihama, Y. Nabeshima, and M. Hoshino, “Cdk5 phosphorylates and stabilizes p27kip1 contributing to actin organization and cortical neuronal migration,” *Nat Cell Biol*, vol. 8, no. 1, pp. 17–26, Jan. 2006, doi: 10.1038/ncb1338.

[103] Mosch B., Morawski M., Mittag A., Lenz D., Tarnok T, and Arendt T., “Aneuploidy and DNA replication in the normal human brain and Alzheimer’s disease,” *J Neuroscience*, pp. 6859–6867, 2007.

[104] J. M. Frade and M. C. Ovejero-Benito, “Neuronal cell cycle: the neuron itself and its circumstances,” *Cell Cycle*, vol. 14, no. 5, pp. 712–720, Mar. 2015, doi: 10.1080/15384101.2015.1004937.

[105] C. Joseph *et al.*, “Cell Cycle Deficits in Neurodegenerative Disorders: Uncovering Molecular Mechanisms to Drive Innovative Therapeutic Development,” *Aging Dis*, vol. 11, no. 4, p. 946, 2020, doi: 10.14336/AD.2019.0923.

[106] D. R. Kaplan and F. D. Miller, “Neurotrophin signal transduction in the nervous system,” *Curr Opin Neurobiol*, vol. 10, no. 3, pp. 381–391, Jun. 2000, doi: 10.1016/S0959-4388(00)00092-1.

[107] A. Mohammadi, V. G. Amooeian, and E. Rashidi, “Dysfunction in Brain-Derived Neurotrophic Factor Signaling Pathway and Susceptibility to Schizophrenia, Parkinson’s and Alzheimer’s Diseases,” *Curr Gene Ther*, vol. 18, no. 1, pp. 45–63, May 2018, doi: 10.2174/1566523218666180302163029.

[108] H. Tanila, “The role of BDNF in Alzheimer’s disease,” *Neurobiol Dis*, vol. 97, pp. 114–118, Jan. 2017, doi: 10.1016/j.nbd.2016.05.008.

[109] M. C. Ovejero-Benito and J. M. Frade, “Brain-Derived Neurotrophic Factor-Dependent cdk1 Inhibition Prevents G2/M Progression in Differentiating Tetraploid Neurons,” *PLoS One*, vol. 8, no. 5, p. e64890, May 2013, doi: 10.1371/journal.pone.0064890.

[110] S. M. Morillo, E. P. Abanto, M. J. Román, and J. M. Frade, “Nerve Growth Factor-Induced Cell Cycle Reentry in Newborn Neurons Is Triggered by p38 ^{MAPK} -Dependent E2F4 Phosphorylation,” *Mol Cell Biol*, vol. 32, no. 14, pp. 2722–2737, Jul. 2012, doi: 10.1128/MCB.00239-12.

[111] S. Ambrosio *et al.*, “Cell cycle-dependent resolution of DNA double-strand breaks,” *Oncotarget*, vol. 7, no. 4, pp. 4949–4960, Jan. 2016, doi: 10.18632/oncotarget.6644.

[112] L.-S. Zhu, D.-Q. Wang, K. Cui, D. Liu, and L.-Q. Zhu, “Emerging Perspectives on DNA Double-strand Breaks in Neurodegenerative Diseases,” *Curr Neuropharmacol*, vol. 17, no. 12, pp. 1146–1157, Nov. 2019, doi: 10.2174/1570159X17666190726115623.

[113] M. S. Y. Huen and J. Chen, “The DNA damage response pathways: at the crossroad of protein modifications,” *Cell Research 2008 18:1*, vol. 18, no. 1, pp. 8–16, Dec. 2007, doi: 10.1038/cr.2007.109.

[114] Q. Nie *et al.*, “The E3 Ligase PIAS1 Regulates p53 Sumoylation to Control Stress-Induced Apoptosis of Lens Epithelial Cells Through the Proapoptotic Regulator Bax,” *Front Cell Dev Biol*, vol. 9, p. 1214, Jun. 2021, doi: 10.3389/FCELL.2021.660494/BIBTEX.

[115] W. M. Abida, A. Nikolaev, W. Zhao, W. Zhang, and W. Gu, "FBXO11 Promotes the Neddylation of p53 and Inhibits Its Transcriptional Activity," *J Biol Chem*, vol. 282, no. 3, p. 1797, Jan. 2007, doi: 10.1074/JBC.M609001200.

[116] A. Kirtonia, G. Sethi, and M. Garg, "The multifaceted role of reactive oxygen species in tumorigenesis," *Cellular and Molecular Life Sciences*, vol. 77, no. 22, pp. 4459–4483, Nov. 2020, doi: 10.1007/s00018-020-03536-5.

[117] M. Yamaura *et al.*, "NADPH Oxidase 4 Contributes to Transformation Phenotype of Melanoma Cells by Regulating G_2-M Cell Cycle Progression," *Cancer Res*, vol. 69, no. 6, pp. 2647–2654, Mar. 2009, doi: 10.1158/0008-5472.CAN-08-3745.

[118] R. G. Jones *et al.*, "AMP-Activated Protein Kinase Induces a p53-Dependent Metabolic Checkpoint," *Mol Cell*, vol. 18, no. 3, pp. 283–293, Apr. 2005, doi: 10.1016/j.molcel.2005.03.027.

[119] S. Lee *et al.*, "Human mitochondrial Fis1 links to cell cycle regulators at G2/M transition," *Cellular and Molecular Life Sciences*, vol. 71, no. 4, pp. 711–725, Feb. 2014, doi: 10.1007/s00018-013-1428-8.

[120] J. A. Klein *et al.*, "The harlequin mouse mutation downregulates apoptosis-inducing factor," *Nature*, vol. 419, no. 6905, pp. 367–374, Sep. 2002, doi: 10.1038/nature01034.

[121] C. Joseph *et al.*, "Cell Cycle Deficits in Neurodegenerative Disorders: Uncovering Molecular Mechanisms to Drive Innovative Therapeutic Development," *Aging Dis*, vol. 11, no. 4, p. 946, 2020, doi: 10.14336/AD.2019.0923.

[122] E. I. Schwartz *et al.*, "Cell Cycle Activation in Postmitotic Neurons is Essential for DNA Repair," *Cell Cycle*, vol. 6, no. 3, pp. 318–329, Feb. 2007, doi: 10.4161/cc.6.3.3752.

[123] Y. Zhang, X. Song, and K. Herrup, "Context-Dependent Functions of E2F1: Cell Cycle, Cell Death, and DNA Damage Repair in Cortical Neurons," *Mol Neurobiol*, vol. 57, no. 5, pp. 2377–2390, May 2020, doi: 10.1007/s12035-020-01887-5.

[124] B. Malik, A. Currais, and S. Soriano, "Cell cycle-driven neuronal apoptosis specifically linked to amyloid peptide A_{142} exposure is not exacerbated in a mouse model

of presenilin-1 familial Alzheimers disease," *J Neurochem*, vol. 106, no. 2, pp. 912–916, Jul. 2008, doi: 10.1111/j.1471-4159.2008.05446.x.

[125] P. Jiang *et al.*, "Chronic fluoride exposure induces neuronal apoptosis and impairs neurogenesis and synaptic plasticity: Role of GSK-3β/β-catenin pathway," *Chemosphere*, vol. 214, pp. 430–435, Jan. 2019, doi: 10.1016/j.chemosphere.2018.09.095.

[126] S. Singh *et al.*, "Axin-2 knockdown promote mitochondrial biogenesis and dopaminergic neurogenesis by regulating Wnt/β-catenin signaling in rat model of Parkinson's disease," *Free Radic Biol Med*, vol. 129, pp. 73–87, Dec. 2018, doi: 10.1016/j.freeradbiomed.2018.08.033.

[127] J. Zhu, W. Li, and Z. Mao, "Cdk5: Mediator of neuronal development, death and the response to DNA damage," *Mech Ageing Dev*, vol. 132, no. 8–9, pp. 389–394, Aug. 2011, doi: 10.1016/j.mad.2011.04.011.

[128] E. Huang *et al.*, "The role of Cdk5-mediated apurinic/apyrimidinic endonuclease 1 phosphorylation in neuronal death," *Nat Cell Biol*, vol. 12, no. 6, pp. 563–571, Jun. 2010, doi: 10.1038/ncb2058.

[129] T. K. Das, P. Jana, S. K. Chakrabarti, and M. R. W. Abdul Hamid, "Curcumin Downregulates GSK3 and Cdk5 in Scopolamine-Induced Alzheimer's Disease Rats Abrogating Aβ40/42 and Tau Hyperphosphorylation," *J Alzheimers Dis Rep*, vol. 3, no. 1, pp. 257–267, Aug. 2019, doi: 10.3233/ADR-190135.

[130] L. Crews and E. Masliah, "Molecular mechanisms of neurodegeneration in Alzheimer's disease," *Hum Mol Genet*, vol. 19, no. R1, pp. R12–R20, Apr. 2010, doi: 10.1093/hmg/ddq160.

[131] J. Mendoza, M. Sekiya, T. Taniguchi, K. M. Iijima, R. Wang, and K. Ando, "Global Analysis of Phosphorylation of Tau by the Checkpoint Kinases Chk1 and Chk2 *in vitro*," *J Proteome Res*, vol. 12, no. 6, pp. 2654–2665, Jun. 2013, doi: 10.1021/pr400008f.

[132] K. Iijima, A. Gatt, and K. Iijima-Ando, "Tau Ser262 phosphorylation is critical for A 42-induced tau toxicity in a transgenic Drosophila model of Alzheimer's disease," *Hum Mol Genet*, vol. 19, no. 15, pp. 2947–2957, Aug. 2010, doi: 10.1093/hmg/ddq200.

[133] Y. Chen, D. L. McPhie, J. Hirschberg, and R. L. Neve, "The Amyloid Precursor Protein-binding Protein APP-BP1 Drives the Cell Cycle through the S-M Checkpoint and Causes Apoptosis in Neurons," *Journal of Biological Chemistry*, vol. 275, no. 12, pp. 8929–8935, Mar. 2000, doi: 10.1074/jbc.275.12.8929.

[134] R. Sharma, D. Kumar, N. K. Jha, S. K. Jha, R. K. Ambasta, and P. Kumar, "Re-expression of cell cycle markers in aged neurons and muscles: Whether cells should divide or die?," *Biochimica et Biophysica Acta (BBA) - Molecular Basis of Disease*, vol. 1863, no. 1, pp. 324–336, Jan. 2017, doi: 10.1016/j.bbadis.2016.09.010.

[135] H. Lee *et al.*, "Cell cycle re-entry mediated neurodegeneration and its treatment role in the pathogenesis of Alzheimer's disease," *Neurochem Int*, vol. 54, no. 2, pp. 84–88, Feb. 2009, doi: 10.1016/j.neuint.2008.10.013.

[136] A. Currais, T. Hortobágyi, and S. Soriano, "The neuronal cell cycle as a mechanism of pathogenesis in Alzheimer's disease," *Aging*, vol. 1, no. 4, pp. 363–371, Apr. 2009, doi: 10.18632/aging.100045.

[137] B. Malik *et al.*, "Loss of neuronal cell cycle control as a mechanism of neurodegeneration in the Presenilin-1 Alzheimer's disease brain," *Cell Cycle*, vol. 7, no. 5, pp. 637–646, Mar. 2008, doi: 10.4161/cc.7.5.5427.

[138] J. Busser, D. S. Geldmacher, and K. Herrup, "Ectopic Cell Cycle Proteins Predict the Sites of Neuronal Cell Death in Alzheimer's Disease Brain," *The Journal of Neuroscience*, vol. 18, no. 8, pp. 2801–2807, Apr. 1998, doi: 10.1523/JNEUROSCI.18-08-02801.1998.

[139] Y. Yang, E. J. Mufson, and K. Herrup, "Neuronal Cell Death Is Preceded by Cell Cycle Events at All Stages of Alzheimer's Disease," *The Journal of Neuroscience*, vol. 23, no. 7, pp. 2557–2563, Apr. 2003, doi: 10.1523/JNEUROSCI.23-07-02557.2003.

[140] P. K. Modi, N. Komaravelli, N. Singh, and P. Sharma, "Interplay between MEK-ERK signaling, cyclin D1, and cyclin-dependent kinase 5 regulates cell cycle reentry and apoptosis of neurons," *Mol Biol Cell*, vol. 23, no. 18, pp. 3722–3730, Sep. 2012, doi: 10.1091/mbc.e12-02-0125.

[141] J. Folch *et al.*, "Role of Cell Cycle Re-Entry in Neurons: A Common Apoptotic Mechanism of Neuronal Cell Death," *Neurotox Res*, vol. 22, no. 3, pp. 195–207, Oct. 2012, doi: 10.1007/s12640-011-9277-4.

[142] S. Veeriah, L. Morris, D. Solit, and T. A. Chan, “The familial Parkinson Disease gene PARK2 is a multisite tumor suppressor on chromosome 6q25.2-27 that regulates cyclin E,” *Cell Cycle*, vol. 9, no. 8, pp. 1451–1452, Apr. 2010, doi: 10.4161/cc.9.8.11583.

[143] R. Roufayel and N. Murshid, “CDK5: Key Regulator of Apoptosis and Cell Survival,” *Biomedicines*, vol. 7, no. 4, p. 88, Nov. 2019, doi: 10.3390/biomedicines7040088.

[144] D. Qu *et al.*, “Role of Cdk5-Mediated Phosphorylation of Prx2 in MPTP Toxicity and Parkinson’s Disease,” *Neuron*, vol. 55, no. 1, pp. 37–52, Jul. 2007, doi: 10.1016/j.neuron.2007.05.033.

[145] J. Tran *et al.*, “Therapeutic effects of TP5, a Cdk5/p25 inhibitor, in in vitro and in vivo models of Parkinson’s disease,” *Current Research in Neurobiology*, vol. 2, p. 100006, 2021, doi: 10.1016/j.crneur.2021.100006.

[146] K.-Y. Liu *et al.*, “Disruption of the nuclear membrane by perinuclear inclusions of mutant huntingtin causes cell-cycle re-entry and striatal cell death in mouse and cell models of Huntington’s disease,” *Hum Mol Genet*, vol. 24, no. 6, pp. 1602–1616, Mar. 2015, doi: 10.1093/hmg/ddu574.

[147] M. S. Hipp *et al.*, “Indirect inhibition of 26S proteasome activity in a cellular model of Huntington’s disease,” *Journal of Cell Biology*, vol. 196, no. 5, pp. 573–587, Mar. 2012, doi: 10.1083/jcb.201110093.

[148] S. W. Park and U. Ozcan, “Potential for therapeutic manipulation of the UPR in disease,” *Semin Immunopathol*, vol. 35, no. 3, pp. 351–373, May 2013, doi: 10.1007/s00281-013-0370-z.

[149] M. R. Fernandez-Fernandez, I. Ferrer, and J. J. Lucas, “Impaired ATF6α processing, decreased Rheb and neuronal cell cycle re-entry in Huntington’s disease,” *Neurobiol Dis*, vol. 41, no. 1, pp. 23–32, Jan. 2011, doi: 10.1016/j.nbd.2010.08.014.

[150] K. Bečanović *et al.*, “A SNP in the HTT promoter alters NF-κB binding and is a bidirectional genetic modifier of Huntington disease,” *Nat Neurosci*, vol. 18, no. 6, pp. 807–816, Jun. 2015, doi: 10.1038/nn.4014.

[151] I. Ferrer and R. Blanco, “N-myc and c-myc expression in Alzheimer disease, Huntington disease and Parkinson disease,” *Molecular Brain Research*, vol. 77, no. 2, pp. 270–276, May 2000, doi: 10.1016/S0169-328X(00)00062-0.

[152] C. Pelegrí *et al.*, “Cell cycle activation in striatal neurons from Huntington’s disease patients and rats treated with 3-nitropropionic acid,” *International Journal of Developmental Neuroscience*, vol. 26, no. 7, pp. 665–671, Nov. 2008, doi: 10.1016/j.ijdevneu.2008.07.016.

[153] M. Kandasamy and L. Aigner, “Reactive Neuroblastosis in Huntington’s Disease: A Putative Therapeutic Target for Striatal Regeneration in the Adult Brain,” *Front Cell Neurosci*, vol. 12, Mar. 2018, doi: 10.3389/fncel.2018.00037.

[154] J. Dong, T. E. Ochsner, M. Zreda, M. H. Cosh, and C. B. Zou, “Calibration and Validation of the COSMOS Rover for Surface Soil Moisture Measurement,” *Vadose Zone Journal*, vol. 13, no. 4, pp. 1–8, Apr. 2014, doi: 10.2136/vzj2013.08.0148.

[155] A. Barzilai, S. Biton, and Y. Shiloh, “The role of the DNA damage response in neuronal development, organization and maintenance,” *DNA Repair (Amst)*, vol. 7, no. 7, pp. 1010–1027, Jul. 2008, doi: 10.1016/j.dnarep.2008.03.005.

[156] S. Di Giovanni *et al.*, “Cell cycle inhibition provides neuroprotection and reduces glial proliferation and scar formation after traumatic brain injury,” *Proceedings of the National Academy of Sciences*, vol. 102, no. 23, pp. 8333–8338, Jun. 2005, doi: 10.1073/pnas.0500989102.

[157] J. Woods, M. Snape, and M. A. Smith, “The cell cycle hypothesis of Alzheimer’s disease: Suggestions for drug development,” *Biochimica et Biophysica Acta (BBA) - Molecular Basis of Disease*, vol. 1772, no. 4, pp. 503–508, Apr. 2007, doi: 10.1016/j.bbadis.2006.12.004.

[158] J. Wu, B. A. Stoica, and A. I. Faden, “Cell Cycle Activation and Spinal Cord Injury,” *Neurotherapeutics*, vol. 8, no. 2, pp. 221–228, Apr. 2011, doi: 10.1007/s13311-011-0028-2.

[159] L. Meijer *et al.*, “Biochemical and Cellular Effects of Roscovitine, a Potent and Selective Inhibitor of the Cyclin-Dependent Kinases cdc2, cdk2 and cdk5,” *Eur J Biochem*, vol. 243, no. 1–2, pp. 527–536, Jan. 1997, doi: 10.1111/j.1432-1033.1997.t01- 2-00527.x.

[160] R. Abraham *et al.*, "Cellular effects of olomoucine, an inhibitor of cyclin-dependent kinases," *Biol Cell*, vol. 83, no. 2–3, pp. 105–120, 1995, doi: 10.1016/0248-4900(96)81298-6.

[161] N. S. Elsisi, S. Darling-Reed, E. Y. Lee, E. T. Oriaku, and K. F. Soliman, "Ibuprofen and apigenin induce apoptosis and cell cycle arrest in activated microglia," *Neurosci Lett*, vol. 375, no. 2, pp. 91–96, Feb. 2005, doi: 10.1016/j.neulet.2004.10.087.

[162] M. Cascella, S. Bimonte, M. R. Muzio, V. Schiavone, and A. Cuomo, "The efficacy of Epigallocatechin-3-gallate (green tea) in the treatment of Alzheimer's disease: an overview of pre-clinical studies and translational perspectives in clinical practice," *Infect Agent Cancer*, vol. 12, no. 1, p. 36, Dec. 2017, doi: 10.1186/s13027-017-0145-6.

[163] Y. Ding, A. Qiao, and G.-H. Fan, "Indirubin-3'-monoxime rescues spatial memory deficits and attenuates β-amyloid-associated neuropathology in a mouse model of Alzheimer's disease," *Neurobiol Dis*, vol. 39, no. 2, pp. 156–168, Aug. 2010, doi: 10.1016/j.nbd.2010.03.022.

[164] J. Inokoshi *et al.*, "Neuronal Differentiation of Neuro 2a Cells by Inhibitors of Cell Cycle Progression, Trichostatin A and Butyrolactone I," *Biochem Biophys Res Commun*, vol. 256, no. 2, pp. 372–376, Mar. 1999, doi: 10.1006/bbrc.1999.0316.

[165] Y. Xiao *et al.*, "Tetrahydrocurcumin ameliorates Alzheimer's pathological phenotypes by inhibition of microglial cell cycle arrest and apoptosis via Ras/ERK signaling," *Biomedicine & Pharmacotherapy*, vol. 139, p. 111651, Jul. 2021, doi: 10.1016/j.biopha.2021.111651.

[166] Q. Quan, X. Li, J. Feng, J. Hou, M. Li, and B. Zhang, "Ginsenoside Rg1 reduces β-amyloid levels by inhibiting CD5K-induced PPARγ phosphorylation in a neuron model of Alzheimer's disease," *Mol Med Rep*, Aug. 2020, doi: 10.3892/mmr.2020.11424.

[167] A. Nakajima and Y. Ohizumi, "Potential Benefits of Nobiletin, A Citrus Flavonoid, against Alzheimer's Disease and Parkinson's Disease," *Int J Mol Sci*, vol. 20, no. 14, p. 3380, Jul. 2019, doi: 10.3390/ijms20143380.

[168] S. Ahmad, M. H. Jo, M. Ikram, A. Khan, and M. O. Kim, "Deciphering the Potential Neuroprotective Effects of Luteolin against Aβ1–42-Induced Alzheimer's Disease," *Int J Mol Sci*, vol. 22, no. 17, p. 9583, Sep. 2021, doi: 10.3390/ijms22179583.

[169] L.-J. Zhou and X.-Z. Zhu, “Reactive Oxygen Species-Induced Apoptosis in PC12 Cells and Protective Effect of Bilobalide,” *Journal of Pharmacology and Experimental Therapeutics*, vol. 293, no. 3, p. 982, Jun. 2000, [Online]. Available: http://jpet.aspetjournals.org/content/293/3/982.abstract

[170] J. Xiang *et al.*, “Bilobalide inhibits inflammation and promotes the expression of Aβ degrading enzymes in astrocytes to rescue neuronal deficiency in AD models,” *Transl Psychiatry*, vol. 11, no. 1, p. 542, Dec. 2021, doi: 10.1038/s41398-021-01594-2.

[171] M. Zhang, J. Li, P. Chakrabarty, B. Bu, and I. Vincent, “Cyclin-Dependent Kinase Inhibitors Attenuate Protein Hyperphosphorylation, Cytoskeletal Lesion Formation, and Motor Defects in Niemann-Pick Type C Mice,” *Am J Pathol*, vol. 165, no. 3, pp. 843–853, Sep. 2004, doi: 10.1016/S0002-9440(10)63347-0.

[172] L. Wei *et al.*, “A Butyrolactone Derivative 3BDO Alleviates Memory Deficits and Reduces Amyloid-β Deposition in an AβPP/PS1 Transgenic Mouse Model,” *Journal of Alzheimer’s Disease*, vol. 30, no. 3, pp. 531–543, Jun. 2012, doi: 10.3233/JAD-2012-111985.

[173] A. Wilkaniec, M. Gąssowska-Dobrowolska, M. Strawski, A. Adamczyk, and G. A. Czapski, “Inhibition of cyclin-dependent kinase 5 affects early neuroinflammatory signalling in murine model of amyloid beta toxicity,” *J Neuroinflammation*, vol. 15, no. 1, p. 1, Dec. 2018, doi: 10.1186/s12974-017-1027-y.

[174] G. M. Leggio *et al.*, “The antineoplastic drug flavopiridol reverses memory impairment induced by Amyloid-ß 1-42 oligomers in mice,” *Pharmacol Res*, vol. 106, pp. 10–20, Apr. 2016, doi: 10.1016/j.phrs.2016.02.007.

[175] A. Khan *et al.*, “Neuroprotective Effect of Quercetin Against the Detrimental Effects of LPS in the Adult Mouse Brain,” *Front Pharmacol*, vol. 9, Dec. 2018, doi: 10.3389/fphar.2018.01383.

[176] N. S. Dourado *et al.*, “Neuroimmunomodulatory and Neuroprotective Effects of the Flavonoid Apigenin in in vitro Models of Neuroinflammation Associated With Alzheimer’s Disease,” *Front Aging Neurosci*, vol. 12, May 2020, doi: 10.3389/fnagi.2020.00119.

[177] N. S. Elsisi, S. Darling-Reed, E. Y. Lee, E. T. Oriaku, and K. F. Soliman, "Ibuprofen and apigenin induce apoptosis and cell cycle arrest in activated microglia," *Neurosci Lett*, vol. 375, no. 2, pp. 91–96, Feb. 2005, doi: 10.1016/j.neulet.2004.10.087.

[178] M. Cascella, S. Bimonte, M. R. Muzio, V. Schiavone, and A. Cuomo, "The efficacy of Epigallocatechin-3-gallate (green tea) in the treatment of Alzheimer's disease: an overview of pre-clinical studies and translational perspectives in clinical practice," *Infect Agent Cancer*, vol. 12, no. 1, p. 36, Dec. 2017, doi: 10.1186/s13027-017-0145-6.

[179] P. LIczbiński and B. Bukowska, "Tea and coffee polyphenols and their biological properties based on the latest in vitro investigations," *Ind Crops Prod*, vol. 175, p. 114265, Jan. 2022, doi: 10.1016/j.indcrop.2021.114265.

[180] Z. Li, B. Zhang, W. Yao, C. Zhang, L. Wan, and Y. Zhang, "APC-Cdh1 Regulates Neuronal Apoptosis Through Modulating Glycolysis and Pentose-Phosphate Pathway After Oxygen-Glucose Deprivation and Reperfusion," *Cell Mol Neurobiol*, vol. 39, no. 1, pp. 123–135, Jan. 2019, doi: 10.1007/s10571-018-0638-x.

[181] T. Fuchsberger, S. Martínez-Bellver, E. Giraldo, V. Teruel-Martí, A. Lloret, and J. Viña, "Aβ Induces Excitotoxicity Mediated by APC/C-Cdh1 Depletion That Can Be Prevented by Glutaminase Inhibition Promoting Neuronal Survival," *Sci Rep*, vol. 6, no. 1, p. 31158, Nov. 2016, doi: 10.1038/srep31158.

[182] S. A. Mandel, T. Fishman-Jacob, and M. B. H. Youdim, "Genetic reduction of the E3 ubiquitin ligase element, SKP1A and environmental manipulation to emulate cardinal features of Parkinson's disease," *Parkinsonism Relat Disord*, vol. 18, pp. S177–S179, Jan. 2012, doi: 10.1016/S1353-8020(11)70055-4.

[183] J. F. Staropoli, C. McDermott, C. Martinat, B. Schulman, E. Demireva, and A. Abeliovich, "Parkin Is a Component of an SCF-like Ubiquitin Ligase Complex and Protects Postmitotic Neurons from Kainate Excitotoxicity," *Neuron*, vol. 37, no. 5, pp. 735–749, Mar. 2003, doi: 10.1016/S0896-6273(03)00084-9.

[184] H. Ino and T. Chiba, "Cyclin-Dependent Kinase 4 and Cyclin D1 Are Required for Excitotoxin-Induced Neuronal Cell Death *In Vivo*," *The Journal of Neuroscience*, vol. 21, no. 16, pp. 6086–6094, Aug. 2001, doi: 10.1523/JNEUROSCI.21-16-06086.2001.

[185] S. Marathe, S. Liu, E. Brai, M. Kaczarowski, and L. Alberi, “Notch signaling in response to excitotoxicity induces neurodegeneration via erroneous cell cycle reentry,” *Cell Death Differ*, vol. 22, no. 11, pp. 1775–1784, Nov. 2015, doi: 10.1038/cdd.2015.23.

[186] A. Currais, T. Hortobágyi, and S. Soriano, “The neuronal cell cycle as a mechanism of pathogenesis in Alzheimer’s disease,” *Aging*, vol. 1, no. 4, pp. 363–371, Apr. 2009, doi: 10.18632/aging.100045.

[187] S. Demuro, R. M. C. Di Martino, J. A. Ortega, and A. Cavalli, “GSK-3β, FYN, and DYRK1A: Master Regulators in Neurodegenerative Pathways,” *Int J Mol Sci*, vol. 22, no. 16, p. 9098, Aug. 2021, doi: 10.3390/ijms22169098.

[188] C. H. van Dyck *et al.*, “Effect of AZD0530 on Cerebral Metabolic Decline in Alzheimer Disease,” *JAMA Neurol*, vol. 76, no. 10, p. 1219, Oct. 2019, doi: 10.1001/jamaneurol.2019.2050.

[189] D.-D. Li, Y.-H. Zhang, W. Zhang, and P. Zhao, “Meta-Analysis of Randomized Controlled Trials on the Efficacy and Safety of Donepezil, Galantamine, Rivastigmine, and Memantine for the Treatment of Alzheimer’s Disease,” *Front Neurosci*, vol. 13, May 2019, doi: 10.3389/fnins.2019.00472.

[190] M. M. Zhu, H. L. Li, L. H. Shi, X. P. Chen, J. Luo, and Z. L. Zhang, “The pharmacogenomics of valproic acid,” *Journal of Human Genetics 2017 62:12*, vol. 62, no. 12, pp. 1009–1014, Sep. 2017, doi: 10.1038/jhg.2017.91.

[191] M. Catarina Silva and S. J. Haggarty, “Tauopathies: Deciphering Disease Mechanisms to Develop Effective Therapies,” *International Journal of Molecular Sciences 2020, Vol. 21, Page 8948*, vol. 21, no. 23, p. 8948, Nov. 2020, doi: 10.3390/IJMS21238948.

[192] F. Coppede, “Targeting the epigenome to treat neurodegenerative diseases or delay their onset: a perspective,” *Neural Regen Res*, vol. 17, no. 8, p. 1745, Aug. 2022, doi: 10.4103/1673-5374.332145.

[193] W. M. A. D. B. Fernando *et al.*, “Sodium Butyrate Reduces Brain Amyloid-β Levels and Improves Cognitive Memory Performance in an Alzheimer’s Disease Transgenic Mouse Model at an Early Disease Stage,” *J Alzheimers Dis*, vol. 74, no. 1, pp. 91–99, 2020, doi: 10.3233/JAD-190120.

[194] A. Sharma and C. V. Preuss, “Bortezomib,” *StatPearls*, Sep. 2023, Accessed: Dec. 16, 2023. [Online]. Available: https://www.ncbi.nlm.nih.gov/books/NBK519559/

[195] M. Paranjpe, A. Taubes, and M. Sirota, “Insights into Computational Drug Repurposing for Neurodegenerative Disease”, doi: 10.1016/j.tips.2019.06.003.

[196] J. Haneczok, M. Delijewski, and R. Moldzio, “AI molecular property prediction for Parkinson’s Disease reveals potential repurposing drug candidates based on the increase of the expression of PINK1,” *Comput Methods Programs Biomed*, vol. 241, p. 107731, Nov. 2023, doi: 10.1016/J.CMPB.2023.107731.

[197] Z. Kuang *et al.*, “A Machine-Learning Based Drug Repurposing Approach Using Baseline Regularization,” *Methods Mol Biol*, vol. 1903, p. 255, 2019, doi: 10.1007/978-1-4939-8955-3_15.

[198] A. Gottlieb, G. Y. Stein, E. Ruppin, and R. Sharan, “PREDICT: a method for inferring novel drug indications with application to personalized medicine,” *Mol Syst Biol*, vol. 7, 2011, doi: 10.1038/MSB.2011.26.

[199] D. Szklarczyk *et al.*, “The STRING database in 2023: protein–protein association networks and functional enrichment analyses for any sequenced genome of interest,” *Nucleic Acids Res*, vol. 51, no. D1, pp. D638–D646, Jan. 2023, doi: 10.1093/nar/gkac1000.

[200] P. Shannon *et al.*, “Cytoscape: A Software Environment for Integrated Models of Biomolecular Interaction Networks,” *Genome Res*, vol. 13, no. 11, pp. 2498–2504, Nov. 2003, doi: 10.1101/gr.1239303.

[201] H. Zhao *et al.*, “NPASS database update 2023: quantitative natural product activity and species source database for biomedical research,” *Nucleic Acids Res*, vol. 51, no. D1, pp. D621–D628, Jan. 2023, doi: 10.1093/NAR/GKAC1069.

[202] M. Naveed *et al.*, “Comparative toxicity assessment of fisetin-aided artificial intelligence-assisted drug design targeting epibulbar dermoid through phytochemicals,” *Open Chem*, vol. 22, no. 1, Jan. 2024, doi: 10.1515/CHEM-2023-0197/MACHINEREADABLECITATION/RIS.

[203] F. Wu *et al.*, "Computational Approaches in Preclinical Studies on Drug Discovery and Development," *Front Chem*, vol. 8, p. 546712, Sep. 2020, doi: 10.3389/FCHEM.2020.00726/BIBTEX.

[204] X. Luo *et al.*, "Discovery of new small-molecule cyclin-dependent kinase 6 inhibitors through computational approaches," *Mol Divers*, vol. 25, no. 1, pp. 367–382, Feb. 2021, doi: 10.1007/S11030-020-10120-3/FIGS/7.

[205] S. Sarma, D. Dowerah, M. Basumatary, A. Phonglo, and R. C. Deka, "Inhibitory potential of furanocoumarins against cyclin dependent kinase 4 using integrated docking, molecular dynamics and ONIOM methods," *J Biomol Struct Dyn*, Dec. 2023, doi: 10.1080/07391102.2023.2300755.

[206] A. Daina, O. Michielin, and V. Zoete, "SwissADME: a free web tool to evaluate pharmacokinetics, drug-likeness and medicinal chemistry friendliness of small molecules," *Scientific Reports 2017 7:1*, vol. 7, no. 1, pp. 1–13, Mar. 2017, doi: 10.1038/srep42717.

[207] M. Naveed *et al.*, "Integrated track of nano-informatics coupling with the enrichment concept in developing a novel nanoparticle targeting ERK protein in Naegleria fowleri," *Open Chem*, vol. 22, no. 1, Jan. 2024, doi: 10.1515/CHEM-2023-0198/MACHINEREADABLECITATION/RIS.

[208] V. Blay, B. Tolani, S. P. Ho, and M. R. Arkin, "High-Throughput Screening: today's biochemical and cell-based approaches," *Drug Discov Today*, vol. 25, no. 10, pp. 1807–1821, Oct. 2020, doi: 10.1016/J.DRUDIS.2020.07.024.

[209] T. N. Doman *et al.*, "Molecular docking and high-throughput screening for novel inhibitors of protein tyrosine phosphatase-1B," *J Med Chem*, vol. 45, no. 11, pp. 2213–2221, May 2002, doi: 10.1021/JM010548W.

[210] V. Eynde, R. Barretta, S. Kralj, M. Jukič, and U. Bren, "Molecular Filters in Medicinal Chemistry," *Encyclopedia 2023, Vol. 3, Pages 501-511*, vol. 3, no. 2, pp. 501–511, Apr. 2023, doi: 10.3390/ENCYCLOPEDIA3020035.

[211] A. Chauhan *et al.*, "Designing the 5HT2BR structure and its modulation as a therapeutic target for repurposing approach in drug-resistant epilepsy," *Epilepsy Res*, vol. 194, p. 107168, Aug. 2023, doi: 10.1016/J.EPLEPSYRES.2023.107168.

[212] D. Van Der Spoel, E. Lindahl, B. Hess, G. Groenhof, A. E. Mark, and H. J. C. Berendsen, "GROMACS: Fast, flexible, and free," *J Comput Chem*, vol. 26, no. 16, pp. 1701–1718, Dec. 2005, doi: 10.1002/JCC.20291.

[213] N. Bharatham, S. W. Chi, and H. S. Yoon, "Molecular Basis of Bcl-XL-p53 Interaction: Insights from Molecular Dynamics Simulations," *PLoS One*, vol. 6, no. 10, p. 26014, 2011, doi: 10.1371/JOURNAL.PONE.0026014.

[214] P. J. Day *et al.*, "Crystal structure of human CDK4 in complex with a D-type cyclin," *Proc Natl Acad Sci U S A*, vol. 106, no. 11, pp. 4166–4170, Mar. 2009, doi: 10.1073/PNAS.0809645106.

[215] E. E. Abola, N. O. Manning, J. Prilusky, D. R. Stampf, and J. L. Sussman, "The Protein Data Bank: Current status and future challenges," *J Res Natl Inst Stand Technol*, vol. 101, no. 3, p. 231, May 1996, doi: 10.6028/jres.101.025.

[216] F. A. Yousif, A. A. Alzain, A. M. Alraih, and W. Ibraheem, "Repurposing of approved drugs for targeting CDK4/6 and aromatase protein using molecular docking and molecular dynamics studies," *PLoS One*, vol. 18, no. 9, p. e0291256, Sep. 2023, doi: 10.1371/JOURNAL.PONE.0291256.

[217] L. O. Anifowose, O. K. Paimo, O. M. Ogunyemi, R. O. Akano, S. F. Hammad, and M. A. Ghazy, "Molecular Docking Appraisal of Dysphania ambrosioides Phytochemicals as Potential Inhibitor of a Key Triple-negative Breast Cancer Driver Gene," Apr. 2023, doi: 10.21203/RS.3.RS-2854790/V1.

[218] M. Sorokina, P. Merseburger, K. Rajan, M. A. Yirik, and C. Steinbeck, "COCONUT online: Collection of Open Natural Products database," *J Cheminform*, vol. 13, no. 1, pp. 1–13, Dec. 2021, doi: 10.1186/S13321-020-00478-9/FIGS/4.

[219] H. Kuwahara and X. Gao, "Analysis of the effects of related fingerprints on molecular similarity using an eigenvalue entropy approach," *J Cheminform*, vol. 13, no. 1, p. 27, Dec. 2021, doi: 10.1186/s13321-021-00506-2.

[220] D. Bajusz, A. Rácz, and K. Héberger, "Why is Tanimoto index an appropriate choice for fingerprint-based similarity calculations?," *J Cheminform*, vol. 7, no. 1, pp. 1–13, Dec. 2015, doi: 10.1186/S13321-015-0069-3/FIGS/7.

[221] S. Khan, R. Hussain, Y. Khan, T. Iqbal, T. Aziz, and M. Alharbi, “Correlation between in vitro anti-urease activity and in silico molecular modeling approach of novel imidazopyridine–oxadiazole hybrids derivatives,” *Open Chem*, vol. 22, no. 1, Jan. 2024, doi:10.1515/CHEM-2023-0210/ASSET/GRAPHIC/J_CHEM-2023- 0210.

[222] A. Daina, O. Michielin, and V. Zoete, “SwissADME: a free web tool to evaluate pharmacokinetics, drug-likeness and medicinal chemistry friendliness of small molecules,” *Sci Rep*, vol. 7, no. 1, p. 42717, Mar. 2017, doi: 10.1038/srep42717.

[223] Y. Kochnev, E. Hellemann, K. C. Cassidy, and J. D. Durrant, “Webina: an open-source library and web app that runs AutoDock Vina entirely in the web browser,” *Bioinformatics*, vol. 36, no. 16, pp. 4513–4515, Aug. 2020, doi: 10.1093/BIOINFORMATICS/BTAA579.

[224] S. Sharma and P. Kumar, “Dissecting the functional significance of HSP90AB1 and other heat shock proteins in countering glioblastomas and ependymomas using omics analysis and drug prediction using virtual screening,” *Neuropeptides*, vol. 102, p. 102383, Dec. 2023, doi: 10.1016/J.NPEP.2023.102383.

[225] C. Jiang and X. Jin, “Quick Way to Port Existing C/C++ Chemoinformatics Toolkits to the Web Using Emscripten,” *J Chem Inf Model*, vol. 57, no. 10, pp. 2407–2412, Oct. 2017, doi: 10.1021/ACS.JCIM.7B00434.

[226] Z. Wang *et al.*, “fastDRH: a webserver to predict and analyze protein–ligand complexes based on molecular docking and MM/PB(GB)SA computation,” *Brief Bioinform*, vol. 23, no. 5, pp. 1–10, Sep. 2022, doi: 10.1093/BIB/BBAC201.

[227] I. Fatima *et al.*, “Revolutionizing and identifying novel drug targets in Citrobacter koseri via subtractive proteomics and development of a multi-epitope vaccine using reverse vaccinology and immuno-informatics,” *J Biomol Struct Dyn*, 2024, doi: 10.1080/07391102.2024.2316762.

[228] J. Eberhardt, D. Santos-Martins, A. F. Tillack, and S. Forli, “AutoDock Vina 1.2.0: New Docking Methods, Expanded Force Field, and Python Bindings,” *J Chem Inf Model*, vol. 61, no. 8, pp. 3891–3898, Aug. 2021, doi: 10.1021/ACS.JCIM.1C00203/SUPPL_FILE/CI1C00203_SI_002.ZIP.

[229] K. Dutta, S. Shityakov, and F. Maruyama, “DSF inactivator RpfB homologous FadD upregulated in Bradyrhizobium japonicum under iron limiting conditions,” *Scientific Reports 2023 13:1*, vol. 13, no. 1, pp. 1–14, May 2023, doi: 10.1038/s41598-023-35487-9.

[230] N. Bharatham, S.-W. Chi, H. Sup Yoon, and V. N. Uversky, “Molecular Basis of Bcl-XL-p53 Interaction: Insights from Molecular Dynamics Simulations,” *PLoS One*, vol. 6, no. 10, p. 26014, 2011, doi: 10.1371/journal.pone.0026014.

[231] G. Zahoránszky-Kőhalmi, C. G. Bologa, and T. I. Oprea, “Impact of similarity threshold on the topology of molecular similarity networks and clustering outcomes,” *J Cheminform*, vol. 8, no. 1, p. 16, Dec. 2016, doi: 10.1186/s13321-016-0127-5.

[232] M. Naveed *et al.*, “GC–MS profiling of Bacillus spp. metabolites with an in vitro biological activity assessment and computational analysis of their impact on epithelial glioblastoma cancer genes,” *Front Chem*, vol. 11, p. 1287599, Dec. 2023, doi: 10.3389/FCHEM.2023.1287599/BIBTEX.

[233] M. Yousuf *et al.*, “Inhibiting CDK6 Activity by Quercetin Is an Attractive Strategy for Cancer Therapy,” *ACS Omega*, vol. 5, no. 42, pp. 27480–27491, Oct. 2020, doi: 10.1021/acsomega.0c03975.

[234] T. Paysan-Lafosse *et al.*, “InterPro in 2022,” *Nucleic Acids Res*, vol. 51, no. D1, pp. D418–D427, Jan. 2023, doi: 10.1093/NAR/GKAC993.

[235] R. A. Laskowski, J. Jabłońska, L. Pravda, R. S. Vařeková, and J. M. Thornton, “PDBsum: Structural summaries of PDB entries,” *Protein Science*, vol. 27, no. 1, pp. 129–134, Jan. 2018, doi: 10.1002/PRO.3289.

[236] R. Islam *et al.*, “Computational and structural based approach to identify malignant nonsynonymous single nucleotide polymorphisms associated with CDK4 gene,” *PLoS One*, vol. 16, no. 11, Nov. 2021, doi: 10.1371/JOURNAL.PONE.0259691.

[237] N. Rani, M. Sahu, R. K. Ambasta, and P. Kumar, “Triaging between post-translational modification of cell cycle regulators and their therapeutics in neurodegenerative diseases,” *Ageing Res Rev*, vol. 94, p. 102174, Feb. 2024, doi: 10.1016/J.ARR.2023.102174.

[238] G. Maggiora, M. Vogt, D. Stumpfe, and J. Bajorath, “Molecular Similarity in Medicinal Chemistry,” *J Med Chem*, vol. 57, no. 8, pp. 3186–3204, Apr. 2014, doi: 10.1021/jm401411z.

[239] V. Kumar *et al.*, “Identification of cdk7 inhibitors from natural sources using pharmacoinformatics and molecular dynamics simulations,” *Biomedicines*, vol. 9, no. 9, p. 1197, Sep. 2021, doi: 10.3390/BIOMEDICINES9091197/S1.

LIST OF PUBLICATIONS

Cumulative impact factor of all publications = 24.5

h-index = 1

Number of citations = 9

PUBLICATIONS FROM THESIS

1. **Rani, N.,** Kumar, P. Exploring Natural Compounds as Potential CDK4 Inhibitors for Therapeutic Intervention in Neurodegenerative Diseases through Computational Analysis. *Mol Biotechnol* (2024). https://doi.org/10.1007/s12033-024-01258-8 **(SCIE IF 2.4)**

2. **Rani, N.**, Sahu, M., Ambasta, R.K., Kumar, P., 2024. Triaging between post-translational modification of cell cycle regulators and their therapeutics in neurodegenerative diseases. Ageing Res Rev 94, 102174. https://doi.org/10.1016/J.ARR.2023.102174 **(SCIE IF 12.5)**

3. **Rani, N.,** Kaushik, A., Kardam, S., Kag, S., Raj, V. S., Ambasta, R. K., & Kumar, P. (2024). Reimagining old drugs with new tricks: Mechanisms, strategies and notable success stories in drug repurposing for neurological diseases. Progress in Molecular Biology and Translational Science. https://doi.org/10.1016/BS.PMBTS.2024.03.029 **(IF 3.6)**

OTHER PUBLICATIONS

1. Sahu, M., **Rani, N.** & Kumar, P. Simulation and Computational Study of RING Domain Mutants of BRCA1 and Ube2k in AD/PD Pathophysiology. Mol Biotechnol 66, 1095–1115 (2024). https://doi.org/10.1007/s12033-023-01006-4 **(SCIE IF 2.4)**

CONFERENCES PROCEEDINGS

1. N. **Rani** and P. Kumar, "Understanding the role of alkaloids in therapeutic targeting of UBE3A in Alzheimer's Disease," 2023 3rd International Conference on Innovative Sustainable Computational Technologies (CISCT), Dehradun, India, 2023, pp. 1-4, doi: 10.1109/CISCT57197.2023.10351490.
2. **N. Rani** and P. Kumar, "Leuconoxine as a prospective therapeutic candidate targeting CDK6 in combating Alzheimer's disease," the World Congress of Neurology (WCN 2023) Journal of the Neurological Sciences Volume 455, SUPPLEMENT,121442, https://doi.org/10.1016/j.jns.2023.121442 **(SCIE IF 3.6)**
3. **N. Rani** and P. Kumar, "Revolutionizing Antimicrobial Defence: Unleashing CDK5 as a Molecular Maestro Against Drug Resistance," 3rd International Conference on "Antimicrobial Resistance, Novel Drug Discovery and Vaccine Development: Challenges and Opportunities", Delhi, India 2024.

WORKSHOP

1. On-site SNCI symposium titled *"Neurochemical Legacy of Neurological Disorders: Brainstorming of Novel Approaches",* 9th March 2022, Jamia

Hamdard University, New Delhi.

2. DST STUTI Training Program on "*Synergistic Approach of Alternative Models in Toxicological Research"*, 10th to 16th March 2022, Department of Toxicology, School of Chemical and Life Sciences, Jamia Hamdard University, New Delhi.
3. DST STUTI Training Program on "Understanding *Neurological Disorders: Technical Approaches and Advancements"*, 20th to 26th December 2022, Department of Toxicology, School of Chemical and Life Sciences, Jamia Hamdard University, New Delhi.
4. Two-day workshop titled "*Hands–on workshop on Cell Culture Techniques*", 26th- 27th September 2023, University College of Medical Sciences (University of Delhi) and Guru Teg Bahadur Hospital.

BIOSKETCH

NEETU RANI

Corresponding address:

H. NO.- 394 VILLAGE JHARERA DELHI CANTT 110010 (India) neetulohia2@gmail.com;
+(91) 8800769264

EDUCATION/TRAINING

INSTITUTION /UNIVERSITY	POSITION	YEAR(s)	FIELD OF STUDY
Delhi Technological University (Formerly Delhi College of Engineering), Delhi	PhD (CSIR-UGC JRF)	August 2021-present	Neurodegenerative Diseases, Cell Cycle, Ubiquitin Proteasome System and Neuroscience
Ch. Charan Singh University, Meerut (India)	M.Sc. Biotechnology	2007-2009	Biotechnology

Deen Dayal Upadhayay College, Universityof Delhi (India)	B.Sc. Life Sciences	2004-2007	Life Sciences
Victoria Girls Senior Secondary School, Delhi (India)	Higher Secondary School Examination, C.B.S.E.	2004	Physics, Chemistry, Biology,English,
Nav Jeevan Adarsh Public School, Delhi (India)	Senior Secondary School Examination, C.B.S.E.	2002	Science, Mathematics, SocialSciences, Hindi, English,

SALIENT FEATURES OF YOUR RESEARCH WORK

Therapeutics Research: Expertise in CDK4, CDK6, and UBE3A-related pathways and drug targets

In silico experimental Design: Designing experiments for microarray analysis, protein interactions, and MD simulation

Literature Review: In-depth review of scientific literature related to neurodegenerative diseases, cell cycle regulation, and therapeutics

- CSIR-UGC fellow

PEER-REVIEWED PUBLICATIONS

Cumulative impact factor of all publications = **24.5**

h-index = **1**

Total number of citations = **9**

1. **Rani, N.,** Kumar, P. Exploring Natural Compounds as Potential CDK4 Inhibitors for Therapeutic Intervention in Neurodegenerative Diseases through Computational Analysis. *Mol Biotechnol* (2024). https://doi.org/10.1007/s12033-024-01258-8 **[SCIE IF 2.4]**

2. **Rani, N.**, Sahu, M., Ambasta, R.K., Kumar, P., 2024. Triaging between post-translational modification of cell cycle regulators and their therapeutics in neurodegenerative diseases. Ageing Res Rev 94, 102174. https://doi.org/10.1016/J.ARR.2023.102174 **[SCIE IF 12.5]**

3. **Rani, N.,** Kaushik, A., Kardam, S., Kag, S., Raj, V. S., Ambasta, R. K., & Kumar, P. (2024). Reimagining old drugs with new tricks: Mechanisms, strategies and notable success stories in drug repurposing for neurological diseases. Progress in Molecular Biology and Translational Science. https://doi.org/10.1016/BS.PMBTS.2024.03.029 **[IF 3.6]**

4. Sahu, M., **Rani, N.** & Kumar, P. Simulation and Computational Study of RING Domain Mutants of BRCA1 and Ube2k in AD/PD Pathophysiology. Mol Biotechnol 66, 1095–1115 (2024). https://doi.org/10.1007/s12033-023-01006-4 **[SCIE IF 2.4]**

CONFERENCE, PROCEEDINGS AND SYMPOSIUM

- N. Rani and P. Kumar, "Understanding the role of alkaloids in therapeutic targeting of UBE3A in Alzheimer's Disease," 2023 3rd International Conference on Innovative Sustainable Computational Technologies (CISCT), Dehradun, India, 2023, pp. 1-4, doi: 10.1109/CISCT57197.2023.10351490. [**Oral presentation**]

- N. Rani and P. Kumar, "Leuconoxine as a prospective therapeutic candidate targeting CDK6 in combating Alzheimer's disease," the World Congress of Neurology (WCN 2023) Journal of the Neurological Sciences Volume 455, SUPPLEMENT,121442, https://doi.org/10.1016/j.jns.2023.121442 **(SCIE IF 3.6) [Poster presentation]**

- N. Rani and P. Kumar, "Revolutionizing Antimicrobial Defence: Unleashing CDK5 as a Molecular Maestro Against Drug Resistance," 3rd International Conference on "Antimicrobial Resistance, Novel Drug Discovery and Vaccine Development: Challenges and Opportunities", Delhi, India 2024 **[Poster presentation]**

- DST STUTI Training Program on "*Synergistic Approach of Alternative Models inToxicological Research"*, 10th to 16th March 2022, Department of Toxicology, School of Chemical and Life Sciences, Jamia Hamdard University, New Delhi.

- DST STUTI Training Program on "Understanding *Neurological Disorders: Technical Approaches and Advancements"*, 20th to 26th December 2022, Department of Toxicology, School of Chemical and Life Sciences, Jamia Hamdard University, New Delhi.

- Two-day workshop titled "*Hands–on workshop on Cell Culture Techniques*", 26th- 27th September 2023, University College of Medical Sciences (University of Delhi) and Guru Teg Bahadur Hospital.

PROFICIENCY IN TECHNIQUES

In-*vitro* characterization:

Cell culture, DNA isolation Protein isolation, SDS-PAGE, Soft agar assayand Drug stability studies.

Gene expression studies:

Gradient PCR, RT-PCR, DNA and RNA isolations from Blood, Cell line and tissue samples.

In-*silico* studies:

Microarray dataset collection and analysis, Drug Repurposing using Molecular Docking, Molecular Dynamic Simulations (MDS) studies using CHARMM Forcefield in GROMACS, CytoScape and Network analysis.

HONOURS AND AWARDS

- Prestigious CSIR-UGC Fellowship (2021-Present)
- GATE qualified

REFERENCES

Professor Pravir Kumar (Ph.D. Supervisor)
Professor and Head, Department of Biotechnology
Molecular Neuroscience and Functional Genomics Laboratory
*Former Dean***,** Delhi Technological University (Formerly Delhi College of Engineering)
Shahbad Daulatpur, Bawana Road, Delhi 110042;
Phone: +91- 9818898622 Email: pravirkumar@dtu.ac.in; kpravir@gmail.com

DELHI TECHNOLOGICAL UNIVERSITY

(Formerly Delhi College of Engineering)
Shahbad Daulatpur, Main Bawana Road, Delhi-42

PLAGIARISM VERIFICATION

Title of the Thesis THERAPEUTIC IMPLICATIONS OF UBIQUITIN PROTEASOME SYSTEM IN NEURODEGENERATIVE DISEASES

Total Pages 144 Name of the Scholar NEETU RANI

Supervisor (s)

(1) PROF. PRAVIR KUMAR

(2)

(3)

Department BIOTECHNOLOGY

This is to report that the above thesis was scanned for similarity detection. Process and outcome is given below:

Software used: TURNITIN Similarity Index: 8%, Total Word Count: 30724

Date: 18-10-2024

Candidate's Signature

21/10/2024

Signature of Supervisor(s)

Similarity Report

PAPER NAME

THERAPEUTIC IMPLICATIONS OF UBIQUITIN PROTEASOME SYSTEM IN NEURODEGENERATIVE DISEASES

AUTHOR

NEETU RANI

WORD COUNT

30724 Words

CHARACTER COUNT

176693 Characters

PAGE COUNT

144 Pages

FILE SIZE

11.0MB

SUBMISSION DATE

Oct 2, 2024 9:55 PM GMT+5:30

REPORT DATE

Oct 2, 2024 9:58 PM GMT+5:30

Verified 21/10/2024

8% Overall Similarity

The combined total of all matches, including overlapping sources, for each database.

- 5% Internet database
- 5% Publications database
- Crossref database
- Crossref Posted Content database
- 4% Submitted Works database

Excluded from Similarity Report

- Bibliographic material
- Quoted material
- Cited material
- Small Matches (Less then 10 words)
- Manually excluded sources

Summary

Similarity Report

8% Overall Similarity

Top sources found in the following databases:

- 5% Internet database
- Crossref database
- 4% Submitted Works database
- 5% Publications database
- Crossref Posted Content database

TOP SOURCES

The sources with the highest number of matches within the submission. Overlapping sources will not be displayed.

1	**frontiersin.org** Internet	<1%
2	**nature.com** Internet	<1%
3	**mdpi.com** Internet	<1%
4	**ncbi.nlm.nih.gov** Internet	<1%
5	**Sukumar Ranjith, Aswathy Sathyan, Senbagam Duraisamy, Ansu Susan...** Crossref	<1%
6	**link.springer.com** Internet	<1%
7	**Chunye Zhang, Yuxiang Sui, Shuai Liu, Ming Yang. "Anti-Viral Activity o...** Crossref	<1%
8	**researchgate.net** Internet	<1%

Sources overview

Similarity Report

9	abis-files.bezmialem.edu.tr Internet	<1%
10	Kwame Nkrumah University of Science and Technology on 2022-07-22 Submitted works	<1%
11	researchsquare.com Internet	<1%
12	National Institute of Technology on 2024-08-20 Submitted works	<1%
13	tandfonline.com Internet	<1%
14	Ipek Kucuk, Didem Nur Ünal, Arzu Karayel, Sevinc Kurbanoglu, Bengi U... Crossref	<1%
15	infospace.mrc.ac.za Internet	<1%
16	academic.oup.com Internet	<1%
17	journals.plos.org Internet	<1%
18	statpearls.com Internet	<1%
19	Dhurgham Al-Fahad, G Ropón-Palacios, Damilola A. Omoboyowa, Gaga... Crossref posted content	<1%
20	Sk Injamamul Islam, Sheikh Sunzid Ahmed, Nasim Habib, Md Akib Ferd... Crossref	<1%

Sources overview

Similarity Report

21	dspace.dtu.ac.in:8080 Internet	<1%
22	biorxiv.org Internet	<1%
23	Keiichi I. Nakayama, Keiko Nakayama. "Ubiquitin ligases: cell-cycle co... Crossref	<1%
24	downloads.hindawi.com Internet	<1%
25	research-management.mq.edu.au Internet	<1%
26	Nishtha Malhotra, Rohan Gupta, Pravir Kumar. "Pharmacological releva... Crossref	<1%
27	assets.researchsquare.com Internet	<1%
28	tmrjournals.com Internet	<1%
29	scholar.deep-time.org Internet	<1%
30	Mapua Institute of Technology on 2024-07-27 Submitted works	<1%
31	Nottingham Trent University on 2024-09-02 Submitted works	<1%
32	Sajad Majeed Zargar, Asmat Farooq, Parvaze Ahmad Sofi, Jebi Sudan, ... Crossref	<1%

Sources overview

Similarity Report

33	University of Wales Swansea on 2021-12-09 Submitted works	<1%
34	Srutishree Sarma, Dikshita Dowerah, Moumita Basumatary, Ambalika ... Crossref posted content	<1%
35	Vodermaier, H.C.. "APC/C and SCF: Controlling Each Other and the Cell... Crossref	<1%
36	portlandpress.com Internet	<1%
37	science.org Internet	<1%
38	docslib.org Internet	<1%
39	finance.yahoo.com Internet	<1%
40	openscience.ub.uni-mainz.de Internet	<1%
41	phd-dissertations.unizik.edu.ng Internet	<1%
42	researchspace.ukzn.ac.za Internet	<1%
43	jcipp.curtin.edu.au Internet	<1%
44	Bilal Malik, Helen Devine, Rickie Patani, Albert R. La Spada, Michael G. ... Crossref	<1%

Sources overview

Similarity Report

45	Diaf, Saousen R.. "Utilizing Molecular Simulation to Understand the Mo... Publication	<1%
46	Higher Education Commission Pakistan on 2024-07-09 Submitted works	<1%
47	Quan Yang, Jinyao Zhao, Dan Chen, Yang Wang. "E3 ubiquitin ligases: ... Crossref	<1%
48	University of Bristol on 2015-03-11 Submitted works	<1%
49	University of Teesside on 2024-08-14 Submitted works	<1%
50	Uttar Pradesh Technical University on 2022-03-05 Submitted works	<1%
51	api.research-repository.uwa.edu.au Internet	<1%
52	dspace.tul.cz Internet	<1%
53	molbiolcell.org Internet	<1%
54	Abbas Khan, Shoaib Adil, Hafiza Ayesha Qudsia, Yasir Waheed, Fahad ... Crossref	<1%
55	City University of Hong Kong on 2022-07-23 Submitted works	<1%
56	Deeksha Tiwari, Nitish Mittal, Hem Chandra Jha. "Unraveling the links ... Crossref	<1%

Sources overview

Similarity Report

57	Imperial College of Science, Technology and Medicine on 2015-04-16 Submitted works	<1%
58	Jan-Michael Peters. "The anaphase promoting complex/cyclosome: a ... Crossref	<1%
59	Khurana, V.. "Connecting cell-cycle activation to neurodegeneration in ... Crossref	<1%
60	Natasha Khatri, Heng-Ye Man. "The Autism and Angelman Syndrome P... Crossref	<1%
61	P. Fasanaro. "Regulation of the endothelial cell cycle by the ubiquitin-p... Crossref	<1%
62	Silvana-Yanina Romero-Zerbo, Nadia Valverde, Silvia Claros, Pablo Za... Crossref	<1%
63	Tanaka, K.. "Ubiquitin, proteasome and parkin", BBA - Molecular Cell R... Crossref	<1%
64	University of Texas Health Science Center on 2011-03-15 Submitted works	<1%
65	Vrije Universiteit Brussel on 2021-08-16 Submitted works	<1%
66	Westminster College on 2011-11-20 Submitted works	<1%
67	purehost.bath.ac.uk Internet	<1%
68	repub.eur.nl Internet	<1%

Sources overview

Similarity Report

69	spandidos-publications.com Internet	<1%
70	"Encyclopedia of Signaling Molecules", Springer Nature, 2018 Crossref	<1%
71	Abdulkadir, Abubakar Shettima. "Diesel Particulate Extract Induced Im... Publication	<1%
72	Ahirwar, Parmanand. "Streptococcus mutans Biofilm Inhibiting Small ... Publication	<1%
73	American University of Beirut on 2017-11-10 Submitted works	<1%
74	Amjad Khan, Tahir Ali, Shafiq Ur Rehman, Muhammad Sohail Khan et al... Crossref	<1%
75	Associatie K.U.Leuven on 2012-01-09 Submitted works	<1%
76	Bilal Malik. "Cell cycle-driven neuronal apoptosis specifically linked to ... Crossref	<1%
77	Canterbury Christ Church University on 2022-04-28 Submitted works	<1%
78	Clara F.G. Laursen, Federica Genovese, M.A. Karsdal. "Aging—the most... Crossref	<1%
79	Daskivich, Grant Joseph. "Characterization and Contextualization of Pr... Publication	<1%
80	F. Macdonald, C.H.J. Ford, A.G. Casson. "Molecular Biology of Cancer",... Publication	<1%

Sources overview

Similarity Report

81	Fakultät Bauingenieurwesen Bergische Universität Wuppertal on 2024-... Submitted works	<1%
82	Friedrich Marks, Ursula Klingmüller, Karin Müller-Decker. "Cellular Sign... Publication	<1%
83	Jawaharlal Nehru University (JNU) on 2021-11-04 Submitted works	<1%
84	Jennifer Sigmond, Godefridus J. Peters. "Pyrimidine and Purine Analog... Crossref	<1%
85	Joshua Santos, Mark Tristan Quimque, Rhenz Alfred Liman, Jay Carl A... Crossref	<1%
86	Maria Velez-Brochero, Padmanava Behera, Kazi Sabrina Afreen, Abby ... Crossref	<1%
87	Md. Masudur Rahman Munna, Md. Touki Tahamid Tusar, Saima Sajnin ... Crossref	<1%
88	Osheen Sahay, Ganesh Kumar Barik, Tanisha Sharma, Ajay D. Pillai, Sri... Crossref	<1%
89	Paula Mariana Kustiawan, Khalish Arsy Al Khairy Siregar, Putri Hawa S... Crossref	<1%
90	Rodriguez Serrano, Alan Fernando. "Engineering Small Molecule Biose... Publication	<1%
91	Sahasrabuddhe, Anagh A., and Kojo S. J. Elenitoba-Johnson. "Role of t... Crossref	<1%
92	The University of Manchester on 2014-04-03 Submitted works	<1%

Sources overview

Similarity Report

93	UT, Dallas on 2014-12-01 Submitted works	<1%
94	University of Florida on 2023-02-15 Submitted works	<1%
95	University of Liverpool on 2017-11-03 Submitted works	<1%
96	Zhi-Xiang Zhou, Zhong Ren, Bin-Jie Yan, Shun-Lin Qu, Zhi-Han Tang, D... Crossref	<1%
97	article.sciencepublishinggroup.com Internet	<1%
98	cyberleninka.org Internet	<1%
99	eprints.soton.ac.uk Internet	<1%
100	iris.unige.it Internet	<1%
101	studentsrepo.um.edu.my Internet	<1%
102	ensani.ir Internet	<1%
103	freepatentsonline.com Internet	<1%
104	ir.juit.ac.in:8080 Internet	<1%

Sources overview

Similarity Report

105 rcsb.org
Internet

<1%

Sources overview

Similarity Report

Excluded from Similarity Report

- Bibliographic material
- Cited material
- Manually excluded sources
- Quoted material
- Small Matches (Less then 10 words)

EXCLUDED SOURCES

Neetu Rani, Mehar Sahu, Rashmi K. Ambasta, Pravir Kumar. "Triaging betwee... Crossref	**34%**
Neetu Rani, Mehar Sahu, Rashmi K. Ambasta, Pravir Kumar. "Triaging betwee... Crossref	**34%**
Neetu Rani, Pravir Kumar. "Exploring Natural Compounds as Potential CDK4 I... Crossref	**26%**
Neetu Rani, Aastha Kaushik, Shefali Kardam, Sonika Kag, V. Samuel Raj, Rash... Crossref	**5%**
Neetu Rani, Pravir Kumar. "Understanding the role of alkaloids in therapeutic t... Crossref	**4%**
Mehar Sahu, Neetu Rani, Pravir Kumar. "Simulation and Computational Study ... Crossref	**<1%**

Ageing Research Reviews 94 (2024) 102174

Contents lists available at ScienceDirect

Ageing Research Reviews

journal homepage: www.elsevier.com/locate/arr

Review article

Triaging between post-translational modification of cell cycle regulators and their therapeutics in neurodegenerative diseases

Neetu Rani [a], Mehar Sahu [a], Rashmi K. Ambasta [a,b,*], Pravir Kumar [a,**,1]

[a] Molecular Neuroscience and Functional Genomics Laboratory, Department of Biotechnology, Delhi Technological University (Formerly DCE), Delhi 110042
[b] Department of Biotechnology and Microbiology, SRM University, Sonepat, Haryana, India

ARTICLE INFO

Keywords:
Neurodegenerative diseases
Post-mitotic cell division
Cyclin-dependent kinase
Post-translational modifications
Acetylation
Ubiquitination

ABSTRACT

Neurodegenerative diseases, such as Alzheimer's disease, Parkinson's disease, and Huntington's disease, present challenges in healthcare because of their complicated etiologies and absence of healing remedies. Lately, the emerging role of post-translational modifications (PTMs), in the context of cell cycle regulators, has garnered big interest as a potential avenue for therapeutic intervention. The review explores the problematic panorama of PTMs on cell cycle regulators and their implications in neurodegenerative diseases. We delve into the dynamic phosphorylation, acetylation, ubiquitination, SUMOylation, Glycation, and Neddylation that modulate the key cell cycle regulators, consisting of cyclins, cyclin-dependent kinases (CDKs), and their inhibitors. The dysregulation of these PTMs is related to aberrant cell cycle in neurons, which is one of the factors involved in neurodegenerative pathologies. Moreover, the effect of exogenous activation of CDKs and CDK inhibitors through PTMs on the signaling cascade was studied in postmitotic conditions of NDDs. Furthermore, the therapeutic implications of CDK inhibitors and associated alteration in PTMs were discussed. Lastly, we explored the putative mechanism of PTMs to restore normal neuronal function that might reverse NDDs.

Abbreviations: AD, Alzheimer's Disease; Aβ, Amyloid β; AGEs, Advanced glycation end products; AIF, Apoptosis inducing factor; Ape1-Human AP, endonuclease 1; AP-1, Activator protein – 1; APC, Anaphase-promoting complex; APP, Amyloid precursor protein; APP-BP1, Amyloid precursor protein-binding protein; ATM, Ataxia Telangiectasia mutated; ATP, Adenosine triphosphate;; ATR, Ataxia Telangiectasia and Rad-3 related; BDNF, Brain-derived neurotrophic factor; BrdU, Bromodeoxyuridine; βTrCP, β-transducin repeat-containing protein; CaMK, Calcium/Calmodulin-dependent protein kinase II; CCR, Cell Cycle re-entry; CDKs, Cyclin Dependent Kinases; CDK5, Cyclin dependent kinase 5; ChK 1, Checkpoint Kinase 1; ChK 2, Checkpoint Kinase 2; CIP/KIP, CDK interacting protein/Kinase inhibitory protein; CKIs, Cyclin Dependent Kinase Inhibitors; CNS, Central Nervous System; CPT, Camptothecin; DCRNs, Differentiating chick retinal neurons; DDR, DNA Damage Response; Drp1, Dynamin-1, like protein; DUBs, Deubiquitinating enzymes; ERK, Extracellular-signal regulated kinase;; FOXO 1, Forkhead box protein O1; GPX, Glutathione peroxidase; GSK3β, Glycogen synthase kinase 3β; HAT, Histone acetyl transferase; HDAC, Histone deacetylase; HD, Huntington's Disease; HMT, histone methyltransferases; Hq, Harlequin; IGF 1, insulin-like growth factor 1; JNK, c-Jun N-terminal kinase; KLF4, Krüppel-like factor 4; MAPK, mitogen-activated protein kinase; MeF2, Myocyte Enhancer Factor; MEF2D, Myocyte-specific enhancer factor 2D; MPTP, 1-methyl-4-phenyl-1,2,3,6-tetrahydropyridine; NAD, Nicotinamide adenine dinucleotide; NADH, Nicotinamide adenine dinucleotide hydride; NADPH, Nicotinamide adenine dinucleotide phosphate hydrogen; NDDs, Neurodegenerative Disease; Nek2, NIMA related kinase 2; NFTs, Neurofibrillary tangles; NGF, Nerve Growth Factor; NHEJ, Nonhomologous end joining; NMDA R, N-methyl-D-aspartate receptor; PCNA, Proliferating cell nuclear antigen; PD, Parkinson's Disease; PI3K, Phosphoinositide 3-kinases; PIAS, Protein Inhibitor of Activated Signal; PLCγ, Phospholipase C γ; PLK, Polo like kinase; PP1, Protein Phosphatases 1; PQ, Paraquat; PRX, Peroxiredoxin; Prx2, Peroxiredoxin 2; PS1, Presenilin 1; PTM, Post translational modification; RAGE, Receptor for Advanced Glycation end products; RGCs, Retinal ganglion cells; Rhes, Ras Homolog Enriched in Striatum; ROS, Reactive Oxygen Species; SCF, Skp, Cullin; F, box containing complex; SIRT, sirtuin; SOD, Superoxide dismutase; SKP, S-phase kinase associated protein; TBI, Traumatic Brain Injury; TrKB, tropomyosin receptor kinase; VPA, Valproic acid; UPS, ubiquitin-proteasome system.

* Corresponding author at: Department of Biotechnology and Microbiology, SRM University, Sonepat, Haryana, India.
** Correspondence to: Professor, Head (Biotechnology), Dean (international Affairs); Department of Biotechnology, Molecular Neuroscience and Functional Genomics Laboratory, Room# FW4TF3, Mechanical Engineering Building, Shahbad Daulatpur, Bawana Road, Delhi 110042, India.
E-mail addresses: rashmi.ambasta@srmuniversity.ac.in (R.K. Ambasta), pravirkumar@dtu.ac.in (P. Kumar).
[1] ORCID ID: 0000–0001-7444–2344

https://doi.org/10.1016/j.arr.2023.102174
Received 10 November 2023; Received in revised form 18 December 2023; Accepted 18 December 2023
Available online 21 December 2023

Molecular Biotechnology
https://doi.org/10.1007/s12033-024-01258-8

ORIGINAL PAPER

Exploring Natural Compounds as Potential CDK4 Inhibitors for Therapeutic Intervention in Neurodegenerative Diseases through Computational Analysis

Neetu Rani[1] · Pravir Kumar[1,2]

Received: 27 March 2024 / Accepted: 3 July 2024

Abstract

CDK4 is a member of the serine-threonine kinase family, which has been found to be overexpressed in a plethora of studies related to neurodegenerative diseases. CDK4 is one of the most validated therapeutic targets for neurodegenerative diseases. Hence, the discovery of potent inhibitors of CDK4 is a promising candidate in the drug discovery field. Firstly, the reference drug Palbociclib was identified from the available literature as a potential candidate against target CDK4. In the present study, the Collection of Open Natural Products (COCONUT) database was accessed for determining potential CDK4 inhibitors using computational approaches based on the Tanimoto algorithm for similarity with the target drug, i.e., Palbociclib. The potential candidates were analyzed using SWISSADME, and the best candidates were filtered based on Lipinski's Rule of 5, Brenk, blood–brain barrier permeability, and Pains parameter. Further, the molecular docking protocol was accessed for the filtered compounds to anticipate the CDK4-ligand binding score, which was validated by the fastDRH web-based server. Based on the best docking score so obtained, the best four natural compounds were chosen for further molecular dynamic simulation to assess their stability with CDK4. In this study, two natural products, with COCONUT Database compound ID—CNP0396493 and CNP0070947, have been identified as the most suitable candidates for neuroprotection.

Graphical Abstract

Overexpression of CDK4 in NDDs has been considered as prominent target for therapeutics. Possible CDK4 inhibitors have been explored using computational techniques and the COCONUT database, which keeps Palbociclib as the reference drug. Using several criteria, such as molecular docking and Lipinski's Rule of 5, 110 natural compounds have been obtained. In addition to molecular docking, this study utilized Molecular Mechanics Generalised Born Surface Area (MM-GBSA) analysis to further filter and assess the binding affinity and stability of the top 4 natural compounds. Further evaluation was carried

✉ Pravir Kumar
pravirkumar@dtu.ac.in; kpravir@gmail.com

[1] Molecular Neuroscience and Functional Genomics Laboratory, Department of Biotechnology, Delhi Technological University (Formerly DCE), Shahbad Daulatpur, Bawana Road, Delhi 110042, India

[2] Molecular Neuroscience and Functional Genomics Laboratory, Department of Biotechnology, Delhi Technological University, Delhi 110042, India

Published online: 29 August 2024

Understanding the role of alkaloids in therapeutic targeting of UBE3A in Alzheimer's Disease

Neetu Rani ; Pravir Kumar All Authors •••

Abstract:
Neurodegenerative diseases (NDDs) such as Alzheimer's Diseases (AD) are characterised by accumulation of misfolded proteins. The Ubiquitin Proteosome System (UPS) has an ... **View more**

Metadata

Abstract:
Neurodegenerative diseases (NDDs) such as Alzheimer's Diseases (AD) are characterised by accumulation of misfolded proteins. The Ubiquitin Proteosome System (UPS) has an important role in regulation of protein homeostasis in the cell. In this study, common differentially expressed genes (DEGs) (i.e.E3 ligase) were screened after comparing DEGs from GSE5281 dataset and the KSBP2 E3 ligases dataset, based on the applied filters of adj p value < 0.05 and Log FC value. Further Gene set enrichment analysis was performed to assess the biological, cellular, and molecular processes of E3 ligase. These E3 ligase were further screened for protein-protein interaction with the help of STRING and cytoscape tools from where 15 E3 ligases were extracted. In this study, E3 ligase biomarkers (UBE3A, UBE4B, RCHY1, UBOX5, UBE3C, CBL) have been identified based on Gene set enrichment analysis and pathway analysis. UBE3A has been selected for further analysis due to its highest Log FC value among selected biomarkers and its active involvement in enrichment interpretation. Natural compounds (alkaloids) were used against UBE3A. Molecular docking analysis predicted that Leuconoxine, Jamine and Panamine have maximum binding affinity scores. In this study, Leuconoxine, Jamine and Panamine have been found to be promising therapeutic agents against AD.

Published in: 2023 3rd International Conference on Innovative Sustainable Computational Technologies (CISCT)

Date of Conference: 08-09 September 2023

DOI: 10.1109/CISCT57197.2023.10351490

Date Added to IEEE *Xplore*: 21 December 2023

Publisher: IEEE

ISBN Information:

Conference Location: Dehradun, India

Funding Agency:

CHAPTER THREE

Reimagining old drugs with new tricks: Mechanisms, strategies and notable success stories in drug repurposing for neurological diseases

Neetu Rani[a], Aastha Kaushik[a], Shefali Kardam[a], Sonika Kag[a], V. Samuel Raj[b], Rashmi K. Ambasta[b], and Pravir Kumar[a,*]

[a]Molecular Neuroscience and Functional Genomics Laboratory, Department of Biotechnology, Delhi Technological University, Delhi, India
[b]Department of Biotechnology and Microbiology, SRM University, Sonepat, Haryana, India
*Corresponding author. e-mail address: pravirkumar@dtu.ac.in

Contents

Progress in Molecular Biology and Translational Science, Volume 205
ISSN 1877-1173, https://doi.org/10.1016/bs.pmbts.2024.03.029

strongly associated with neuropsychological assessments than plasma p-tau181. Taken together, our study suggests that plasma p-tau181 may aid in evaluating individuals by identifying those with underlying early AD.

doi:10.1016/j.jns.2023.121441

121442

Leuconoxine as a prospective therapeutic candidate targeting CDK6 in combating Alzheimer's disease

Neetu Rani, Pravir Kumar, *Delhi Technological University, Biotchnology, Delhi, India*

Background and aims

Alzheimer's Disease (AD) is manifested as the aggregation of toxic proteins amyloid beta and results in the cognitive decline. Various mechanisms are involved in the pathophysiology of AD such as oxidative stress, ubiquitin proteosome system dysfunction, cell cycle re-entry and others. Herein, we investigated the cell cycle related biomarkers involved in the pathophysiology and natural compounds as therapeutics agents for AD.

Methods

In this study we extracted GSE5281 from GEO database consisting of AD and control patients and cell cycle related (CCR) genes were extracted from KEGG web-based server. Further, differential gene expression, protein-protein interaction (PPI), gene set enrichment analysis was performed to identify the cell cycle related biomarkers. Subsequently, 40 natural compounds and molecular docking was performed with cell cycle related biomarker.

Results

Based on PPI and GSEA analysis we extracted the CCR biomarkers CDK6, ATR, and RB1. The CDK6 was selected as potential CCR marker based on involvement in maximum functional pathways. In molecular docking interpretation with selected natural compound, we analysed that leuconoxine demonstrated maximum binding affinity (−10.78 Kcal/mol) with CDK6, followed by Jamine (−10.49 Kcal/mol), ormosanine (−10.34 Kcal/mol) and panamine (−10.34Kcal/mol) in comparison to the control drug fiestin (−9.652 Kcal/mol).

Conclusions

In this study we identified leuconoxine as a potential therapeutic agent against CDK6 in AD.

doi:10.1016/j.jns.2023.121442

121443

Deep learning brain connectivity augmentation for differentiating Alzheimer's disease from mild cognitive impairment using limited data

Oben Ozgur[a], Arwa Rekik[b], Islem Rekik[c], *[a]Faculty of Computer and Informatics, Istanbul Technical University, Istanbul, Turkey, Computer and Informatics, Istanbul, Turkey, [b]Sahloul hospital Sousse Tunisia, Neurology, Sousse, Tunisia, [c]BASIRA lab, Imperial-X Translation and Innovation Hub Computing, Imperial College London, UK, Artificial Intelligence, London, United Kingdom*

Background and aims

The challenges of collecting large-scale neuroimaging datasets with neurological disorders, to train deep models capable of performing efficiently and accurately in clinical diagnosis tasks paved the way for models which learn from a few brains. In our study, we aimed to design an augmentator graph neural network to generate synthetic brain networks(GNNs) from a single brain connectivity template in order to circumvent the lack of training neuroimaging data and then test the performance's boost in differentiating Alzheimer's disease(AD) from late mild cognitive impairment(LMCI).

Methods

We evaluated our method on brain connectomes diagnosed with AD and late mild LMCI using brain MRI scans extracted from the Alzheimer's Disease Neuroimaging Initiative database GO public dataset. For each brain scan, the networks are derived from maximum principal curvature, the mean cortical thickness, sulcal depth, the average curvature, cortical surface area, and minimum principle area. We used an augmentation network that generates synthetic brain graphs from a single connectional brain template.

Results

The dataset included 70 subjects(35 AD and 35LMCI). Regarding our augmentation network, we have achieved higher accuracy (54 vs.51) and higher sensitivity (69.3vs.39.8). We have observed that Pericalcarine cortex(PrC) and precuneus connectivity is specific to AD patients and that dissimilar connections of the the PrC with the inferior parietal cortex and with the caudal middle frontal gyrus represent fingerprints of LMCI.

Conclusions

Our study pointed out strategic morphological connectivities singular to AD and LMCI. Data augmentation method from one brain template did not only boost the accuracy of our model, but helped tackle the limited date issue.

doi:10.1016/j.jns.2023.121443

121444

The experience acquired during the first prevention clinical trial in Alzheimer's disease in Colombia

Silvia Rios-Romenets[a], Marisol Londoño Castaño[a], Gustavo Villegas[a], Claudia Muñoz[a], Sindy Duque[a], Eugenia Cardona[a], Ernesto Luna[a], Hugo Lopez[a], Liliana Lopez[a], Yury Valencia[a], Erika Gallego[a], Claudia Ramos[a], Margarita Giraldo[a], Natalia Acosta-Baena[a], Kaycee Sink[b], Pierre Tariot[c], Eric Reiman[c], Francisco Lopera[a], *[a]University of Antioquia, Neurosciences Group of Antioquia, Medellin, Colombia, [b]Genentech Inc, Product Development Neuroscience, South San Francisco, United States of America, [c]Banner Alzheimer's Institute, Banner Alzheimer's Institute, Phoenix, United States of America*

Background and aims

The Colombian Alzheimer's Prevention Initiative (API) Autosomal Dominant AD (ADAD) trial was a collaborative project involving the Neurosciences Group of Antioquia (GNA), Banner Alzheimer's Institute, Genentech/Roche, and National Institute on Aging. The trial evaluated the treatment with crenezumab in cognitively unimpaired 30–60 year-old presenilin 1 (PSEN1) E280A members of the world's largest ADAD kindred. We will describe the strategies we employed to recruit and retain participants of the kindred throughout the trial.